CLNS 03/1835
PITHA 03/06
hep-ph/0308039
August 4, 2003

QCD factorization for $B \to PP$ and $B \to PV$ decays

Martin Beneke[a] and Matthias Neubert[b]

[a]*Institut für Theoretische Physik E, RWTH Aachen*
D–52056 Aachen, Germany

[b]*Newman Laboratory for Elementary-Particle Physics, Cornell University*
Ithaca, NY 14853, USA

Abstract

A comprehensive study of exclusive hadronic B-meson decays into final states containing two pseudoscalar mesons (PP) or a pseudoscalar and a vector meson (PV) is presented. The decay amplitudes are calculated at leading power in $\Lambda_{\rm QCD}/m_b$ and at next-to-leading order in α_s using the QCD factorization approach. The calculation of the relevant hard-scattering kernels is completed. Important classes of power corrections, including "chirally-enhanced" terms and weak annihilation contributions, are estimated and included in the phenomenological analysis. Predictions are presented for the branching ratios of the complete set of the 96 decays of B^-, $\bar{B}^0$, and $\bar{B}_s$ mesons into PP and PV final states, and for most of the corresponding CP asymmetries. Several decays and observables of particular phenomenological interest are discussed in detail, including the magnitudes of the penguin amplitudes in PP and PV final states, an analysis of the $\pi\rho$ system, and the time-dependent CP asymmetry in the $K\phi$ and $K\eta'$ final states.

1 Introduction

As the B factories [1, 2] continue to accumulate large data samples, an increasing number of different B-decay modes becomes accessible to investigation. Many of these modes carry interesting information on CP-violating interactions or hadronic flavor-changing neutral currents, but except for a number of decay channels considered "theoretically clean" a theoretical framework is required to correct for the effects of the strong interaction.

For a long time, exclusive two-body B-decay amplitudes have been estimated in the "naive" factorization approach (see, e.g., [3, 4, 5, 6, 7] and references therein) or modifications thereof. In many cases this approach provides the correct order of magnitude of branching fractions, but it cannot predict direct CP asymmetries due to the assumption of no strong rescattering. It is therefore no longer adequate for a detailed phenomenological analysis of B-factory data. Naive factorization has now been superseded by QCD factorization [8, 9]. Although not yet proved rigorously, this scheme provides the means to compute two-body decay amplitudes from first principles. Its accuracy is limited only by power corrections to the heavy-quark limit and the uncertainties of theoretical inputs such as quark masses, form factors, and light-cone distribution amplitudes. For the charmless decays considered in this paper the lowest-order approximation in QCD factorization coincides with "naive" factorization.

Among the charmless hadronic B decays, the modes $B \to \pi\pi$ and $B \to \pi K$ have been studied first and most extensively within QCD factorization [8, 10, 11, 12, 13], because they are the simplest decays for which a significant interference of tree and penguin amplitudes is expected. Other specific final states that have been investigated include those with vector mesons and exotic mesons [14, 15, 16, 17], as well as η or η' along with a pseudoscalar or vector kaon [18]. In the present paper, we complete the phenomenology of hadronic B decays into two light pseudoscalar mesons or one pseudoscalar and one vector meson, all from the ground-state nonet. We consider the complete set of 96 decay modes, including decays of B_s mesons, and decays into mesons with flavor-singlet components. We also summarize in a compact notation all the required decay coefficients and hard-scattering kernels up to the next-to-leading order in α_s. In a series of recent papers [19, 20, 21] Du et al. have considered a subset of these decay modes, including decays of B_s mesons. In [22, 23] fits to the data on pseudoscalar–vector meson final states based on the generalization of the hard-scattering kernels of [10] to these final states have been performed. While we agree qualitatively with the conclusions reached from these fits, we believe that it is currently more useful to investigate in more detail the dynamical origin of agreements and discrepancies with experimental data. In this respect the analysis presented in this paper is more complete than the fits performed previously as far as decay channels, error estimates, and analysis of observables are concerned.

The motivation for our analysis is threefold: First, the larger set of decay channels provides additional information on the CKM phase γ and on hadronic flavor-changing currents, complementary to the $\pi\pi$ and πK final states. Second, the different strong-interaction dynamics underlying specific decay modes provides valuable tests of the QCD factorization framework. Being able to compute correctly a large number of decays, including "uninteresting" ones, increases our confidence in the reliability of the approach where it is necessary to extract fundamental parameters. An example of this concerns the role of so-called scalar penguin operators, which are an important contribution to the penguin amplitude in decays to pions and kaons, but which are expected to be suppressed for decays into vector mesons [15, 24]. Finally, our analysis provides up-to-date expectations for the branching fractions of decay modes yet to be discovered.

The outline of the paper is as follows: In the rather technical Section 2 we briefly review the QCD factorization approach and then collect the notation, definitions, and analytic formulae required to compute the complete set of $B \to PP$ and $B \to PV$ decay amplitudes at next-to-leading order. This includes a new notation for the parameterization of flavor amplitudes, which we find more convenient than the conventional notation in terms of parameters a_i. Sections 3 and 4 contain a summary of the input parameters entering our analysis and an outline of the adopted analysis strategy for the large set of final states. Also included in Section 4 is a discussion of the $B^- \to \pi^-\pi^0$ tree amplitude.

We then analyze separately penguin-dominated $\Delta S = 1$ and $\Delta D = 1$ decays, and tree-dominated $\Delta D = 1$ decays in Sections 5 and 6, respectively. We begin with an investigation of the magnitude of the penguin amplitude in $\Delta S = 1$ decays, which dominates the overall decay rate. The factorization approach makes distinct predictions for this amplitude depending on whether the final state is PP, PV, or VP. The comparison with existing data provides important information on the usefulness of next-to-leading order calculations in QCD factorization and simultaneously on the magnitude of penguin weak annihilation. We proceed to discuss ratios of branching fractions, and a few observations that we find difficult to accommodate in the Standard Model: we quantify the correction to the measurement of $\sin 2\beta$ in the final states ϕK_S and $\eta' K_S$, and we define a new ratio involving the $\pi^0 \bar{K}^0$ final state that may suggest an anomaly in the electroweak penguin sector. We also consider penguin-dominated $\Delta D = 1$ decays, which have small branching fractions, and discuss empirical constraints on the size of weak annihilation contributions.

Section 6 on tree-dominated decays focuses on the information that results from the measurement of $\pi\rho$ final states. In addition to CP-averaged branching fractions, direct CP asymmetries, and certain ratios of branching fractions, we consider the five asymmetries that can be defined in the time-dependent study of the final states $\pi^\mp\rho^\pm$. We find that the asymmetry S is well-suited to constrain γ. S together with the analogous quantity in $B \to \pi^+\pi^-$ decay imply $\gamma = 70^\circ$ with an error of about 10° at 1σ. In this analysis as in the rest of the paper we adopt the quasi two-body assumption, which considers the vector mesons as stable, neglecting interference effects related to the non-negligible widths of the decaying vector mesons.

In Section 7 we summarize the results for final states containing η or η', which complete those of [18], where an additional K or K^* in the final state was assumed. We briefly discuss the decays of B_s mesons in Section 8, and conclude in Section 9. In three appendices we collect: (i) the complete set of decay amplitudes expressed in terms of the amplitude parameters α_i (formerly a_i) and β_i, including weak annihilation; (ii) the convolutions of the new hard-scattering kernels with the distribution amplitudes of vector mesons up to the second Gegenbauer moment; and (iii) the results of the BaBar, Belle, and CLEO experiments, from which we computed the experimental averages used in the paper.

Guide to reading the paper

Since, in the course of time, this paper has grown to an undue volume, we have structured it such that most sections can be read independently of each other. Most of the material in Section 2 and Appendices A and B provides an up-to-date summary of the technical work necessary to implement QCD factorization at next-to-leading order. The reader familiar with the basic ideas of the theoretical framework may read only Section 2.1. The reader interested only in a specific phenomenological applications should consult Sections 3 and 4 (omitting perhaps Section 4.3) and the introduction to Section 5, where we specify the theoretical input, the general strategy of the analysis, and the definition of specific analysis scenarios. The analysis sections 4.3 (tree amplitude in $B \to \pi\pi$ decays), 5 (penguin-dominated decays), 6 (tree-dominated decays), 7 (final states with η or η'), and 8 (B_s decays) could then be read independently.

2 Two-body decay amplitudes

In this section we detail the theoretical framework within which our results for the decay amplitudes are computed. We begin with a brief summary of the QCD factorization method. We then introduce a new notation for the basic transition operator $\mathcal{T}$, which allows us to describe pseudoscalar and vector mesons in the final two-body state in terms of a single expression. The decay amplitude for $\bar{B} \to M_1 M_2$ is proportional to the matrix element $\langle M_1 M_2 | \mathcal{T} | \bar{B} \rangle$. The transition operator is decomposed into a complete basis of "flavor operators" accounting for the different topologies of the various decay mechanisms (tree, penguin, annihilation, etc.). After a summary of light-cone distribution amplitudes we collect the results for the coefficients of the different terms in the transition operator. This discussion is necessarily rather technical, as one of our goals is to provide a reference for the decay amplitudes and hard-scattering kernels in QCD factorization at next-to-leading order. Some readers may wish to read only Section 2.1 and then continue with Section 3.

2.1 The QCD factorization approach

A detailed discussion of the QCD factorization approach can be found in [8, 9, 10]. Here we recapitulate the basic formulae to set up the notation. The effective weak Hamiltonian for charmless hadronic B decays consists of a sum of local operators Q_i multiplied by short-distance coefficients C_i and products of elements of the quark mixing matrix, $\lambda_p^{(D)} = V_{pb} V_{pD}^*$, where $D = d, s$ can be a down or strange quark depending on the decay mode under consideration, and $p = u, c, t$. Using the unitarity relation $\lambda_u^{(D)} + \lambda_c^{(D)} + \lambda_t^{(D)} = 0$ we write

$$\mathcal{H}_{\rm eff} = \frac{G_F}{\sqrt{2}} \sum_{p=u,c} \lambda_p^{(D)} \left(C_1\, Q_1^p + C_2\, Q_2^p + \sum_{i=3}^{10} C_i\, Q_i + C_{7\gamma}\, Q_{7\gamma} + C_{8g}\, Q_{8g} \right) + \text{h.c.}\,, \tag{1}$$

where $Q_{1,2}^p$ are the left-handed current–current operators arising from W-boson exchange, $Q_{3,\dots,6}$ and $Q_{7,\dots,10}$ are QCD and electroweak penguin operators, and $Q_{7\gamma}$ and Q_{8g} are the electromagnetic and chromomagnetic dipole operators as given in [10]. The effective Hamiltonian describes the quark transitions $b \to u\bar{u}D$, $b \to c\bar{c}D$, $b \to D\bar{q}q$ with $q = u, d, s, c, b$, and $b \to Dg$, $b \to D\gamma$, as appropriate for decay modes with interference of "tree" and "penguin" contributions. The Wilson coefficients are evaluated at next-to-leading order, consistent with the calculation of operator matrix elements described below. For the coefficients of electroweak penguin operators the evaluation described in [10], which incorporates some terms normally counted as next-to-next-to-leading order, is employed.

The QCD factorization formalism allows us to compute systematically the matrix elements of the effective weak Hamiltonian in the heavy-quark limit for certain two-body final states $M_1' M_2'$. In condensed notation, the matrix element of every operator in the effective Hamiltonian is evaluated as

$$\begin{aligned} \langle M_1' M_2' | Q_i | \bar{B} \rangle = & \sum_{\{M_1, M_2\} \in \{M_1', M_2'\}} F_j^{B\to M_1}\, T_{ij}^I * f_{M_2} \Phi_{M_2} \\ & + T_i^{II} * f_B \Phi_B * f_{M_1'} \Phi_{M_1'} * f_{M_2'} \Phi_{M_2'}\,, \end{aligned} \tag{2}$$

where $F_j^{B\to M_1}$ is an appropriate form factor, Φ_M are leading-twist light-cone distribution amplitudes, and the star products imply an integration over the light-cone momentum fractions of the constituent quarks inside the mesons. A graphical representation of this result is shown in Figure 1. Whenever the spectator antiquark line goes from the $\bar{B}$ meson to one of the final-state mesons we call this meson M_1 and the other one M_2. The sum in the first term on the right-hand side of (2) accounts for the possibility that for particular final states the spectator antiquark can end up in either one of the two mesons. If the spectator antiquark is annihilated we use the convention that M_1 is the meson that carries away the antiquark from the weak decay vertex.

A justification of the factorization formula for final states in which M_1 is a heavy meson (applicable to D mesons in the heavy-quark limit) can be found in [9, 25]. In this case the term in the second line of (2) is absent. For final states with two light mesons factorization has been proved at order α_s [8], but a complete proof has not yet been given (for recent developments in this direction, see [26]). The factorization formula reduces the complicated hadronic matrix elements of four-quark operators to simpler non-perturbative quantities and calculable hard-scattering kernels T_{ij}^I and T_i^{II}. In this paper we complete the calculation of all relevant kernels at next-to-leading order in α_s.

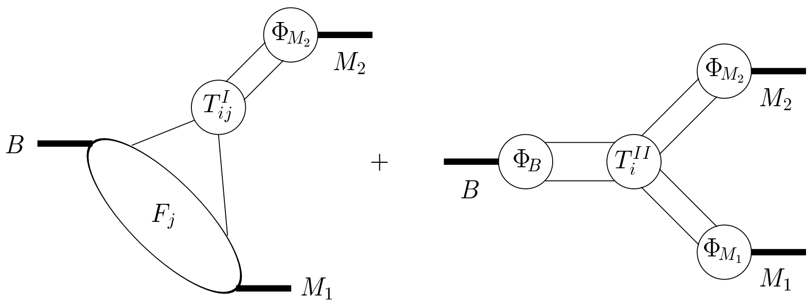

Figure 1: Graphical representation of the factorization formula (2). Only one of the two form-factor terms is shown for simplicity.

The light-cone expansion implies that only leading-twist distribution amplitudes are needed in the heavy-quark limit. There exist however a number of subleading quark–antiquark distribution amplitudes of twist 3, which have large normalization factors for pseudoscalar mesons, e.g. for the pion

$$r_\chi^\pi(\mu) = \frac{2m_\pi^2}{m_b(\mu)\,(m_u+m_d)(\mu)} \sim \frac{\Lambda_{\rm QCD}}{m_b}\,. \tag{3}$$

For realistic b-quark masses these "chirally-enhanced" terms are not much suppressed numerically. We therefore include in our analysis all quark–antiquark twist-3 amplitudes. (The quark–antiquark–gluon amplitude at twist-3 does not have an anomalously large normalization.) In order to perform the same analysis for all final states we also include the quark–antiquark twist-3 amplitudes for vector mesons, even though there is no particular enhancement in this case, r_χ being replaced by $2m_V/m_b$ times a ratio of two decay constants (see below), with m_V the vector-meson mass.

The inclusion of chirally-enhanced terms is important to account for the large branching fractions of penguin-dominated decay modes with pseudoscalar final-state mesons, such as $B\to\pi K$ [10], but it also causes a number of conceptual problems. Factorization is not expected to hold at subleading order in $\Lambda_{\rm QCD}/m_b$ and, somewhat unfortunately, is indeed violated by some of the chirally-enhanced terms [8]. In contrast to the leading-twist distribution amplitudes, the twist-3 two-particle amplitudes do not vanish at the endpoints but rather approach constants. The kernels T^I_{ij} in the first term of the factorization formula also approach constants at the endpoints (modulo logarithms), and hence there is no difficulty with this term. These kernels include the important scalar penguin amplitude mentioned in the introduction, conventionally denoted by a_6. However, the second term in the factorization formula, which accounts for the interactions with the spectator quark, contains integrals that are dominated by the endpoint regions if the distribution amplitudes do not vanish at the endpoint. These integrals formally diverge logarithmically in a perturbative framework. This implies a non-factorizable soft interaction with the spectator quark, while M_1 is formed in a highly asymmetric configuration, in which one quark carries almost all the momentum of the meson. Similar factorization-breaking effects occur in weak annihilation contributions, which are also suppressed by at least one power of $\Lambda_{\rm QCD}/m_b$ in the heavy-quark expansion.

In [10] we have parameterized the power corrections from chirally-enhanced and weak annihilation terms in an *ad hoc* way and included a variation of the corresponding parameters in our error estimate. Based on the analysis of $\pi\pi$ and πK final states we concluded that these factorization-breaking terms introduce a sometimes substantial uncertainty into the theory but do not render the framework unpredictive. In particular, the data so far give no indication that these corrections should be outside the range specified by our error estimate. Given this situation, we follow our previous analysis strategy as regards twist-3 and annihilation effects. The inclusion of twist-3 effects for vector mesons then allows us to estimate the impact of some power-suppressed effects, which turn out to be small. But we should stress that this is far from a complete account of such contributions. We also note that some other classes of power corrections have been analyzed using the method of light-cone QCD sum rules [27, 28].

The pseudoscalar mesons η and η', which contain a flavor-singlet component in their wave function, require special attention, because they can be formed from two gluons at leading twist. The new effects associated with this possibility have been worked out in the context of QCD factorization in [18]. For these mesons the factorization formula (2) holds provided it is extended by an additional non-local form-factor term. At the order we are working the corresponding complications do not appear for vector mesons, since they do not have a two-gluon component. There is, however, one novel effect for neutral vector mesons, namely that they can be produced via a virtual photon. Although this effect is very small, we shall discuss it, because it is of the same order as other electroweak contributions to the decay amplitudes.

2.2 Flavor operators

In the literature on QCD factorization the result of computing the hard-scattering kernels for the various operators in the effective weak Hamiltonian is usually presented in terms of "factorized operators" with coefficients $a_i(M_1 M_2)$. (The matrix element of a factorized operator is simply proportional to a form factor times a decay constant.) The reasons for this are largely historical. Besides containing some redundancy, such a notation leads to inconveniences for vector mesons since the factorized operator $\sum_q (\bar{q}b)_{S-P} \otimes (\bar{D}q)_{S+P}$ vanishes, while there exist non-vanishing terms at order α_s that one would naturally associate with the corresponding coefficient a_6. Here we introduce a new notation that eliminates these inconveniences, and which at the same time is sufficiently general and explicit to facilitate the construction of the decay amplitude for any particular decay with either pseudoscalar or vector mesons in the final state. The main point of the new notation is to keep track of only the flavor structure of an operator. Its Dirac structure, which distinguishes some of the $a_i(M_1 M_2)$ coefficients in the conventional notation, becomes irrelevant, since operators with different Dirac structure (but identical flavor structure) always contribute in the same combination to a particular final state.

We first introduce our phase convention for the flavor wave functions. We take the light quark triplet as (u, d, s) and the antitriplet as $(\bar{u}, \bar{d}, \bar{s})$. Consequently,

$$B^- \sim \bar{u}b\,, \qquad \bar{B}_d \sim \bar{d}b\,, \qquad \bar{B}_s \sim \bar{s}b\,. \tag{4}$$

Assuming isospin symmetry, the non-singlet members of the light nonet of pseudoscalar mesons are given by

$$\begin{aligned} \pi^0 &\sim \frac{1}{\sqrt{2}}\,(\bar{u}u - \bar{d}d), \qquad \pi^- \sim \bar{u}d\,, \qquad \pi^+ \sim \bar{d}u\,, \\ \bar{K}^0 &\sim \bar{d}s\,, \qquad K^0 \sim \bar{s}d\,, \qquad K^- \sim \bar{u}s\,, \qquad K^+ \sim \bar{s}u\,, \end{aligned} \tag{5}$$

and analogous expressions hold for the corresponding vector mesons. The treatment of mesons containing a flavor-singlet component in their wave function has been explained in detail in the dedicated paper [18], to which we refer the reader for all details. The mesons η and η' (and similarly the vector mesons ω and ϕ) can be treated as coherent superpositions of the flavor components, e.g.

$$\eta_q \sim \frac{1}{\sqrt{2}}\,(\bar{u}u + \bar{d}d)\,, \qquad \eta_s \sim \bar{s}s\,, \tag{6}$$

and similarly for η', ω, and ϕ. This should not be confused with the representation of the meson state as a superposition of flavor states, but simply means that these mesons have matrix elements of $\bar{s}s$ and $\bar{u}u$ (or $\bar{d}d$, these two being equal due to the assumed isospin symmetry) operators that are a priori unrelated. Consequently, each meson is described by two decay constants; for instance, for the η meson

$$\langle \eta(q)|\bar{u}\gamma_\mu\gamma_5 u|0\rangle = -\frac{i}{\sqrt{2}}\,f_\eta^q q_\mu, \qquad \langle \eta(q)|\bar{s}\gamma_\mu\gamma_5 s|0\rangle = -i f_\eta^s q_\mu. \tag{7}$$

Similarly, there are two transition form factors, two leading-twist quark–antiquark distribution amplitudes etc., corresponding to the two distinct flavor components. In addition, for the pseudoscalar case there exist contributions proportional to the two-gluon content of η and η'. Finally, certain contributions to the $b \to Dgg$ amplitude are conveniently interpreted in terms of a $\bar{c}c$ flavor component η_c for η and η'. The QCD factorization approach presented here is sufficiently general to allow for a discussion of states containing flavor-singlet contributions without assumption of a particular flavor-mixing scheme. However, in our phenomenological analysis we will adopt the Feldmann–Kroll–Stech scheme for η and η' mixing, in which it is sufficient to introduce a single mixing angle in the flavor basis [29]. The corresponding expressions for the hadronic matrix elements (decay constants, form factors, etc.) needed in the calculations of the decay amplitudes can be found in [18]. For the vector mesons ω and ϕ we will assume ideal mixing, so that $\omega = \omega_q \sim (\bar{u}u + \bar{d}d)/\sqrt{2}$ and $\phi = \phi_s \sim \bar{s}s$.

We match the effective weak Hamiltonian onto a transition operator such that its matrix element is given by

$$\langle M_1' M_2'|\mathcal{H}_{\text{eff}}|\bar{B}\rangle = \sum_{p=u,c} \lambda_p^{(D)}\,\langle M_1' M_2'|\mathcal{T}_A^p + \mathcal{T}_B^p|\bar{B}\rangle\,. \tag{8}$$

The two terms account for the flavor topologies of the form-factor and hard-scattering terms in (2), respectively, corresponding to the two diagrams of Figure 1. Each term in the transition operator contains several operators labeled only by the flavor composition of the four-quark final state. Note that below we will include in the definition of $\mathcal{T}_B^p$ also some power-suppressed terms, such as weak annihilation contributions.

Including electroweak penguin topologies there are six different flavor structures one can write down for the left diagram of Figure 1. We define (with $D = d$ or s)

$$\begin{aligned}\mathcal{T}_A^p &= \delta_{pu}\,\alpha_1(M_1M_2)\,A([\bar q_s u][\bar u D]) + \delta_{pu}\,\alpha_2(M_1M_2)\,A([\bar q_s D][\bar u u]) \\ &\quad + \alpha_3^p(M_1M_2)\sum_q A([\bar q_s D][\bar q q]) + \alpha_4^p(M_1M_2)\sum_q A([\bar q_s q][\bar q D]) \\ &\quad + \alpha_{3,\mathrm{EW}}^p(M_1M_2)\sum_q \frac{3}{2}\,e_q\,A([\bar q_s D][\bar q q]) + \alpha_{4,\mathrm{EW}}^p(M_1M_2)\sum_q \frac{3}{2}\,e_q\,A([\bar q_s q][\bar q D])\,, \end{aligned} \tag{9}$$

where the sums extend over $q = u, d, s$, and $\bar q_s$ denotes the spectator antiquark. The operators $A([\bar q_{M_1} q_{M_1}][\bar q_{M_2} q_{M_2}])$ also contain an implicit sum over $q_s = u, d, s$ to cover all possible B-meson initial states. The coefficients $\alpha_i^p(M_1M_2)$ contain all dynamical information, while the arguments of A encode the flavor composition of the final state and hence determine the final state to which a given term can contribute. We define

$$\langle M_1' M_2' | \alpha_i^p(M_1M_2)\,A([\ldots][\ldots]) | \bar B_{q_s}\rangle \equiv c\,\alpha_i^p(M_1'M_2')\,A_{M_1'M_2'} \tag{10}$$

whenever the quark flavors of the first (second) square bracket match those of M_1' (M_2'). The constant c is a product of three factors of 1, $\pm 1/\sqrt{2}$ etc. from the flavor composition of the $\bar B$ meson and $M_{1,2}$ as specified above. The quantity $A_{M_1M_2}$ is given by

$$A_{M_1M_2} = i\,\frac{G_F}{\sqrt{2}}\begin{cases} m_B^2 F_0^{B\to M_1}(0) f_{M_2}\,; & \text{if } M_1 = M_2 = P, \\ -2m_V\,\epsilon_{M_1}^*\cdot p_B\,A_0^{B\to M_1}(0) f_{M_2}\,; & \text{if } M_1 = V,\ M_2 = P, \\ -2m_V\,\epsilon_{M_2}^*\cdot p_B\,F_+^{B\to M_1}(0) f_{M_2}\,; & \text{if } M_1 = P,\ M_2 = V. \end{cases} \tag{11}$$

Here $F_{+,0}$ and A_0 denote pseudoscalar (P) and vector (V) meson form factors in the standard convention (see, e.g., [3]). The decay constants f_{M_2} are normalized according to

$$\langle \pi^-(q)|\bar d\gamma_\mu\gamma_5 u|0\rangle = -if_\pi q_\mu\,, \qquad \langle \rho^-(q)|\bar d\gamma_\mu u|0\rangle = -if_\rho m_\rho \epsilon_\mu^*\,. \tag{12}$$

For a vector meson, $f_V \equiv f_V^{||}$ always refers to the decay constant of a longitudinally polarized meson. We neglect corrections to the decay amplitudes quadratic in the light meson masses, so that all form factors are evaluated at $q^2 = 0$. (At this kinematic point, the form factors F_+ and F_0 coincide.) Parameters referring to the B meson depend on whether the decaying meson is B_s or $B_{u,d}$. This will be implicitly understood in the following. The above expression can be simplified by replacing $2m_V\,\epsilon^*\cdot p_B \to m_B^2$, since the left-hand side squared and summed over the polarizations of the vector meson gives m_B^4 (neglecting again quadratic meson-mass corrections). As expected by angular momentum conservation the final-state vector meson is longitudinally polarized. When the replacement above is done the polarization sum for vector mesons must be omitted, and the decay rate is simply given by

$$\Gamma = \frac{S}{16\pi m_B}\,\left|\langle M_1' M_2' |\mathcal{H}_{\rm eff}|\bar B\rangle\right|^2 , \tag{13}$$

where $S = 1/2$ if M_1' and M_2' are identical, and $S = 1$ otherwise.

We do not discuss in this paper final states containing two vector mesons. The extension to this case is straightforward, since the leading amplitude in the heavy-quark limit is the one for two longitudinally polarized vector mesons, which in many ways behave like pseudoscalar mesons.

In order to exemplify the notation consider the decay $\bar B_d \to \pi^0\rho^0$, for which $q_s = d$ and $D = d$. The spectator quark can go to either one of the two mesons, so M_1 can be π^0 or ρ^0. Hence, e.g.

$$\langle\pi^0\rho^0|\alpha_4^p(M_1 M_2)\sum_q A([\bar d q][\bar q d])|\bar B_d\rangle = -\frac12\left[\alpha_4^p(\pi^0\rho^0)\,A_{\pi^0\rho^0} + \alpha_4^p(\rho^0\pi^0)\,A_{\rho^0\pi^0}\right] . \tag{14}$$

The order of the arguments of α_4^p is relevant as will be seen from the explicit expressions given in Section 2.4 below. The factor $c = 1/2$ arises from the flavor wave functions of the mesons. On the other hand,

$$\langle\pi^0\rho^0|\alpha_3^p(M_1 M_2)\sum_q A([\bar d d][\bar q q])|\bar B_d\rangle = 0 , \tag{15}$$

since $q = u, d$ contribute equally but with opposite sign for the mesons π^0 and ρ^0.

We now discuss the flavor structure of the hard-scattering term in (2), i.e., the second diagram in Figure 1. Since all six quarks participate in the hard scattering, the generic flavor operator in $\mathcal{T}_B^p$ is of the form $B([\bar q_{M_1} q_{M_1}][\bar q_{M_2} q_{M_2}][\bar q_s b])$ with possible sums over quarks from penguin transitions or flavor-singlet conversion $g \to \bar q q$. We define the matrix element of a B-operator as

$$\langle M_1 M_2|B([\ldots][\ldots]][\ldots])|\bar B_q\rangle \equiv c\, B_{M_1 M_2} , \quad \text{with} \quad B_{M_1 M_2} = \pm i\,\frac{G_F}{\sqrt2}\,f_{B_q} f_{M_1} f_{M_2} , \tag{16}$$

whenever the quark flavors of the three brackets match those of M_1, M_2, and $\bar B_q$. The constant c is the same as in (10). The upper sign in the definition of $B_{M_1 M_2}$ applies when both mesons are pseudoscalar, and the lower when one of the mesons is a vector meson. This matches the sign conventions for the quantities $A_{M_1 M_2}$ in (11). The most important case of spectator scattering is when the spectator-quark line goes from the B meson to a final-state meson, which we then call M_1. These are the hard spectator interactions, which are the only terms of leading power in the heavy-quark limit. (We refer to all other contributions to $\mathcal{T}_B^p$ as annihilation.) This special case implies $\bar q_s = \bar q_{M_1}$, leaving six different amplitudes that are in one-to-one correspondence with the six A-operators defined above, because

$$B([\bar{q}_s q_{M_1}][\bar{q}_{M_2} q_{M_2}][\bar{q}_s b]) = \frac{B_{M_1 M_2}}{A_{M_1 M_2}}\, A([\bar{q}_s q_{M_1}][\bar{q}_{M_2} q_{M_2}])\,. \tag{17}$$

We therefore absorb the spectator scattering contributions into the definition of the coefficients $\alpha_i^p(M_1 M_2)$.

With parts of $\mathcal{T}_B^p$ absorbed into $\mathcal{T}_A^p$, the transition operator $\mathcal{T}_A^p$ now contains all scattering mechanisms except weak annihilation. In particular, it contains all contributions of leading power in the heavy-quark limit. The remaining, power-suppressed annihilation part of $\mathcal{T}_B^p$ is parameterized in its most general form as

$$\begin{aligned}
\mathcal{T}_B^p = {} & \delta_{pu}\, b_1(M_1 M_2) \sum_{q'} B([\bar{u}q'][\bar{q}'u][\bar{D}b]) + \delta_{pu}\, b_2(M_1 M_2) \sum_{q'} B([\bar{u}q'][\bar{q}'D][\bar{u}b]) \\
& + b_3^p(M_1 M_2) \sum_{q,q'} B([\bar{q}q'][\bar{q}'D][\bar{q}b]) + b_4^p(M_1 M_2) \sum_{q,q'} B([\bar{q}q'][\bar{q}'q][\bar{D}b]) \\
& + b_{3,\mathrm{EW}}^p(M_1 M_2) \sum_{q,q'} \frac{3}{2}\, e_q\, B([\bar{q}q'][\bar{q}'D][\bar{q}b]) + b_{4,\mathrm{EW}}^p(M_1 M_2) \sum_{q,q'} \frac{3}{2}\, e_q\, B([\bar{q}q'][\bar{q}'q][\bar{D}b]) \\
& + \delta_{pu}\, b_{S1}(M_1 M_2) \sum_{q'} B([\bar{u}u][\bar{q}'q'][\bar{D}b]) + \delta_{pu}\, b_{S2}(M_1 M_2) \sum_{q'} B([\bar{u}D][\bar{q}'q'][\bar{u}b]) \\
& + b_{S3}^p(M_1 M_2) \sum_{q,q'} B([\bar{q}D][\bar{q}'q'][\bar{q}b]) + b_{S4}^p(M_1 M_2) \sum_{q,q'} B([\bar{q}q][\bar{q}'q'][\bar{D}b]) \\
& + b_{S3,\mathrm{EW}}^p(M_1 M_2) \sum_{q,q'} \frac{3}{2}\, e_q\, B([\bar{q}D][\bar{q}'q'][\bar{q}b]) + b_{S4,\mathrm{EW}}^p(M_1 M_2) \sum_{q,q'} \frac{3}{2}\, e_q\, B([\bar{q}q][\bar{q}'q'][\bar{D}b])\,,
\end{aligned} \tag{18}$$

where the sums extend over $q, q' = u, d, s$. The sum over q' arises because a quark–antiquark pair must be created by $g \to \bar{q}'q'$ after the spectator quark is annihilated. The definitions of the first six coefficients coincide with the corresponding definitions in [10] for $\pi\pi$ and πK final states. Note that the operator $\sum_{q,q'} B([\bar{q}q'][\bar{q}'D][\bar{q}b])$ is redundant, because it is equivalent to $\sum_q A([\bar{q}_s q][\bar{q}D])$ (which includes an implicit sum over q_s). We allow this redundancy to keep the parameterization of annihilation effects separate from the others. The six new coefficients with subscript 'S' contribute only to final states containing flavor-singlet mesons or neutral vector mesons and were not needed in our previous analysis. It will be convenient to use the notation

$$\beta_i^p(M_1 M_2) \equiv \frac{B_{M_1 M_2}}{A_{M_1 M_2}}\, b_i^p(M_1 M_2) \tag{19}$$

whenever $A_{M_1 M_2}$ does not vanish. However, for some pure annihilation decays such as $\bar{B}_s \to \pi^+\pi^-$, where β_i^p is not defined since $F_0^{B_s\to\pi}(0) = 0$, we express the decay amplitude in terms of the coefficients b_i^p. The redundancy mentioned above implies that $\alpha_4^p(M_1 M_2)$ and $\beta_3^p(M_1 M_2)$ always appear in the combination

$$\hat{\alpha}_4^p(M_1 M_2) \equiv \alpha_4^p(M_1 M_2) + \beta_3^p(M_1 M_2)\,. \tag{20}$$

It is now straightforward to express the $\bar{B}_q \to M_1' M_2'$ decay amplitude in terms of linear combinations of the coefficients α_i^p and β_i^p. The results are collected in Appendix A, where we also give a convenient master formula suitable for implementation in a computer program, which generates the entire set of 96 decay amplitudes by evaluating a single expression. It remains to express the flavor coefficients in terms of the hard-scattering kernels of the QCD factorization approach.

2.3 Distribution amplitudes

We now summarize the definitions of the light-cone distribution amplitudes for light pseudoscalar and vector mesons. The corresponding amplitudes for B mesons have been discussed in [30, 31]. While our treatment of the leading-twist distributions is completely general, at the level of twist-3 power corrections we work in the approximation of neglecting the $q\bar{q}g$ Fock state of the meson. The motivation for this approximation is that it retains all effects with large (chirally-enhanced) normalization factors but neglects "ordinary" power corrections of order $\Lambda_{\rm QCD}/m_b$. The following discussion relies on the analysis of distribution amplitudes in coordinate space presented in [32, 33], while the momentum-space projectors are taken from [31]. A more detailed discussion of the pseudoscalar case can be found in [10, 34].

We recall that in general the collinear approximation for the parton momenta can be taken only after the light-cone projection has been applied. We therefore assign momenta

$$k_1^\mu = x p^\mu + k_\perp^\mu + \frac{\vec{k}_\perp^2}{2x\,p\cdot\bar{p}}\,\bar{p}^\mu\,, \qquad k_2^\mu = \bar{x} p^\mu - k_\perp^\mu + \frac{\vec{k}_\perp^2}{2\bar{x}\,p\cdot\bar{p}}\,\bar{p}^\mu \tag{21}$$

to the quark and antiquark in a light meson with momentum p, where $\bar{p}$ is a light-like vector whose 3-components point into the opposite direction of $\vec{p}$, and $\bar{x} \equiv 1 - x$. The light-cone projection operator of a light pseudoscalar meson in momentum space, including twist-3 two-particle contributions, then reads

$$M_{\alpha\beta}^P = \frac{if_P}{4}\left\{ \not{p}\,\gamma_5\,\Phi_P(x) - \mu_P\gamma_5\left(\Phi_p(x) - i\sigma_{\mu\nu}\,\frac{p^\mu\,\bar{p}^\nu}{p\cdot\bar{p}}\,\frac{\Phi_\sigma'(x)}{6} + i\sigma_{\mu\nu}\,p^\mu\,\frac{\Phi_\sigma(x)}{6}\,\frac{\partial}{\partial k_{\perp\nu}} \right) \right\}_{\alpha\beta}, \tag{22}$$

where μ_P is defined as $m_b\,r_\chi^P/2$ with r_χ^P defined as in (3). The convention for the projection is that one computes ${\rm tr}\,(M^P A)$ if $\bar{u}Av$ is the scattering amplitude with an on-shell quark and antiquark. The derivative acts on the scattering amplitude A, and it is understood that, after the derivative is taken, the momenta k_1 and k_2 are set equal to xp and $\bar{x}p$, respectively. The overall sign of (22) corresponds to defining the projector (in coordinate space) through the matrix element $\langle P(p)|\bar{q}_\beta(z)q_\alpha(0)|0\rangle$ rather than the opposite ordering of the quark fields. (For simplicity, we suppress the gauge string connecting the two fermion fields.) The meson η (and similarly η', ω, and ϕ) is described by two quark–antiquark distribution amplitudes corresponding to the two independent flavor components η_q and η_s in (6).

The leading-twist distribution amplitude is conventionally expanded in Gegenbauer polynomials,

$$\Phi_P(x,\mu) = 6x(1-x)\left[1+\sum_{n=1}^{\infty}\alpha_n^P(\mu)\,C_n^{(3/2)}(2x-1)\right], \tag{23}$$

since the Gegenbauer moments $\alpha_n^P(\mu)$ are multiplicatively renormalized. When three-particle contributions are neglected, the twist-3 two-particle distribution amplitudes are determined completely by the equations of motion, which then require

$$\Phi_p(x) = 1\,, \qquad \frac{\Phi'_\sigma(x)}{6} = \bar{x}-x\,, \qquad \frac{\Phi_\sigma(x)}{6} = x\bar{x}\,. \tag{24}$$

It is not difficult to derive from this the simpler projector [35]

$$M^P_{\alpha\beta} = \frac{if_P}{4}\left(\not{p}\,\gamma_5\,\Phi_P(x) - \mu_P\gamma_5\,\frac{\not{k}_2\,\not{k}_1}{k_2\cdot k_1}\,\Phi_p(x)\right)_{\alpha\beta}. \tag{25}$$

The η and η' mesons also have a two-particle two-gluon distribution amplitude at leading twist, for which we adopt the convention given in [18].

The corresponding equations for vector mesons are very similar. In general, the light-cone projection operator in momentum space contains two terms, $M^V = M^V_\parallel + M^V_\perp$. However, the transverse projector does not contribute to the $B\to PV$ decay amplitudes at leading and first subleading power in $\Lambda_{\rm QCD}/m_b$. The longitudinal projector is given by

$$\begin{aligned}\left(M^V_\parallel\right)_{\alpha\beta} = -\frac{if_V}{4}\Bigg\{&\not{p}\,\Phi_V(x) + \frac{m_V f_V^\perp}{f_V}\Bigg(\frac{h_\parallel'^{(s)}(x)}{2} - i\sigma_{\mu\nu}\,\frac{p^\mu\,\bar{p}^\nu}{p\cdot\bar{p}}\,h_\parallel^{(t)}(x)\\ &+ i\sigma_{\mu\nu}\,p^\mu\int_0^x dv\left[h_\parallel^{(t)}(v)-\Phi_\perp(v)\right]\frac{\partial}{\partial k_{\perp\nu}}\Bigg)\Bigg\}_{\alpha\beta}.\end{aligned} \tag{26}$$

The polarization vector has been replaced by $\epsilon^*_\mu \to p_\mu/m_V$, which is correct up to corrections quadratic in the meson mass. After this replacement no polarization sum must be taken after squaring the decay amplitude. The leading-twist distribution amplitude $\Phi_V(x)$ is expanded in Gegenbauer polynomials exactly as in (23), but with Gegenbauer moments $\alpha_n^V(\mu)$. When three-particle amplitudes are neglected, the twist-3 amplitudes that appear in (26) can all be expressed in terms of the leading-twist amplitude $\Phi_\perp(x)$ of a *transversely* polarized vector meson [33]. We define

$$\Phi_v(x) \equiv \int_0^x dv\,\frac{\Phi_\perp(v)}{\bar{v}} - \int_x^1 dv\,\frac{\Phi_\perp(v)}{v} = 3\sum_{n=0}^{\infty}\alpha_{n,\perp}^V(\mu)\,P_{n+1}(2x-1)\,, \tag{27}$$

where $\alpha_{0,\perp}^V = 1$, and $P_n(x)$ are the Legendre polynomials. The second equation is obtained by inserting the Gegenbauer expansion of $\Phi_\perp(x)$. The equations of motion then lead to the Wandzura–Wilczek relations [33]

$$\frac{h_{\parallel}'^{(s)}(x)}{2} = -\Phi_v(x)\,, \qquad h_{\parallel}^{(t)}(x) = -(\bar{x}-x)\,\Phi_v(x)\,,$$
$$\int_0^x dv\,\left[h_{\parallel}^{(t)}(v) - \Phi_\perp(v)\right] = -x\bar{x}\,\Phi_v(x)\,, \tag{28}$$

which allow us to express the twist-3 two-particle projection in terms of the single function $\Phi_v(x)$. Comparing the vector meson projection in (26) with the pseudoscalar projection in (22) we see that the function $\Phi_v(x)$ is analogous to $\Phi_p(x)$. In analogy with the pseudoscalar case we obtain the simpler projector

$$\left(M_{\parallel}^V\right)_{\alpha\beta} = -\frac{if_V}{4}\left(\not{p}\,\Phi_V(x) - \frac{m_V f_V^\perp}{f_V}\,\frac{\not{k}_2\,\not{k}_1}{k_2\cdot k_1}\,\Phi_v(x)\right)_{\alpha\beta}, \tag{29}$$

valid in the approximation where one neglects three-particle contributions. Like $\Phi_p(x)$, the function $\Phi_v(x)$ does not vanish at the endpoints $x = 0, 1$. We note, however, the vanishing of the integral

$$\int_0^1 dx\,\Phi_v(x) = 0\,. \tag{30}$$

With these remarks, we can obtain the hard-scattering kernels for vector mesons in the final state from those for two pseudoscalars given in [10] by performing the replacements $\Phi_P(x) \to \Phi_V(x)$, $\Phi_p(x) \to \Phi_v(x)$, $f_P \to f_V$, and by interpreting r_χ as in (32), (33) below. However, one must pay attention to certain sign changes arising from the absence of γ_5 in the vector-meson projector (29) and in the matrix elements that define vector-meson form factors. This leads to the sign alternations in the definitions of α_3^p, α_4^p, $\alpha_{3,\mathrm{EW}}^p$, and $\alpha_{4,\mathrm{EW}}^p$ in (31) below, and to sign alternations in the weak annihilation terms to be discussed later.

2.4 Coefficients of the decay operators in QCD factorization

In the following we give the expressions for the coefficients of the decay operator up to the next-to-leading order. First, some comments on the treatment of electromagnetic corrections and electroweak penguin effects, and on the treatment of weak annihilation, are in order.

Electroweak penguin effects and electromagnetic corrections

1) We neglect electromagnetic corrections to the QCD coefficients α_1, α_2, α_3^p, and α_4^p, since these are much smaller than the next-to-leading order QCD corrections. We also neglect corrections of order $\alpha_s C_{7-10}$ to these coefficients, since the Wilson coefficients C_{7-10} are proportional to the electromagnetic coupling α.

2) In leading order the electroweak penguin coefficients $\alpha^p_{3,\rm EW}$ and $\alpha^p_{4,\rm EW}$ involve only the Wilson coefficients C_{7-10}. We include the QCD corrections of order $\alpha_s C_{7-10}$ to $\alpha^p_{3,\rm EW}$ and $\alpha^p_{4,\rm EW}$.

3) We include electromagnetic corrections to $\alpha^p_{3,\rm EW}$ and $\alpha^p_{4,\rm EW}$ only when they are proportional to the large Wilson coefficients $C_{1,2,7\gamma}$, i.e., we include the corrections of order $\alpha\, C_{1,2,7\gamma}$, but neglect those proportional to $\alpha\, C_{3-10}$.

Weak annihilation

1) We neglect weak annihilation mechanisms involving photons ($\gamma \to \bar{q}'q'$), which in fact would introduce more operators in (18), i.e., we drop annihilation terms of order $\alpha\, C_i$, but keep terms of order $\alpha_s\, C_i$. The reason for this is that the former can never be CKM-enhanced when one of the large Wilson coefficients $C_{1,2}$ is involved.

2) We use an approximation where all singlet annihilation coefficients are set to zero except for β_{S3}, see below and [18].

In the following we first give the generic results for the α_i and β_i coefficients applicable to all final states, and then discuss contributions specific to particular pseudoscalar or vector mesons.

A-operators (generic results)

The coefficients of the flavor operators α^p_i can be expressed in terms of the coefficients a^p_i defined in [8, 10] as follows:[1]

$$
\begin{aligned}
\alpha_1(M_1M_2) &= a_1(M_1M_2)\,,\\
\alpha_2(M_1M_2) &= a_2(M_1M_2)\,,\\
\alpha_3^p(M_1M_2) &= \begin{cases} a_3^p(M_1M_2) - a_5^p(M_1M_2)\,; & \text{if } M_1M_2 = PP,\, VP\,,\\ a_3^p(M_1M_2) + a_5^p(M_1M_2)\,; & \text{if } M_1M_2 = PV\,,\end{cases}\\
\alpha_4^p(M_1M_2) &= \begin{cases} a_4^p(M_1M_2) + r_\chi^{M_2}\, a_6^p(M_1M_2)\,; & \text{if } M_1M_2 = PP,\, PV\,,\\ a_4^p(M_1M_2) - r_\chi^{M_2}\, a_6^p(M_1M_2)\,; & \text{if } M_1M_2 = VP\,,\end{cases}\\
\alpha_{3,\rm EW}^p(M_1M_2) &= \begin{cases} a_9^p(M_1M_2) - a_7^p(M_1M_2)\,; & \text{if } M_1M_2 = PP,\, VP\,,\\ a_9^p(M_1M_2) + a_7^p(M_1M_2)\,; & \text{if } M_1M_2 = PV\,,\end{cases}\\
\alpha_{4,\rm EW}^p(M_1M_2) &= \begin{cases} a_{10}^p(M_1M_2) + r_\chi^{M_2}\, a_8^p(M_1M_2)\,; & \text{if } M_1M_2 = PP,\, PV\,,\\ a_{10}^p(M_1M_2) - r_\chi^{M_2}\, a_8^p(M_1M_2)\,; & \text{if } M_1M_2 = VP\,.\end{cases}
\end{aligned}
\tag{31}
$$

[1]The numerical values of the coefficients $\alpha_i(M_1M_2)$ also depend on the nature of the initial-state B meson. This dependence is not indicated explicitly by our notation. The same remark applies to the annihilation coefficients b^p_i defined below.

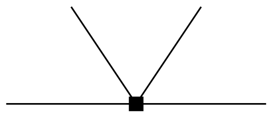

Figure 2: Leading-order contribution to the coefficients a_i^p. The weak decay of the b quark through a four-fermion operator is represented by the black square. The b-quark line comes in from the left. The outgoing line to the right represents the quark in M_1. The two lines directed upward represent the meson M_2. The spectator antiquark is not drawn, because it does not participate in the hard scattering.

Note that the order of the arguments in $\alpha_i^p(M_1M_2)$ and $a_i^p(M_1M_2)$ is relevant. For pions and kaons, the ratios $r_\chi^{M_2}$ are defined as

$$r_\chi^\pi(\mu) = \frac{2m_\pi^2}{m_b(\mu)\,2m_q(\mu)}\,, \qquad r_\chi^K(\mu) = \frac{2m_K^2}{m_b(\mu)\,(m_q+m_s)(\mu)}\,, \tag{32}$$

while their generalizations to η and η' can be found in [18]. All quark masses are running masses defined in the $\overline{\rm MS}$ scheme, and m_q denotes the average of the up and down quark masses. For vector mesons we have

$$r_\chi^V(\mu) = \frac{2m_V}{m_b(\mu)}\,\frac{f_V^\perp(\mu)}{f_V}\,, \tag{33}$$

where the scale-dependent transverse decay constant is defined as

$$\langle V(p,\varepsilon^*)|\bar q\sigma_{\mu\nu}q'|0\rangle = f_V^\perp(p_\mu\varepsilon_\nu^* - p_\nu\varepsilon_\mu^*)\,. \tag{34}$$

Note that all the terms proportional to $r_\chi^{M_2}$ are formally suppressed by one power of $\Lambda_{\rm QCD}/m_b$ in the heavy-quark limit. Numerically, however, these terms are not always small.

The general form of the coefficients a_i^p at next-to-leading order in α_s is

$$\begin{aligned} a_i^p(M_1M_2) &= \left(C_i + \frac{C_{i\pm1}}{N_c}\right) N_i(M_2) \\ &\quad + \frac{C_{i\pm1}}{N_c}\,\frac{C_F\alpha_s}{4\pi}\left[V_i(M_2) + \frac{4\pi^2}{N_c}\,H_i(M_1M_2)\right] + P_i^p(M_2)\,, \end{aligned} \tag{35}$$

where the upper (lower) signs apply when i is odd (even). It is understood that the superscript 'p' is to be omitted for $i=1,2$. The quantities $V_i(M_2)$ account for one-loop vertex corrections, $H_i(M_1M_2)$ for hard spectator interactions, and $P_i^p(M_1M_2)$ for penguin contractions. We now present the explicit expressions for these objects, extending the results of [10] to the case when M_1 or M_2 is a vector meson.

Figure 3: Next-to-leading order vertex contribution to the coefficients a_i^p. The meaning of the external lines is the same as in Figure 2.

Leading order (Figure 2). The leading-order coefficient $N_i(M_2)$ is simply the normalization integral of the relevant light-cone distribution amplitude $\Phi_{P,V}$ or $\Phi_{p,v}$. It follows that

$$N_i(M_2) = \begin{cases} 0\,; & i = 6, 8 \text{ and } M_2 = V, \\ 1\,; & \text{all other cases.} \end{cases} \tag{36}$$

The special case for vector mesons arises because of the vanishing integral (30). This implies the absence of scalar penguin contributions for vector mesons at tree level, since the coefficients $a_{6,8}^p$ originate from $(V-A)\otimes(V+A)$ penguin operators in the weak Hamiltonian, which must be Fierz-transformed into the Form $(-2)(S-P)\otimes(S+P)$ to match the quark flavors in the second $(S+P)$ current with those of the meson M_2.

Vertex terms (Figure 3). The vertex corrections are given by

$$V_i(M_2) = \begin{cases} \displaystyle\int_0^1 dx\, \Phi_{M_2}(x)\, \Big[12 \ln\frac{m_b}{\mu} - 18 + g(x) \Big]\,; & i = 1\text{–}4, 9, 10, \\ \displaystyle\int_0^1 dx\, \Phi_{M_2}(x)\, \Big[-12 \ln\frac{m_b}{\mu} + 6 - g(1-x) \Big]\,; & i = 5, 7, \\ \displaystyle\int_0^1 dx\, \Phi_{m_2}(x)\, \Big[-6 + h(x) \Big]\,; & i = 6, 8, \end{cases} \tag{37}$$

with

$$\begin{aligned} g(x) &= 3\left(\frac{1-2x}{1-x} \ln x - i\pi \right) \\ &\quad + \left[2\,\mathrm{Li}_2(x) - \ln^2 x + \frac{2\ln x}{1-x} - (3+2i\pi)\ln x - (x \leftrightarrow 1-x) \right], \\ h(x) &= 2\,\mathrm{Li}_2(x) - \ln^2 x - (1+2\pi i)\,\ln x - (x \leftrightarrow 1-x)\,. \end{aligned} \tag{38}$$

The expression for $g(x)$ has already been presented in [10], while the kernel $h(x)$ is new. The constants -18, 6, -6 are scheme dependent and correspond to using the NDR scheme for γ_5. The light-cone distribution amplitude Φ_{M_2} is one of the leading-twist amplitudes $\Phi_{P,V}$, depending on whether M_2 is a pseudoscalar or vector meson, whereas Φ_{m_2} is one of the twist-3 amplitudes $\Phi_{p,v}$. We recall that $\Phi_p(x) = 1$, so $\int dx\, \Phi_{m_2}(x)\,[-6 + h(x)] = -6$ for pseudoscalar mesons, which reproduces the result of [10]. On the other hand, because of (30) the scheme-dependent constant -6 does not contribute for vector mesons as it should be, since there is no leading-order contribution that could cause a scheme dependence at next-to-leading order.

Figure 4: Next-to-leading order penguin contribution to the coefficients a_i^p.

Penguin terms (Figure 4). At order α_s a correction from penguin contractions is present only for $i = 4, 6$. For $i = 4$ we obtain

$$
\begin{aligned}
P_4^p(M_2) = \frac{C_F\alpha_s}{4\pi N_c} \Bigg\{ & C_1 \left[\frac{4}{3} \ln\frac{m_b}{\mu} + \frac{2}{3} - G_{M_2}(s_p) \right] + C_3 \left[\frac{8}{3} \ln\frac{m_b}{\mu} + \frac{4}{3} - G_{M_2}(0) - G_{M_2}(1) \right] \\
& + (C_4 + C_6) \left[\frac{4n_f}{3} \ln\frac{m_b}{\mu} - (n_f - 2)\, G_{M_2}(0) - G_{M_2}(s_c) - G_{M_2}(1) \right] \\
& - 2C_{8g}^{\rm eff} \int_0^1 \frac{dx}{1-x}\, \Phi_{M_2}(x) \Bigg\} \,, \qquad (39)
\end{aligned}
$$

where $n_f = 5$ is the number of light quark flavors, and $s_u = 0$, $s_c = (m_c/m_b)^2$ are mass ratios involved in the evaluation of the penguin diagrams. Small electroweak corrections from C_{7-10} are neglected within the approximations discussed above. The function $G_{M_2}(s)$ is given by

$$
\begin{aligned}
G_{M_2}(s) &= \int_0^1 dx\, G(s - i\epsilon, 1 - x)\, \Phi_{M_2}(x) \,, \\
G(s, x) &= -4 \int_0^1 du\, u(1-u) \ln[s - u(1-u)x] \qquad (40) \\
&= \frac{2(12s + 5x - 3x\ln s)}{9x} - \frac{4\sqrt{4s - x}\,(2s + x)}{3x^{3/2}} \arctan\sqrt{\frac{x}{4s - x}} \,.
\end{aligned}
$$

The interpretation of Φ_{M_2} is the same as in the discussion of vertex corrections. For $i = 6$, the result for the penguin contribution is

$$
\begin{aligned}
P_6^p(M_2) = \frac{C_F\alpha_s}{4\pi N_c} \Bigg\{ & C_1 \left[\frac{4}{3} \ln\frac{m_b}{\mu} + \frac{2}{3} - \hat{G}_{M_2}(s_p) \right] + C_3 \left[\frac{8}{3} \ln\frac{m_b}{\mu} + \frac{4}{3} - \hat{G}_{M_2}(0) - \hat{G}_{M_2}(1) \right] \\
& + (C_4 + C_6) \left[\frac{4n_f}{3} \ln\frac{m_b}{\mu} - (n_f - 2)\, \hat{G}_{M_2}(0) - \hat{G}_{M_2}(s_c) - \hat{G}_{M_2}(1) \right] - 2C_{8g}^{\rm eff} \Bigg\} \qquad (41)
\end{aligned}
$$

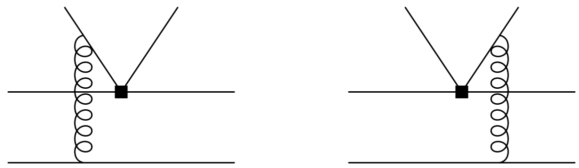

Figure 5: Hard spectator-scattering contribution to the coefficients a_i^p. The meaning of the external lines is the same as in Figure 2, but the spectator-quark line is now included in the drawing.

if M_2 is a pseudoscalar meson, and

$$P_6^p(M_2) = -\frac{C_F\alpha_s}{4\pi N_c}\Bigg\{C_1\,\hat{G}_{M_2}(s_p) + C_3\left[\hat{G}_{M_2}(0) + \hat{G}_{M_2}(1)\right] + (C_4 + C_6)\left[(n_f - 2)\,\hat{G}_{M_2}(0) + \hat{G}_{M_2}(s_c) + \hat{G}_{M_2}(1)\right]\Bigg\} \tag{42}$$

if M_2 is a vector meson. In analogy with (40), the function $\hat{G}_{M_2}(s)$ is defined as

$$\hat{G}_{M_2}(s) = \int_0^1 dx\, G(s - i\epsilon, 1 - x)\,\Phi_{m_2}(x)\,. \tag{43}$$

As mentioned above we take into account electromagnetic corrections only for $\alpha_{3,\rm EW}^p$ and $\alpha_{4,\rm EW}^p$, and only if they are proportional to the large Wilson coefficients $C_{1,2}$ and $C_{7\gamma}^{\rm eff}$. These corrections are present for $i = 8, 10$ and correspond to the penguin diagrams of Figure 4 with the gluon replaced by a photon. (An additional contribution for neutral vector mesons will be discussed separately below). For $i = 10$ we obtain

$$P_{10}^p(M_2) = \frac{\alpha}{9\pi N_c}\left\{(C_1 + N_c C_2)\left[\frac{4}{3}\ln\frac{m_b}{\mu} + \frac{2}{3} - G_{M_2}(s_p)\right] - 3C_{7\gamma}^{\rm eff}\int_0^1 \frac{dx}{1-x}\,\Phi_{M_2}(x)\right\}. \tag{44}$$

For $i = 8$ we find

$$P_8^p(M_2) = \frac{\alpha}{9\pi N_c}\left\{(C_1 + N_c C_2)\left[\frac{4}{3}\ln\frac{m_b}{\mu} + \frac{2}{3} - \hat{G}_{M_2}(s_p)\right] - 3C_{7\gamma}^{\rm eff}\right\} \tag{45}$$

if M_2 is a pseudoscalar meson, and

$$P_8^p(M_2) = -\frac{\alpha}{9\pi N_c}\,(C_1 + N_c C_2)\,\hat{G}_{M_2}(s_p) \tag{46}$$

if M_2 is a vector meson.

Hard spectator terms (Figure 5). The correction from hard gluon exchange between M_2 and the spectator quark is given by

$$H_i(M_1M_2) = \frac{B_{M_1M_2}}{A_{M_1M_2}} \frac{m_B}{\lambda_B} \int_0^1 dx \int_0^1 dy \left[\frac{\Phi_{M_2}(x)\Phi_{M_1}(y)}{\bar{x}\bar{y}} + r_\chi^{M_1} \frac{\Phi_{M_2}(x)\Phi_{m_1}(y)}{x\bar{y}} \right] \tag{47}$$

for $i = 1$–4,9,10,

$$H_i(M_1M_2) = -\frac{B_{M_1M_2}}{A_{M_1M_2}} \frac{m_B}{\lambda_B} \int_0^1 dx \int_0^1 dy \left[\frac{\Phi_{M_2}(x)\Phi_{M_1}(y)}{x\bar{y}} + r_\chi^{M_1} \frac{\Phi_{M_2}(x)\Phi_{m_1}(y)}{\bar{x}\bar{y}} \right] \tag{48}$$

for $i = 5, 7$, and $H_i(M_1M_2) = 0$ for $i = 6, 8$. In these results λ_B is defined by [8]

$$\int_0^1 \frac{d\xi}{\xi}\, \Phi_B(\xi) \equiv \frac{m_B}{\lambda_B} \tag{49}$$

with $\Phi_B(\xi)$ one of the two light-cone distribution amplitudes of the B meson. We recall that the term involving $r_\chi^{M_1}$ is suppressed by a factor of $\Lambda_{\rm QCD}/m_b$ in heavy-quark power counting. Since the twist-3 distribution amplitude $\Phi_{m_1}(y)$ does not vanish at $y = 1$, the power-suppressed term is divergent. We extract this divergence by defining a parameter $X_H^{M_1}$ through

$$\begin{aligned}
\int_0^1 \frac{dy}{\bar{y}}\, \Phi_{m_1}(y) &= \Phi_{m_1}(1) \int_0^1 \frac{dy}{\bar{y}} + \int_0^1 \frac{dy}{\bar{y}} \Big[\Phi_{m_1}(y) - \Phi_{m_1}(1) \Big] \\
&\equiv \Phi_{m_1}(1)\, X_H^{M_1} + \int_0^1 \frac{dy}{[\bar{y}]_+}\, \Phi_{m_1}(y)\,.
\end{aligned} \tag{50}$$

The remaining integral is finite (it vanishes for pseudoscalar mesons since $\Phi_p(y) = 1$), but $X_H^{M_1}$ is an unknown parameter representing a soft-gluon interaction with the spectator quark. Since the divergence that appears in an attempt to compute this soft interaction perturbatively is regulated by a physical scale of order $\Lambda_{\rm QCD}$ (i.e. at $\bar{y} \sim \Lambda_{\rm QCD}/m_b$), we expect that $X_H^M \sim \ln(m_b/\Lambda_{\rm QCD})$, however with a potentially complex coefficient, since multiple soft scattering can introduce a strong-interaction phase. A consequence of this is that power corrections to the spectator interaction, including chirally-enhanced ones for pseudoscalar mesons, are unavoidably model dependent. As in [10], our model consists of varying $X_H^{M_1}$ within a certain range (specified later) and to treat the resulting variation of the coefficients α_i^p as an uncertainty. We also assume that $X_H^{M_1}$ is universal, i.e., that it does not depend on M_1 and on the index i of $H_i(M_1M_2)$.

In [10] the convolution integrals relevant to $B \to PP$ decays were evaluated explicitly up to second non-trivial order in the Gegenbauer expansion. In Appendix B we present the corresponding results for convolution integrals involving the function $\Phi_v(x)$, which appear only in $B \to PV$ decays.

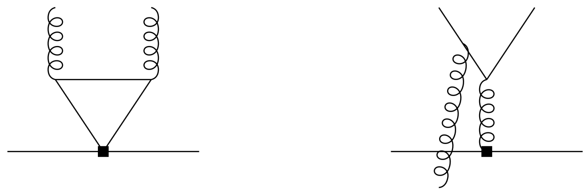

Figure 6: Additional contributions (representative diagrams shown) to the decay amplitude when $M_2 = \eta$ or η'. Left: Charm-loop contribution to the $b \to Dgg$ amplitude. Right: Soft spectator-scattering diagram, which contributes to $\Delta\alpha_3^p(M_1\eta_{q,s})$ in (52). The gluon to the left is soft and part of the operator whose matrix element defines the non-local form factor $\mathcal{F}_g^{B\to M_1}$. The gluon that originates at the weak vertex is semi-hard.

A-operators (particular results)

In addition to the generic expressions given above, there exist additional contributions to the decay amplitudes for final states containing an η or η' meson (related to their two-gluon content), and for final states containing one of the neutral vector mesons ρ^0, ω, ϕ (related to their coupling to the photon).

The contributions specific to $\eta^{(\prime)}$ mesons have been discussed in [18]. There are two effects relevant to the A-operators. First, the leading contribution of the $b \to Dgg$ amplitude can be interpreted in terms of a "charm decay constant" of the $\eta^{(\prime)}$ meson, which is calculable in a $\Lambda_{\rm QCD}/m_c$ expansion (left side of Figure 6). To account for this effect the term

$$\left[\delta_{pc}\,\alpha_2(M_1\eta_c^{(\prime)}) + \alpha_3^p(M_1\eta_c^{(\prime)})\right] A([\bar{q}_s D][\bar{c}c]) \tag{51}$$

is added to $\mathcal{T}_A^p$ in (9). Since this contribution is very small, we will only need the leading-order expressions for the new α_i coefficients, which coincide with the general leading-order result. We will also neglect the corresponding electroweak penguin effect, which is even smaller. Second, there exists an additional form-factor type contribution $\Delta\alpha_3^p(M_1\eta_{q,s}^{(\prime)})$ to the flavor-singlet coefficient $\alpha_3^p(M_1\eta_{q,s}^{(\prime)})$, which is given by

$$\Delta\alpha_3^p(M_1\eta_{q,s}^{(\prime)}) = -\frac{3\alpha_s(\mu_h)}{8\pi N_c}\,C_{8g}^{\rm eff}(\mu_h)\left(\int_0^1 dx\,\frac{\Phi_{\eta_{q,s}^{(\prime)}}(x)}{6x\bar{x}} + \dots\right)\frac{\mathcal{F}_g^{B\to M_1}(0)}{F^{B\to M_1}(0)}\,, \tag{52}$$

where $\mu_h = \sqrt{m_b\Lambda_h}$ with $\Lambda_h = 0.5\,\mathrm{GeV}$ serves as a typical scale for the semi-hard subprocess (right side of Figure 6), and the dots stand for a contribution from the leading-twist two-gluon distribution amplitude of η or η', which vanishes for asymptotic distribution amplitudes. The new feature of (52) is that this contribution is proportional to a non-local "form factor" $\mathcal{F}_g^{B\to M_1}(0)$ (rather than the usual local form factors $F = F_0$, A_0) defined in terms of the $B \to M_1$ matrix element of a bilocal quark–antiquark–gluon operator [18]. The ratio of the two form factors in (52) is of order unity in the heavy-quark limit and has been estimated to be close to 1; however, there is a large uncertainty associated with this estimate.

Figure 7: Additional contributions (representative diagrams shown) to the decay amplitude when $M_2 = \rho^0, \omega, \phi$. Wavy lines denote a photon.

For the vector mesons ρ^0, ω, ϕ the particular contributions are related to the electromagnetic penguin diagrams shown in Figure 7. These contributions are very small, but it is interesting to discuss them from a conceptual point of view. In both diagrams the photon propagator is canceled. The left diagram where the photon originates from the electric dipole operator $Q_{7\gamma}$ is therefore effectively a local vertex. The other diagram in the figure can be calculated explicitly in an expansion in $\Lambda_{\rm QCD}/m_Q$ when the quark in the loop is heavy (with mass m_Q). In the case of a charm quark this produces logarithms of the form $\ln(m_b/m_c)$, which could be summed by introducing a $c\bar{c}$ decay constant and distribution amplitude for the vector mesons, similar to the treatment of the $b \to Dgg$ amplitude for η and η'. The quark loop contains an ultraviolet divergence, which must be subtracted in accordance with the scheme used to define the Wilson coefficients. The scale and scheme dependence after subtraction is required to cancel the scale and scheme dependence of the electroweak penguin coefficients C_{7-10}. When the quark in the loop is massless (light quarks), the loop integral is infrared and ultraviolet divergent. The ultraviolet divergence is subtracted as before. The infrared divergence must be factorized into the longitudinal decay constant of the vector meson. As a consequence, parameters such as f_{ρ^0} become scale-dependent.[2] The reason for this is that the operator $\bar{q}\gamma^\mu q$ has a non-vanishing anomalous dimension in the presence of electromagnetic interactions. With these remarks it is straightforward to compute the additional contribution $\Delta\alpha^p_{3,\rm EW}(M_1V)$ to the electromagnetic penguin amplitude $\alpha^p_{3,\rm EW}(M_1V)$ when $V = \rho^0, \omega, \phi$. Within our approximation of keeping only the $\alpha C_{1,2,7\gamma}$ corrections we find

$$\Delta\alpha^p_{3,\rm EW}(M_1V) = \frac{2\alpha}{27\pi}\left\{4(C_1 + N_c C_2)\left(\frac{1}{2} - \delta_{pc}\ln\frac{\mu}{m_c} - \delta_{pu}\ln\frac{\mu}{\nu}\right) - 9C^{\rm eff}_{7\gamma}\right\}. \qquad (53)$$

Here μ refers to the renormalization scale of the Wilson coefficients $C_i(\mu)$, and ν to the scale of the decay constant $f_V(\nu)$. The ν dependence of (53) cancels the ν dependence of the leading-order decay amplitude to order α. In our analysis we set $\nu = \mu$.

B-operators/weak annihilation (generic results)

We now turn to a discussion of power-suppressed weak annihilation effects. Except for certain sign changes the "non-singlet" annihilation coefficients can be taken from [10].

[2] Strictly speaking, we should then distinguish $f_{\rho^0}(\nu)$ from f_{ρ^+}, which is scale-independent. However, given the smallness of the effect we set the two decay constants equal at $\nu = \mu$.

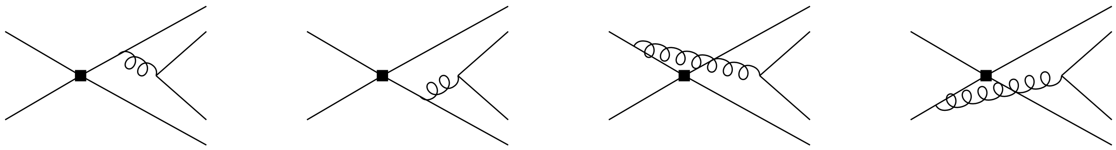

Figure 8: Weak annihilation contributions.

We consider b-quark decay and use the convention that M_1 contains an antiquark from the weak vertex with longitudinal momentum fraction $\bar{y}$. For non-singlet annihilation M_2 then contains a quark from the weak vertex with momentum fraction x. The basic building blocks when both mesons are pseudoscalar are given by (omitting the argument $M_1 M_2$ for brevity)

$$\begin{aligned}
A_1^i &= \pi\alpha_s \int_0^1 dxdy\,\left\{\Phi_{M_2}(x)\,\Phi_{M_1}(y)\left[\frac{1}{y(1-x\bar{y})}+\frac{1}{\bar{x}^2 y}\right]+r_\chi^{M_1} r_\chi^{M_2}\,\Phi_{m_2}(x)\,\Phi_{m_1}(y)\,\frac{2}{\bar{x}y}\right\},\\
A_1^f &= 0\,,\\
A_2^i &= \pi\alpha_s \int_0^1 dxdy\,\left\{\Phi_{M_2}(x)\,\Phi_{M_1}(y)\left[\frac{1}{\bar{x}(1-x\bar{y})}+\frac{1}{\bar{x}y^2}\right]+r_\chi^{M_1} r_\chi^{M_2}\,\Phi_{m_2}(x)\,\Phi_{m_1}(y)\,\frac{2}{\bar{x}y}\right\},\\
A_2^f &= 0\,, \qquad\qquad (54)\\
A_3^i &= \pi\alpha_s \int_0^1 dxdy\,\left\{r_\chi^{M_1}\,\Phi_{M_2}(x)\,\Phi_{m_1}(y)\,\frac{2\bar{y}}{\bar{x}y(1-x\bar{y})}-r_\chi^{M_2}\,\Phi_{M_1}(y)\,\Phi_{m_2}(x)\,\frac{2x}{\bar{x}y(1-x\bar{y})}\right\},\\
A_3^f &= \pi\alpha_s \int_0^1 dxdy\,\left\{r_\chi^{M_1}\,\Phi_{M_2}(x)\,\Phi_{m_1}(y)\,\frac{2(1+\bar{x})}{\bar{x}^2 y}+r_\chi^{M_2}\,\Phi_{M_1}(y)\,\Phi_{m_2}(x)\,\frac{2(1+y)}{\bar{x}y^2}\right\}.
\end{aligned}$$

When M_1 is a vector meson and M_2 a pseudoscalar, one has to change the sign of the second (twist-4) term in A_1^i, the first (twist-2) term in A_2^i, and the second term in A_3^i and A_3^f. When M_2 is a vector meson and M_1 a pseudoscalar, one only has to change the overall sign of A_2^i.

In (54) the superscripts 'i' and 'f' refer to gluon emission from the initial and final-state quarks, respectively (see Figure 8. The subscript 'k' on $A_k^{i,f}$ refers to one of the three possible Dirac structures $\Gamma_1 \otimes \Gamma_2$, which arise when the four-quark operators in the effective weak Hamiltonian are Fierz-transformed into the form $(\bar{q}_1 b)_{\Gamma_1}(\bar{q}_2 q_3)_{\Gamma_2}$, such that the quarks in the first bracket refer to the constituents of the $\bar{B}$ meson. Specifically, we have $k=1$ for $(V-A)\otimes(V-A)$, $k=2$ for $(V-A)\otimes(V+A)$, and $k=3$ for $(-2)(S-P)\otimes(S+P)$. The power suppression of weak annihilation terms compared to the leading spectator interaction via gluon exchange is evident from the fact that annihilation terms are proportional to f_B rather than $f_B m_B/\lambda_B$.

In terms of these building blocks the non-singlet annihilation coefficients are given by

$$\begin{aligned}
b_1 &= \frac{C_F}{N_c^2}\, C_1 A_1^i\,, \qquad b_3^p = \frac{C_F}{N_c^2}\Big[C_3 A_1^i + C_5 (A_3^i + A_3^f) + N_c C_6 A_3^f\Big]\,,\\
b_2 &= \frac{C_F}{N_c^2}\, C_2 A_1^i\,, \qquad b_4^p = \frac{C_F}{N_c^2}\Big[C_4 A_1^i + C_6 A_2^i\Big]\,,\\
b_{3,\rm EW}^p &= \frac{C_F}{N_c^2}\Big[C_9 A_1^i + C_7 (A_3^i + A_3^f) + N_c C_8 A_3^f\Big]\,,\\
b_{4,\rm EW}^p &= \frac{C_F}{N_c^2}\Big[C_{10} A_1^i + C_8 A_2^i\Big]\,,
\end{aligned} \tag{55}$$

omitting again the argument $M_1 M_2$. These coefficients correspond to current–current annihilation (b_1, b_2), penguin annihilation (b_3, b_4), and electroweak penguin annihilation $(b_3^{\rm EW}, b_4^{\rm EW})$, where within each pair the two coefficients correspond to different flavor structures as defined in (18).

The weak annihilation kernels exhibit endpoint divergences, which we treat in the same manner as the power corrections to the hard spectator scattering. The divergent subtractions are interpreted as

$$\int_0^1 \frac{dy}{y} \to X_A^{M_1}\,, \qquad \int_0^1 dy\, \frac{\ln y}{y} \to -\frac{1}{2}\,(X_A^{M_1})^2\,, \tag{56}$$

and similarly for M_2 with $y \to \bar{x}$. The treatment of weak annihilation is model-dependent in the QCD factorization approach, and the explicit results of this subsection are useful mainly to keep track of overall factors from Wilson coefficients and color. We treat X_A^M as an unknown complex number of order $\ln(m_b/\Lambda_{\rm QCD})$ and make the simplifying assumption that this number is independent of the identity of the meson M and the weak decay vertex. (The first assumption will be relaxed in a specific scenario, where we allow different X_A for the three cases PP, PV, and VP.) Since the treatment of annihilation is model-dependent anyway, we further simplify our results by evaluating the convolution integrals with asymptotic distribution amplitudes $\Phi(x) = \Phi_\|(x) = 6x\bar{x}$, $\Phi_p(x) = 1$, and $\Phi_v(x) = 3(x - \bar{x})$. We then find the simple expressions

$$\begin{aligned}
A_1^i &\approx A_2^i \approx 2\pi\alpha_s \left[9\left(X_A - 4 + \frac{\pi^2}{3}\right) + r_\chi^{M_1} r_\chi^{M_2} X_A^2\right],\\
A_3^i &\approx 6\pi\alpha_s\, (r_\chi^{M_1} - r_\chi^{M_2}) \left(X_A^2 - 2X_A + \frac{\pi^2}{3}\right),\\
A_3^f &\approx 6\pi\alpha_s\, (r_\chi^{M_1} + r_\chi^{M_2})\, (2X_A^2 - X_A)\,,
\end{aligned} \tag{57}$$

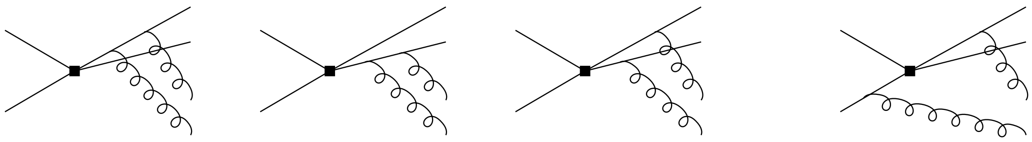

Figure 9: Examples of flavor-singlet annihilation graphs. Diagrams where both gluons attach to the constituents of the $\bar{B}$ meson belong to the $B \to \eta^{(\prime)}$ form factors. The fourth diagram and similar ones with one of the two gluons attached to the constituents of the B meson do not contribute to β^p_{S3}.

and $A^f_1 = A^f_2 = 0$ when both final state mesons are pseudoscalar, whereas

$$\begin{aligned}
A^i_1 &\approx -A^i_2 \approx 6\pi\alpha_s \left[3\left(X_A - 4 + \frac{\pi^2}{3} \right) + r_\chi^{M_1} r_\chi^{M_2} (X_A^2 - 2X_A) \right], \\
A^i_3 &\approx 6\pi\alpha_s \left[-3r_\chi^{M_1} \left(X_A^2 - 2X_A - \frac{\pi^2}{3} + 4 \right) + r_\chi^{M_2} \left(X_A^2 - 2X_A + \frac{\pi^2}{3} \right) \right], \\
A^f_3 &\approx 6\pi\alpha_s \left[3r_\chi^{M_1} (2X_A - 1)(2 - X_A) - r_\chi^{M_2} (2X_A^2 - X_A) \right],
\end{aligned} \tag{58}$$

and $A^f_1 = A^f_2 = 0$ when M_1 is a vector meson and M_2 a pseudoscalar. For the opposite case of a pseudoscalar M_1 and a vector M_2, one exchanges $r_\chi^{M_1} \leftrightarrow r_\chi^{M_2}$ in the previous equations and changes the sign of A^f_3.

B-operators/weak annihilation (particular results)

The calculation of the singlet weak annihilation coefficients b_{Si} is even more uncertain. Some of the diagrams that can contribute to these quantities are shown in Figure 9. Since we consider only diagrams formally proportional to α_s, the second meson M_2 must have a two-gluon content, hence the effect vanishes for vector mesons. We shall also make the approximation adopted in [18], in which the small electroweak singlet annihilation coefficients $b_{S3,\rm EW}$ and $b_{S4,\rm EW}$ are neglected, and in which also b_{S1} and b_{S2} are not computed and only b_{S3} is kept. The reason for neglecting b_{S1} and b_{S2} is not that these terms are smaller than b_{S3}, but that in decay amplitudes they always appear together with the large tree coefficients α_1 and α_2. On the other hand, b_{S3} appears in conjunction with the singlet penguin amplitude α^p_3. The singlet weak annihilation effect is then confined to final states with an η or η' meson.

With these approximations only the first three diagrams shown in the figure (and the corresponding crossed diagrams) have to be calculated. The result is [18]

$$b_{S3}(M_1 P_{q,s}) = \frac{C_F}{N_c^2} (C_5 + N_c C_6) \, \frac{3\pi\alpha_s}{2} \int_0^1 dy \, \frac{r_\chi^{M_1} \Phi_{m1}(y)}{y\bar{y}} \int_0^1 dx \, \Phi_{Pg}(x) \, \frac{x - \bar{x}}{x^2 \bar{x}^2}, \tag{59}$$

where $\Phi_{Pg}(x)$ is the leading-twist two-gluon distribution amplitude of P, whose Gegenbauer expansion reads

$$\Phi_{Pg}(x) = 5B_2^{Pg}(\mu)\, x^2\bar{x}^2\,(x-\bar{x}) + \dots\,. \tag{60}$$

The coefficient $B_2^{Pg}(\mu)$ as well as all higher Gegenbauer moments vanish for $\mu \to \infty$. Expression (59) is endpoint-divergent as any other weak annihilation term. Introducing $X_A^{M_1}$ as before, and truncating the Gegenbauer expansion of $\Phi_{Pg}(x)$ after the leading term, we obtain the estimate

$$b_{S3}(M_1 P_{q,s}) = \frac{C_F}{N_c^2}\,(C_5 + N_c C_6)\; 5\pi\alpha_s B_2^{Pg}(\mu_h) X_A^{M_1}\,, \tag{61}$$

which we will use in our numerical analysis below. The process $\gamma\gamma^* \to \eta^{(\prime)}$ can in principle be used to constrain $B_2^{Pg}(\mu)$. In our normalization convention the analysis performed in [36] gives $B_2^{Pg}(1\,\mathrm{GeV}) = 2 \pm 3$. Note, however, that the second Gegenbauer moment of the singlet quark–antiquark amplitude is much smaller, of order -0.1.

3 Input parameters

The predictions obtained using the QCD factorization approach depend on many input parameters. First there are Standard Model parameters such as the elements of the CKM matrix, quark masses, and the strong coupling constant. Of those our results are most sensitive to the strange-quark mass, which sets the scale for the ratios r_χ for pseudoscalar mesons defined in (32). (We work with a fixed ratio m_q/m_s, hence r_χ^π implicitly depends on m_s.) Some branching ratios, and in particular the direct CP asymmetries, are also very sensitive to the value of $|V_{ub}|$ and the weak phase $\gamma = \arg(V_{ub}^*)$. Next there are hadronic parameters that can, in principle, be determined from experiment, such as meson decay constants and transition form factors. In practice, information about these quantities often comes from theoretical calculations such as light-cone QCD sum rules or lattice calculations. The corresponding uncertainties in the form factors are substantial and often have a large impact on our results. Finally, we need predictions for a variety of light-cone distribution amplitudes, which we parameterize by the first two Gegenbauer coefficients in their moment expansion. Experimental information can at best provide indirect constraints on these parameters. Fortunately, it turns out that the sensitivity of our predictions to the Gegenbauer coefficients is usually small. The notable exception is the color-suppressed tree amplitude $\alpha_2(M_1M_2)$, which shows a considerable dependence on the first inverse moment of the B-meson distribution amplitude (λ_B) and the second Gegenbauer moment of the light mesons through the hard-spectator interaction.

A summary of the input parameters entering our numerical analysis is given in Table 1. Some additional parameters related to η and η' mesons, such as their decay constants, form factors, and the η–η' mixing angle in the quark-flavor basis, can be found in [18]. Not given in this reference are the values of the second Gegenbauer moments of the quark–antiquark twist-2 distribution amplitudes for the flavor components $\eta_q^{(\prime)}$ and $\eta_s^{(\prime)}$, for which we take $\alpha_2^{\eta_{q,s}^{(\prime)}} = 0 \pm 0.3$.

Table 1: Summary of theoretical input parameters. All scale-dependent quantities refer to $\mu = 2\,\mathrm{GeV}$ unless indicated otherwise. Parameters related to η and η' are given in [18].

QCD scale and running quark masses [GeV]				
$\Lambda^{(5)}_{\overline{\mathrm{MS}}}$	$m_b(m_b)$	$m_c(m_b)$	$m_s(2\,\mathrm{GeV})$	m_q/m_s
0.225	4.2	1.3 ± 0.2	0.090 ± 0.020	0.0413

CKM parameters and B-meson lifetimes [ps]					
$\|V_{cb}\|$	$\|V_{ub}/V_{cb}\|$	γ	$\tau(B^-)$	$\tau(B_d)$	$\tau(B_s)$
0.041 ± 0.002	0.09 ± 0.02	$(70 \pm 20)^\circ$	1.67	1.54	1.46

Pseudoscalar-meson decay constants [MeV]			
f_π	f_K	f_B	f_{B_s}
131	160	200 ± 30	230 ± 30

Vector-meson decay constants [MeV]			
f_ρ	f_{K^*}	f_ω	f_ϕ
209 ± 1	218 ± 4	187 ± 3	221 ± 3

Transverse vector-meson decay constants [MeV]			
$f_\rho^\perp$	$f_{K^*}^\perp$	$f_\omega^\perp$	$f_\phi^\perp$
150 ± 25	175 ± 25	150 ± 25	175 ± 25

Form factors for pseudoscalar mesons (at $q^2 = 0$)		
$F_0^{B\to\pi}$	$F_0^{B\to K}$	$F_0^{B_s\to\bar K}$
0.28 ± 0.05	0.34 ± 0.05	0.31 ± 0.05

Form factors for vector mesons (at $q^2 = 0$)				
$A_0^{B\to\rho}$	$A_0^{B\to K^*}$	$A_0^{B\to\omega}$	$A_0^{B_s\to\bar K^*}$	$A_0^{B_s\to\phi}$
0.37 ± 0.06	0.45 ± 0.07	0.33 ± 0.05	0.29 ± 0.05	0.34 ± 0.05

Parameters of pseudoscalar-meson distribution amplitudes				
α_2^π	$\alpha_1^{\bar K}$	$\alpha_2^{\bar K}$	λ_B [MeV]	λ_{B_s} [MeV]
0.1 ± 0.3	0.2 ± 0.2	0.1 ± 0.3	350 ± 150	350 ± 150

Parameters of vector-meson distribution amplitudes				
α_2^ρ, $\alpha_{2,\perp}^\rho$	$\alpha_1^{\bar K^*}$, $\alpha_{1,\perp}^{\bar K^*}$	$\alpha_2^{\bar K^*}$, $\alpha_{2,\perp}^{\bar K^*}$	α_2^ω, $\alpha_{2,\perp}^\omega$	α_2^ϕ, $\alpha_{2,\perp}^\phi$
0.1 ± 0.3	0.2 ± 0.2	0.1 ± 0.3	0 ± 0.3	0 ± 0.3

A few additional comments are in order. The values for the decay constants of pseudoscalar mesons and longitudinally polarized vector mesons can be determined with good accuracy from experimental data on the leptonic decays $\pi^- \to \mu\bar{\nu}_\mu$, $K^- \to \mu\bar{\nu}_\mu$, the semileptonic decay $\tau \to \rho^- \nu_\tau$, and the electromagnetic decays $V \to e^+e^-$ with $V = \rho^0$, ω, or ϕ. We have updated the values obtained in [4] by using the most recent results for the various decay rates. We will neglect the small uncertainties on these parameters in our numerical analysis. The values we take for the decay constants of the B and B_s mesons are in the ball park of many theoretical calculations using QCD sum rules and lattice gauge theory. The values for the heavy-to-light form factors are close to the results of light-cone QCD sum rules where available [37, 38, 39]. In other cases we base our values on a crude estimate of SU(3) flavor symmetry breaking effects. The $B \to \eta^{(\prime)}$ form factors receive an unknown two-gluon contribution. We therefore parameterize the form factor as [18]

$$F_0^{B\to\eta^{(\prime)}} = F_0^{B\to\pi}\,\frac{f_{\eta^{(\prime)}}^q}{f_\pi} + F_2\,\frac{\sqrt{2}f_{\eta^{(\prime)}}^q + f_{\eta^{(\prime)}}^s}{\sqrt{3}f_\pi}\,. \tag{62}$$

(For B_s decay replace $F_0^{B\to\pi}\,f_{\eta^{(\prime)}}^q$ by $F_0^{B\to K}\,f_{\eta^{(\prime)}}^s$.) Information on F_2 can in principle be obtained from semileptonic $B \to \eta\, l\nu$ decay at $q^2 = 0$. At present, however, the parameter F_2 is completely undetermined, and for lack of better knowledge we adopt the value $F_2 = 0$, for which $F_0^{B\to\eta} = 0.23$ and $F_0^{B\to\eta} = 0.19$. The modes with η' in the final state are rather sensitive to this choice. This introduces an additional theoretical uncertainty not taken into account in the error ranges given below (see [18] for the dependence of the $B \to K^{(*)}\eta^{(\prime)}$ modes on the choice of F_2). The values for the transverse decay constants and Gegenbauer moments of vector mesons are rounded numbers taken from [38], however we have inflated the small errors quoted there.[3]

The quark masses are running masses in the $\overline{\text{MS}}$ scheme. Note that the value of the charm-quark mass is given at $\mu = m_b$. The ratio $s_c = (m_c/m_b)^2$ needed for the calculation of the penguin contributions is scale independent. The values of the light quark masses are such that $r_\chi^K = r_\chi^\pi$. Finally, the value of the QCD scale parameter corresponds to $\alpha_s(M_Z) = 0.118$ for the two-loop running coupling in the $\overline{\text{MS}}$ scheme. The corresponding results for the Wilson coefficients C_i are tabulated in [10].

As discussed in detail in [10], there are large theoretical uncertainties related to the modeling of power corrections corresponding to weak annihilation effects and the chirally-enhanced power corrections to hard spectator scattering. As in our earlier work we parameterize these effects in terms of the divergent integrals X_H (hard spectator scattering) and X_A (weak annihilation) introduced in (50) and (56). We model these quantities by using the parameterization

$$X_A = \left(1 + \varrho_A\, e^{i\varphi_A}\right) \ln\frac{m_B}{\Lambda_h}\,; \qquad \varrho_A \le 1\,, \qquad \Lambda_h = 0.5\,\text{GeV}\,, \tag{63}$$

[3] To facilitate the comparison with the results of [10, 18], where they overlap, we note the following changes of input parameters relative to those papers: m_s was (110 ± 25) MeV in [10] and (100 ± 25) MeV in [18]; $|V_{ub}/V_{cb}|$ was 0.085 ± 0.017, f_B was (180 ± 40) MeV, and $F_0^{B\to K}$ was $0.9 f_K/f_\pi F_0^{B\to\pi}$ in [10]; $\alpha_1^{\bar{K}}$ was 0.3 ± 0.3, $\tau(B^-)$ was 1.65 ps, and $\tau(B_d)$ was 1.56 ps in [10, 18].

and similarly for X_H. Here φ_A is an arbitrary strong-interaction phase, which may be caused by soft rescattering. In other words, we assign a 100% uncertainty to the "default value" $X_A = \ln(m_M/\Lambda_h) \approx 2.4$. Unless otherwise stated we assume that X_A and X_H are universal for all decay processes. Finally, in the evaluation of the hard-scattering and annihilation terms we evaluate the running coupling constant and the Wilson coefficients at an intermediate scale $\mu_h \sim (\Lambda_{\rm QCD}\, m_b)^{1/2}$ rather than $\mu \sim m_b$. Specifically, we use $\mu_h = \sqrt{\Lambda_h\, \mu}$.

4 Analysis strategy for B^- and $\bar{B}^0$ decays

We are now in a position to discuss the phenomenological implications of our results, and to compare them to the experimental data compiled in Appendix C. Unless otherwise stated, all results for branching fractions and decay rates refer to an average over CP-conjugate modes, i.e., a result for $\mathrm{Br}(\bar{B} \to \bar{f})$ actually refers to

$$\frac{1}{2}\left[\mathrm{Br}(\bar{B} \to \bar{f}) + \mathrm{Br}(B \to f)\right]. \tag{64}$$

Our convention for the direct CP asymmetry follows the standard "$\bar{B}$ minus B" convention

$$A_{\rm CP}(\bar{f}\,) \equiv \frac{\mathrm{Br}(\bar{B}^0 \to \bar{f}) - \mathrm{Br}(B^0 \to f)}{\mathrm{Br}(\bar{B}^0 \to \bar{f}) + \mathrm{Br}(B^0 \to f)}\,, \tag{65}$$

which is opposite to the sign convention employed in our previous paper [10].

4.1 Outline

In the following sections we will compare the data with our theoretical results. Besides presenting our default values for the branching fractions and CP asymmetries, along with a detailed estimation of the various sources of theoretical uncertainty, we will consider a series of scenarios of specific parameter sets which elucidate correlations between different quantities and their sensitivity to hadronic parameters. Sections 5 to 7 deal with decays of B^- and $\bar{B}^0$ mesons (and their CP conjugates), while B_s decays are treated in Section 8.

The decay modes are categorized according to which flavor topology (tree, penguin, or annihilation) gives the dominant contribution to the amplitude. The $\Delta S = 1$ decay modes are always penguin dominated and are discussed first, in Section 5. They typically have "large" branching ratios of order few times 10^{-6} to few times 10^{-5}. The theoretical predictions for these modes often suffer from large uncertainties due to the strange-quark mass and due to power corrections contributing to the weak annihilation coefficient β_3^c, which is part of the dominant amplitude $\hat{\alpha}_4^c = \alpha_4^c + \beta_3^c$. These two sources of uncertainty are almost fully correlated between the various decay channels, since they always contribute to the penguin coefficients $\hat{\alpha}_4^p$. We illustrate methods that allow one to extract from data the magnitudes and strong phases of the dominant penguin contributions in the three topologies for which $M_1M_2 = PP$, PV, and VP. Once the measurements become more precise, it will be possible to reduce significantly the corresponding correlated theoretical uncertainties. For the time being we consider different scenarios for the unknown annihilation contributions as representatives for modifications of the penguin amplitude $\hat{\alpha}_4^c$ away from our default parameter choices. There are also some $\Delta D = 1$ decays which are penguin or annihilation dominated. In the last part of Section 5 we show how they can be used to derive constraints on annihilation parameters.

Most of the $\Delta D = 1$ decay modes are dominated by tree amplitudes, which do not suffer from a large sensitivity to light quark masses or chirally-enhanced power corrections. These decays are studied in Section 6. In many cases the dominant theoretical uncertainty arises from the variation of CKM parameters or form factors and decay constants. The latter source of uncertainty can be reduced once better data on semileptonic or leptonic B decays become available. The sensitivity to CKM parameters is not a theoretical limitation but rather provides access to $|V_{ub}|$ and γ, which is important for CKM fits.

We omit from our discussion in Sections 5 and 6 the decays with an η or η' meson in the final state. As discussed in [18] these modes are characterized by a complicated interplay of many different flavor topologies and suffer from additional large theoretical uncertainties due to η–η' mixing, the two-gluon component in the $\eta^{(\prime)}$ wave functions, and an annihilation contribution to the $B \to \eta^{(\prime)}$ semileptonic form factors. We will, however, consider modes with an ω or ϕ meson in the final states, taking the flavor wave functions $\omega = \omega_q \sim (\bar{u}u + \bar{d}d)/\sqrt{2}$ and $\phi = \phi_s \sim \bar{s}s$ corresponding to ideal mixing, and neglecting singlet annihilation contributions (which for vector mesons vanish within our approximations). The large number of final states with η or η' mesons is then analyzed briefly in Section 7. The decays with additional pseudoscalar or vector kaons have already been discussed in [18]. Here we give the results for the complete set, concentrating on $B^- \to \pi^-\eta^{(\prime)}$ and $B^- \to \rho^-\eta^{(\prime)}$ decay, which have sizable branching fractions.

4.2 Simplified expressions for the decay amplitudes

Appendix A contains the exact expressions for all 96 decay amplitudes in terms of the flavor parameters α_i and β_i. While these results (along with the expressions for the flavor operators collected in Section 2.4) are used in our numerical evaluations, for a phenomenological analysis is will be very useful to have simpler, approximate expressions at hand, which capture the dominant contributions to the amplitudes. These can be obtained by making the following, approximations:

- $\Delta S = 1$ *Decays:* We neglect annihilation contributions proportional to $\lambda_u^{(s)}$, since they are strongly CKM suppressed with respect to the corresponding terms proportional to $\lambda_c^{(s)}$. This amounts to setting β_1, β_2, β_3^u, and β_4^u to zero in Appendix A. Of the electroweak penguin contributions we only keep $\alpha_{3,\mathrm{EW}}^c$, since all other electroweak penguin terms are strongly suppressed. We neglect in particular all electroweak annihilation contributions.

- $\Delta D = 1$ *Decays:* We neglect all electroweak contributions, since they are never CKM enhanced and formally of order α, hence most likely smaller than unknown QCD corrections of order α_s^2.

Within these approximations the various contributions to the decay amplitudes can be classified as tree topologies (α_1 and α_2), penguin topologies (α_3^p and α_4^p), an electroweak penguin topology ($\alpha_{3,\mathrm{EW}}^c$), and annihilation topologies (β_i). The penguin annihilation contribution β_3^p is always combined with the penguin contribution α_4^p into the combination $\hat{\alpha}_4^p = \alpha_4^p + \beta_3^p$. The electroweak penguin contribution is kept only for $\Delta S = 1$ decays.

4.3 The $B^- \to \pi^-\pi^0$ tree amplitude

Before discussing the various penguin and tree-dominated B-meson decay modes it is instructive to consider the process $B^- \to \pi^-\pi^0$, which among the charmless modes discussed here is the single pure tree decay (within the approximations mentioned above). For the corresponding CP-averaged branching ratio we obtain

$$10^6\,\mathrm{Br}(B^- \to \pi^-\pi^0) = (6.1\,^{+1.1}_{-0.7}) \times \left[\frac{|V_{ub}|}{0.0037}\,\frac{F_0^{B\to\pi}(0)}{0.28}\right]^2 , \qquad (66)$$

where the largest sources of uncertainty come from the parameter λ_B of the B-meson distribution amplitude, the second Gegenbauer moment of the pion distribution amplitude, and the quantity X_H. This value can be compared with the experimental result $\mathrm{Br}(B^- \to \pi^-\pi^0) = (5.3 \pm 0.8) \cdot 10^{-6}$. The good agreement of the central values indicates that the magnitude of the tree amplitude is obtained naturally with the default set of parameters. However, given the substantial uncertainty in the overall normalization due to $|V_{ub}|$ and $F_0^{B\to\pi}(0)$, a similarly good agreement could also result if the amplitude coefficients $\alpha_{1,2}(\pi\pi)$ were to take values rather different from our expectations $|\alpha_1(\pi\pi)| = 0.99\,^{+0.04}_{-0.07}$ and $|\alpha_2(\pi\pi)| = 0.20\,^{+0.17}_{-0.11}$.

The comparison could be made independent of the values of $|V_{ub}|$ and $F_0^{B\to\pi}(0)$ if the semileptonic $B \to \pi\, l\, \nu$ rate were measured near $q^2 = 0$. One could then perform a direct measurement of the tree coefficients via the ratio [40, 41]

$$\frac{\Gamma(B^- \to \pi^-\pi^0)}{d\Gamma(\bar{B}^0 \to \pi^+ l^- \bar{\nu})/dq^2\big|_{q^2=0}} = 3\pi^2 f_\pi^2\, |V_{ud}|^2\, |\alpha_1(\pi\pi) + \alpha_2(\pi\pi)|^2 . \qquad (67)$$

In QCD factorization we find $|\alpha_1(\pi\pi) + \alpha_2(\pi\pi)| = 1.17\,^{+0.11}_{-0.07}$, which yields the value $(0.66\,^{+0.13}_{-0.08})\,\mathrm{GeV}^2$ for the above ratio.

The CLEO collaboration [42] has measured the semileptonic decay spectrum in three q^2 bins. Using their result for the lowest bin,

$$\int_0^{8\,\mathrm{GeV}^2} dq^2\, \frac{d\mathrm{Br}}{dq^2}(\bar{B}^0 \to \pi^+ l^- \bar{\nu}) = (4.31 \pm 1.06) \cdot 10^{-5} , \qquad (68)$$

and making the assumption (fulfilled in all form-factor models) $F_+^{B\to\pi}(q^2) > F_+^{B\to\pi}(0)$ for $q^2 < 8\,\mathrm{GeV}^2$, we obtain the upper bound

$$|V_{ub}|\,F_+^{B\to\pi}(0) < \sqrt{6.05\cdot 10^{-5}}\left(\tau(B_d)\,\frac{G_F^2}{24\pi^3}\int_0^{8\,\mathrm{GeV}^2} dq^2\,|\vec{p}_\pi|^3\right)^{-1/2} = 1.22\cdot 10^{-3} \qquad (69)$$

at 90% confidence level, which is already close to our default input value $(1.03\pm 0.30)\cdot 10^{-3}$. (The central experimental value would give the upper bound $1.03\cdot 10^{-3}$.) With $\mathrm{Br}(B^-\to\pi^-\pi^0) > 4.0\cdot 10^{-6}$ at 90% CL we find

$$|\alpha_1(\pi\pi)+\alpha_2(\pi\pi)| > 0.87 \quad (90\%\,\mathrm{CL})\,, \qquad (70)$$

or > 1.10 for central values. Although the bound at 90% CL is not yet in an interesting range, the limit obtained using central values shows the potential of the ratio (67) for constraining $\alpha_{1,2}(\pi\pi)$ directly. This underlines the importance of the semileptonic decay spectrum for understanding the pattern of non-leptonic $\pi\pi$ final states.

Significantly stronger limits can already be obtained if one assumes a model for the q^2 dependence of the form factor, which may be guided by QCD sum-rule calculations or lattice data at large q^2. A fit of such form factor models to the CLEO decay spectrum and lattice data has recently been performed [43], resulting in

$$|V_{ub}|\,F_+^{B\to\pi}(0) = (0.83\pm 0.16)\cdot 10^{-3} \qquad (71)$$

and a small form factor $F_+^{B\to\pi}(0) = 0.23\pm 0.04$. This would require a sizable value of $|\alpha_1(\pi\pi)+\alpha_2(\pi\pi)|$ to account for the $B^-\to\pi^-\pi^0$ branching fraction.

A scenario where $\alpha_2(\pi\pi)$ is large may be of interest, since the current experimental value of the ratio

$$\frac{\mathrm{Br}(\bar{B}^0\to\pi^-\pi^+)}{\mathrm{Br}(B^-\to\pi^-\pi^0)} = 0.86\pm 0.15 \qquad (72)$$

is not in good agreement with the QCD factorization result $1.47^{+0.37}_{-0.43}$ (with $\gamma = 70^\circ$ and $|V_{ub}/V_{cb}| = 0.09$ fixed). This is often taken as an indication for destructive interference of tree and penguin contributions to $\bar{B}^0\to\pi^-\pi^+$, implying a large value of γ or a large strong phase, in contradiction with factorization. However, another possibility could be that $\bar{B}^0\to\pi^-\pi^0$ is enhanced relative to $\bar{B}^0\to\pi^-\pi^+$ because the color-suppressed tree amplitude $\alpha_2(\pi\pi)$ is large, of order $0.4-0.5$. To keep the $\bar{B}^0\to\pi^-\pi^0$ branching ratio in agreement with its experimental value we must then assume that the $B\to\pi$ form factor $F_0^{B\to\pi}(0)$ is about 0.25, on the lower edge of the range of model predictions, but in agreement with the trend indicated by the semileptonic decay spectrum. Below, when we define a set of parameter scenarios different from the default parameters to exhibit correlations among the decay modes, we shall therefore consider this "large-α_2" scenario as one of our options.

This scenario is not as contrived as it may seem, since it can be realized by simply taking the the second Gegenbauer moment of the pion to be $\alpha_2^\pi = 0.4$ and $\lambda_B = 200\,\mathrm{MeV}$, both at the boundary of our parameter region. Indeed, there is no rigorous information available on the parameter λ_B of the B-meson distribution amplitude, and although the light-cone distribution amplitude of the pion is now believed to be close to the asymptotic form already at small scales (disfavoring a large Gegenbauer moment α_2^π), the calculations of the low-energy hadronic processes from which this information is extracted may have significant theoretical uncertainties. Furthermore, the heavy-to-light form factors at $q^2 = 0$ are usually taken from QCD sum-rule calculations, but it now appears that these form factors exhibit a substantially more complex dynamics than $B \to D$ form factors or pion transition form factors. It remains to be investigated whether the dynamics of these transitions at large momentum transfer is adequately represented in the sum-rule framework.

5 Penguin-dominated decays

All B^- and $\bar{B}^0$ two-body decays with kaons in the final state are dominated by penguin amplitudes. The modes with a single kaon are based on $\Delta S = 1$ transitions and have "large" branching ratios of order few times 10^{-6} to few times 10^{-5}. Modes with two kaons proceed through $\Delta D = 1$ transitions and therefore are expected to have smaller branching fractions. In this section we focus on decays without η or η' mesons in the final state. Those modes will be studied in Section 7.

A successful prediction for the branching ratios and CP asymmetries in rare B decays requires theoretical control over the magnitudes and relative strong-interaction phases of tree topologies, penguin topologies, electroweak penguin topologies, and annihilation topologies. The fact that generically a given decay amplitudes receives several interfering contributions complicates the interpretation of the experimental data in terms of flavor topologies. We expect that our predictions for annihilation effects (as modeled by the complex parameters ϱ_A and φ_A) and for the strong phases of the various contributions are afflicted by the largest theoretical uncertainties. The former effects are incalculable within QCD factorization and so can only be estimated using a simple model. Strong phases are predicted to vanish in the heavy-quark limit. The leading contributions to these phases are then of order α_s and calculable, or of order Λ/m_b and incalculable. Since in practice the two expansion parameters α_s and Λ/m_b are not very different, we expect that our perturbative analysis at one-loop order can only give a rough estimate of the values of strong phases. While we do trust the generic prediction that these phases are small, we expect significant deviations from the values obtained at order α_s from higher-order perturbative and power corrections. This expectation is indeed supported by an analysis of hadronic B decays using the renormalon calculus [44].

Given these limitations, it is instructive to test the reliability of our predictions for the tree, penguin, and annihilation topologies in decays without interference of the different topologies. This will probe the magnitude of these topologies but not their strong-interaction phases. Note that the penguin and annihilation terms cannot be completely separated phenomenologically, since α_4^p and β_3^p always enter in the combination $\hat{\alpha}_4^p = \alpha_4^p + \beta_3^p$. However, some other annihilation contributions can be probed directly.

A discussion of the tree contribution to the decay $B^- \to \pi^-\pi^0$ has already been given in Section 4.3. In the following we present a detailed study of penguin and annihilation terms, using penguin-dominated decay processes based on $\Delta S = 1$ and $\Delta D = 1$ transitions. For each class of decays we give explicit expressions for the decay amplitudes in terms of flavor parameters, adopting the approximations described earlier. We then present numerical predictions for the CP-averaged branching fractions and CP asymmetries and compare them with the world-average experimental data compiled in Appendix C. These results are always obtained using the exact representations of the decay amplitudes in terms of flavor parameters as given in Appendix A.

In the tables we first present our "default results" (column labeled "Theory") along with detailed error estimates corresponding to the different types of theoretical uncertainties detailed in Section 3. The first error shown corresponds to the variation of the CKM parameters $|V_{cb}|$, $|V_{ub}|$, and γ ("CKM"), the second error refers to the variation of the renormalization scale, quark masses, decay constants (except for transverse ones), form factors, and (in later sections) the η–η' mixing angle ("hadronic 1"). The third error corresponds to the uncertainty due to the Gegenbauer moments in the expansion of the light-cone distribution amplitudes, and also includes the scale-dependent transverse decay constants for vector mesons ("hadronic 2"). Finally, the last error reflects our estimate of power corrections parameterized by the quantities X_A and X_H ("power"), for which we adopt the form (63) with $\varrho_{A,H} \le 1$ and arbitrary strong phases $\varphi_{A,H}$.

In order to illustrate correlations between errors we explore four parameter scenarios in which certain parameters are changed within their error ranges while all others take their default values. Specifically, these scenarios are defined as follows:

- Scenario S1 ("large γ"):
  To study the dependence of the various observables on the CP-violating phase γ we use the default parameter values but set $\gamma = 110^\circ$ instead of 70°.

- Scenario S2 ("large α_2"):
  As discussed in Section 4.3, the experimental branching ratios for $\bar{B} \to \pi\pi$ modes can be reproduced in QCD factorization either by using a large value of $\gamma > 90^\circ$, or by enhancing the ratio $\alpha_2(\pi\pi)/\alpha_1(\pi\pi)$ with respect to its default value of about 0.2. This can be done using the form factors $F_0^{B\to\pi}(0) = 0.25$ and $F_0^{B\to K}(0) = 0.31$, the Standard Model parameters $|V_{ub}/V_{cb}| = 0.08$ and $m_s = 70\,\text{MeV}$, as well as the Gegenbauer moments $\lambda_B = 200\,\text{MeV}$ and $\alpha_2^\pi = 0.4$, all of which are within the error ranges specified earlier.

- Scenario S3 ("universal annihilation"):
  The dominant penguin coefficient $\hat{\alpha}_4^p$, which includes the annihilation contribution β_3^p, is rather sensitive to the parameter X_A. While B decays into two pseudoscalar mesons are well described by a small annihilation contribution, certain $B \to PV$ decay amplitudes favor a penguin coefficient that is larger than its default value. Here we adopt the simplest model in which a moderate enhancement of $\hat{\alpha}_4^p$ is attributed to weak annihilation. Specifically, we treat X_A as a universal parameter

obtained by using $\varrho_A = 1$ and a strong phase $\varphi_A = -45°$. The sign of this phase is not predicted, but is chosen such that the sign of the direct CP asymmetry $A_{\rm CP}(\pi^+K^-)$ agrees with the data.

- Scenario S4 ("combined"):
  Here we consider a combination of S2 and S4, but with the more moderate parameter values $m_s = 80\,\text{MeV}$ and $\alpha_2^\pi = 0.3$, as well as non-universal annihilation phases $\varphi_A = -55°$ (PP), $\varphi_A = -20°$ (PV), and $\varphi_A = -70°$ (VP). The signs of these phases are not predicted. As a result, our predictions for the signs of CP asymmetries in this scenario must be taken with caution. While each of the previous scenarios fails to describe well some classes of decay modes, scenario S4 is an attempt to combine certain parameter choices (all within our theoretical error ranges) in such as way as to obtain a good description of all currently available experimental data. In view of this, this is our currently favored scenario.

In Section 5.4 we will also study a modification of scenario S3 in which we use the large value $\varrho_A = 2$ with a universal phase $\varphi_A = -60°$.

5.1 Penguin-dominated $\Delta S = 1$ decays

We start by presenting in Tables 2 and 3 our results for the CP-averaged branching fractions and direct CP asymmetries for the decays $\bar B\to\pi\bar K$, $\bar B\to\pi\bar K^*$, $\bar B\to\bar K\rho$, as well as for the modes $\bar B\to\bar K\omega$ and $\bar B\to\bar K\phi$. The $\bar B\to\pi\bar K$ modes have the largest branching fractions, of order $(1\text{–}2)\cdot 10^{-5}$. The data show that the corresponding rates for the PV modes $\bar B\to\pi\bar K^*$ and $\bar B\to\bar K\rho$ are smaller by about a factor of two, indicating a sizable suppression of the penguin amplitudes in the cases with a final-state vector meson. QCD factorization predicts small direct CP asymmetries for most decay modes, however with a few exceptions. All predictions for CP asymmetries agree with the data within errors.

Adopting the approximations described in the previous section, the $\bar B\to\pi\bar K$ decay amplitudes are given by

$$
\begin{aligned}
\mathcal{A}_{B^-\to\pi^-\bar K^0} &= A_{\pi\bar K}\,\hat\alpha_4^p\,,\\
\sqrt2\,\mathcal{A}_{B^-\to\pi^0K^-} &= A_{\pi\bar K}\Big[\delta_{pu}\,\alpha_1+\hat\alpha_4^p\Big]+A_{\bar K\pi}\Big[\delta_{pu}\,\alpha_2+\delta_{pc}\,\tfrac32\alpha_{3,\rm EW}^c\Big]\,,\\
\mathcal{A}_{\bar B^0\to\pi^+K^-} &= A_{\pi\bar K}\Big[\delta_{pu}\,\alpha_1+\hat\alpha_4^p\Big],\\
\sqrt2\,\mathcal{A}_{\bar B^0\to\pi^0\bar K^0} &= A_{\pi\bar K}\Big[-\hat\alpha_4^p\Big]+A_{\bar K\pi}\Big[\delta_{pu}\,\alpha_2+\delta_{pc}\,\tfrac32\alpha_{3,\rm EW}^c\Big]\,,
\end{aligned}
\tag{73}
$$

where it is understood that each term must be multiplied with $\lambda_p^{(s)}$ and summed over $p=u,c$. The order of the arguments of the coefficients $\alpha_i^p(M_1M_2)$ and $\beta_i^p(M_1M_2)$ is determined by the order of the arguments of the $A_{M_1M_2}$ prefactors. The expressions for

Table 2: CP-averaged branching ratios (in units of 10^{-6}) of penguin-dominated $\bar{B} \to PP$ decays (top) and $\bar{B} \to PV$ decays (bottom) with $\Delta S = 1$. The theoretical errors shown in the first column correspond (in this order) to the uncertainties referred to as "CKM", "hadronic 1", "hadronic 2", and "power" in the text. The numbers shown in the remaining columns correspond to different scenarios of hadronic parameters explained in the text.

Mode	Theory	S1	S2	S3	S4	Experiment
$B^- \to \pi^- \bar{K}^0$	$19.3^{+1.9+11.3+1.9+13.2}_{-1.9-7.8-2.1-5.6}$	18.8	20.7	24.8	20.3	20.6 ± 1.3
$B^- \to \pi^0 K^-$	$11.1^{+1.8+5.8+0.9+6.9}_{-1.7-4.0-1.0-3.0}$	14.0	11.9	14.0	11.7	12.8 ± 1.1
$\bar{B}^0 \to \pi^+ K^-$	$16.3^{+2.6+9.6+1.4+11.4}_{-2.3-6.5-1.4-4.8}$	20.3	18.8	21.0	18.4	18.2 ± 0.8
$\bar{B}^0 \to \pi^0 \bar{K}^0$	$7.0^{+0.7+4.7+0.7+5.4}_{-0.7-3.2-0.7-2.3}$	6.5	8.3	9.3	8.0	11.2 ± 1.4
$B^- \to \pi^- \bar{K}^{*0}$	$3.6^{+0.4+1.5+1.2+7.7}_{-0.3-1.4-1.2-2.3}$	3.4	2.2	7.3	8.4	13.0 ± 3.0
$B^- \to \pi^0 K^{*-}$	$3.3^{+1.1+1.0+0.6+4.4}_{-1.0-0.9-0.6-1.4}$	5.5	2.6	5.4	6.5	< 31
$\bar{B}^0 \to \pi^+ K^{*-}$	$3.3^{+1.4+1.3+0.8+6.2}_{-1.2-1.2-0.8-1.6}$	5.9	2.4	6.6	8.1	15.3 ± 3.8
$\bar{B}^0 \to \pi^0 \bar{K}^{*0}$	$0.7^{+0.1+0.5+0.3+2.6}_{-0.1-0.4-0.3-0.5}$	0.6	0.4	2.1	2.5	< 3.6
$B^- \to \bar{K}^0 \rho^-$	$5.8^{+0.6+7.0+1.5+10.3}_{-0.6-3.3-1.3-3.2}$	5.6	13.6	10.8	9.7	< 48
$B^- \to K^- \rho^0$	$2.6^{+0.9+3.1+0.8+4.3}_{-0.9-1.4-0.6-1.2}$	1.3	6.0	4.7	4.3	< 6.2
$\bar{B}^0 \to K^- \rho^+$	$7.4^{+1.8+7.1+1.2+10.7}_{-1.9-3.6-1.1-3.5}$	4.3	13.9	12.5	10.1	8.9 ± 2.2
$\bar{B}^0 \to \bar{K}^0 \rho^0$	$4.6^{+0.5+4.0+0.7+6.1}_{-0.5-2.1-0.7-2.1}$	5.0	8.4	7.5	6.2	< 12
$B^- \to K^- \omega$	$3.5^{+1.0+3.3+1.4+4.7}_{-1.0-1.6-0.9-1.6}$	1.9	7.9	5.8	5.9	5.3 ± 0.8
$\bar{B}^0 \to \bar{K}^0 \omega$	$2.3^{+0.3+2.8+1.3+4.3}_{-0.3-1.3-0.8-1.3}$	1.9	6.6	4.5	4.9	5.1 ± 1.1
$B^- \to K^- \phi$	$4.5^{+0.5+1.8+1.9+11.8}_{-0.4-1.7-2.1-3.3}$	4.4	2.5	10.1	11.6	9.2 ± 0.7
$\bar{B}^0 \to \bar{K}^0 \phi$	$4.1^{+0.4+1.7+1.8+10.6}_{-0.4-1.6-1.9-3.0}$	4.0	2.3	9.1	10.5	7.7 ± 1.1

the $\bar{B} \to \pi \bar{K}^*$ and $\bar{B} \to \bar{K} \rho$ amplitudes are obtained by replacing $(\pi, \bar{K}) \to (\pi, \bar{K}^*)$ and $(\rho, \bar{K})$, respectively. The remaining amplitudes take the form

$$
\begin{aligned}
\sqrt{2}\,\mathcal{A}_{B^- \to K^- \omega} &= A_{\bar{K}\omega} \Big[\delta_{pu}\, \alpha_2 + 2\alpha_3^p + \delta_{pc}\, \tfrac{1}{2} \alpha_{3,\mathrm{EW}}^c \Big] + A_{\omega \bar{K}} \Big[\delta_{pu}\, \alpha_1 + \hat{\alpha}_4^p \Big] \,, \\
\sqrt{2}\,\mathcal{A}_{\bar{B}^0 \to \bar{K}^0 \omega} &= A_{\bar{K}\omega} \Big[\delta_{pu}\, \alpha_2 + 2\alpha_3^p + \delta_{pc}\, \tfrac{1}{2} \alpha_{3,\mathrm{EW}}^c \Big] + A_{\omega \bar{K}}\, \hat{\alpha}_4^p \,, \\
\mathcal{A}_{B^- \to K^- \phi} &= A_{\bar{K}\phi} \Big[\alpha_3^p + \hat{\alpha}_4^p - \delta_{pc}\, \tfrac{1}{2} \alpha_{3,\mathrm{EW}}^c \Big] \,, \\
\mathcal{A}_{\bar{B}^0 \to \bar{K}^0 \phi} &= A_{\bar{K}\phi} \Big[\alpha_3^p + \hat{\alpha}_4^p - \delta_{pc}\, \tfrac{1}{2} \alpha_{3,\mathrm{EW}}^c \Big] \,.
\end{aligned}
\qquad (74)
$$

An important feature of all these modes is that, within our approximations, annihilation

Table 3: Direct CP asymmetries (in units of 10^{-2}) of penguin-dominated $\bar{B} \to PP$ decays (top) and $\bar{B} \to PV$ decays (bottom) with $\Delta S = 1$. See text for explanations.

Mode	Theory	S1	S2	S3	S4	Experiment
$B^- \to \pi^- \bar{K}^0$	$0.9^{+0.2+0.3+0.1+0.6}_{-0.3-0.3-0.1-0.5}$	0.9	0.8	0.4	0.3	-2 ± 9
$B^- \to \pi^0 K^-$	$7.1^{+1.7+2.0+0.8+9.0}_{-1.8-2.0-0.6-9.7}$	5.7	6.3	-1.3	-3.6	1 ± 12
$\bar{B}^0 \to \pi^+ K^-$	$4.5^{+1.1+2.2+0.5+8.7}_{-1.1-2.5-0.6-9.5}$	3.6	3.0	-3.6	-4.1	-9 ± 4
$\bar{B}^0 \to \pi^0 \bar{K}^0$	$-3.3^{+1.0+1.3+0.5+3.4}_{-0.8-1.6-1.0-3.3}$	-3.5	-3.6	-1.2	0.8	3 ± 37
$B^- \to \pi^- \bar{K}^{*0}$	$1.6^{+0.4+0.6+0.5+2.5}_{-0.5-0.5-0.4-1.0}$	1.7	1.6	0.8	0.8	—
$B^- \to \pi^0 K^{*-}$	$8.7^{+2.1+5.0+2.9+41.7}_{-2.6-4.3-3.4-44.2}$	5.2	8.7	-20.4	-6.5	—
$\bar{B}^0 \to \pi^+ K^{*-}$	$2.1^{+0.6+8.2+5.1+62.5}_{-0.7-7.9-5.8-64.2}$	1.2	1.7	-33.8	-12.1	26 ± 35
$\bar{B}^0 \to \pi^0 \bar{K}^{*0}$	$-12.8^{+4.0+4.7+2.7+31.7}_{-3.2-7.0-4.0-35.3}$	-15.5	-17.7	1.5	1.0	—
$B^- \to \bar{K}^0 \rho^-$	$0.3^{+0.1+0.3+0.2+1.6}_{-0.1-0.4-0.1-1.3}$	0.3	0.4	0.4	0.8	—
$B^- \to K^- \rho^0$	$-13.6^{+4.5+6.9+3.7+62.7}_{-5.7-4.4-3.1-55.4}$	-27.3	-9.3	26.6	31.7	—
$\bar{B}^0 \to K^- \rho^+$	$-3.8^{+1.3+4.4+1.9+34.5}_{-1.4-2.7-1.6-32.7}$	-6.6	-2.6	18.3	20.0	26 ± 15
$\bar{B}^0 \to \bar{K}^0 \rho^0$	$7.5^{+1.7+2.3+0.7+8.8}_{-2.1-2.0-0.4-8.7}$	6.9	5.5	1.4	-2.8	—
$B^- \to K^- \omega$	$-7.8^{+2.6+5.9+2.4+39.8}_{-3.0-3.6-1.9-38.0}$	-14.5	-5.5	18.4	19.3	-5 ± 12
$\bar{B}^0 \to \bar{K}^0 \omega$	$-8.1^{+2.5+3.0+1.7+11.8}_{-2.0-3.3-1.4-12.9}$	-9.6	-4.3	0.0	3.7	—
$B^- \to K^- \phi$	$1.6^{+0.4+0.6+0.5+3.0}_{-0.5-0.5-0.3-1.2}$	1.6	1.7	0.6	0.7	3 ± 7
$\bar{B}^0 \to \bar{K}^0 \phi$	$1.7^{+0.4+0.6+0.5+1.4}_{-0.5-0.5-0.3-0.8}$	1.7	1.9	0.9	0.8	19 ± 68

effects enter the decay amplitudes only through the effective penguin coefficients $\hat{\alpha}_4^c = \alpha_4^c + \beta_3^c$. As a result, these effects can be readily constrained using data. This explains why the $\bar{B} \to \pi \bar{K}$ decay modes have been employed frequently (by many authors and using various analysis strategies) as a way of constraining the phase γ.

Consider first our default results labeled "Theory". While the experimental results for the $\bar{B} \to \pi \bar{K}$ modes are well reproduced within errors, it appears that in the case of the modes $\bar{B} \to \pi \bar{K}^*$ and $\bar{B} \to \bar{K}\phi$ the central values for the branching fractions obtained from QCD factorization are consistently lower than the data by a factor 2 to 3. No significant discrepancy (at the present level of precision) is seen in the modes $\bar{B} \to \bar{K}\rho$ and $\bar{B} \to \bar{K}\omega$, in which the dominant penguin coefficient is $\hat{\alpha}_4^c(VP)$ instead of $\hat{\alpha}_4^c(PV)$ (we may call these modes $B \to VP$). We will come back to this observation below.

In all cases the theoretical predictions suffer from large uncertainties due to the strange-quark mass (largest contribution to the second error), and due to power corrections contributing to the weak annihilation coefficient β_3^c, which is part of the dominant penguin amplitude $\hat{\alpha}_4^c$ (largest contribution to the last error). We stress, however, that these two sources of uncertainty are almost fully correlated between the various decay channels, since they always contribute to the penguin coefficients $\hat{\alpha}_4^p$. Below we will discuss how these coefficients can be directly determined from the data. Once the measurements become more precise it will be possible to reduce significantly the corresponding correlated theoretical uncertainties.

As a final comment, let us add that for some observables in the decays under consideration here (especially $\bar{B} \to \bar{K}\phi$ and $\bar{B} \to \pi\bar{K}$) the present experimental values are inconsistent with Standard Model predictions at the level of 2 to 3 standard deviations. We will discuss these discrepancies at length later. While we will not pursue New Physics explanations of these discrepancies in the present work, the reader should bear in mind that, unless these discrepancies disappear with more precise data, one might expect large deviations also in other observables in these decays, such as their CP-averaged branching fractions. Therefore, deviations of our predictions from experiment do not necessarily imply a failure of the QCD factorization approach.

5.1.1 Magnitudes and phases of penguin coefficients

The decay amplitudes for the three sets of decays $\bar{B} \to \pi\bar{K}$, $\bar{B} \to \pi\bar{K}^*$, and $\bar{B} \to \rho\bar{K}$ shown in (73) are particularly simple. In the $B \to PP$ modes various ratios of CP-averaged decay rates have been used to derive information about the weak phase γ as well as the strong phase of the ratio $\hat{\alpha}_4^c/\alpha_1$ [10, 45, 46, 47, 48, 49].

The amplitudes for the decays $B^- \to \pi^-\bar{K}^0$, $B^- \to \rho^-\bar{K}^0$, and $B^- \to \pi^-\bar{K}^{*0}$ are determined in terms of the coefficients $\hat{\alpha}_4^p$. QCD factorization predicts that $\hat{\alpha}_4^c \approx \hat{\alpha}_4^u$ to a good approximation. Given that $|\lambda_u^{(s)}/\lambda_c^{(s)}| \approx 0.02$, it then follows that the contribution with $p = u$ can be neglected at the present level of accuracy of the experimental data. (This assertion would be invalidated if a significant direct CP asymmetry was found in any of these modes.) It follows that $\Gamma(\bar{B}^- \to \pi^-\bar{K}^0) \propto |\hat{\alpha}_4^c(\pi K)|^2$ and $A_{\rm CP}(\bar{B}^- \to \pi^-\bar{K}^0) \approx 0$ to a very good approximation, and similar relations hold for the other two decays. These decays therefore provide a direct test of the coefficient $\hat{\alpha}_4^c$, which contains the penguin annihilation parameter β_3^c. These penguin annihilation contributions, as well as potential other non-perturbative contributions to the penguin coefficient $\hat{\alpha}_4^c$, are sometimes referred to as "charming penguins" [50].

Uncertainties related to heavy-to-light form factors can be eliminated by normalizing the pure-penguin rates to the pure-tree rate for the decay $B^- \to \pi^-\pi^0$ discussed in Section 4.3. Specifically, the magnitude of the penguin coefficient $\hat{\alpha}_4^c(\pi\bar{K})$ in the decays $B \to \pi K$ can be probed by considering the ratio

$$\left|\frac{\hat{\alpha}_4^c(\pi\bar{K})}{\alpha_1(\pi\pi) + \alpha_2(\pi\pi)}\right| = \left|\frac{V_{ub}}{V_{cb}}\right| \frac{f_\pi}{f_K} \left[\frac{\Gamma(B^- \to \pi^-\bar{K}^0)}{2\Gamma(B^- \to \pi^-\pi^0)}\right]^{1/2} = 0.103 \pm 0.008 \pm 0.023\,, \quad (75)$$

where the numerical value uses the experimental measurements of the decay rates. The first error is experimental while the second reflects the uncertainty in $|V_{ub}|$. This ratio, which is inversely proportional to the quantity called $\varepsilon_{\rm exp}$ in [10], provides a crucial

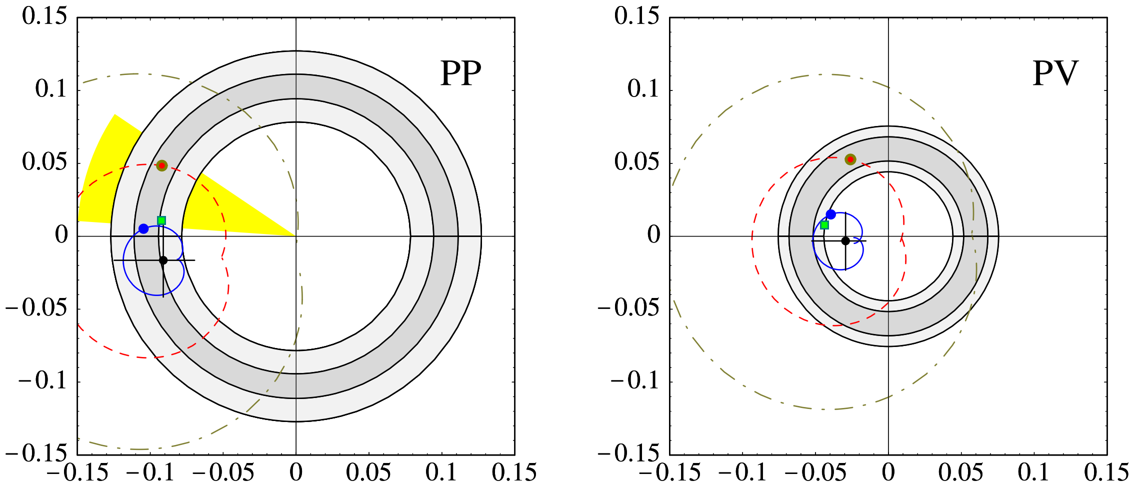

Figure 10: Complex ratios $\hat{\alpha}_4^c(M_1M_2)/(\alpha_1+\alpha_2)(\pi\pi)$ for the cases $M_1M_2 = \pi\bar{K}$ (PP) and $\pi\bar{K}^*$ (PV) (horizontal axis = real part, vertical axis = imaginary part). The rings show the experimental values of the magnitudes of the two ratios with (light) and without (dark) including the uncertainty from $|V_{ub}/V_{cb}|$. The three contour lines in each plot correspond to $\varrho_A = 1$ (solid), 2 (dashed), and 3 (dashed-dotted). The triangular-shaped area in the first plot shows the constraint on the strong phase derived from the direct CP asymmetry in $B^- \to \pi^-\bar{K}^0$ decays. The various symbols indicate theoretical points corresponding to different parameter scenarios: the dots on the solid contours correspond to S3, the squares correspond to S4, and the circles on the dashed contours correspond to the "large annihilation scenario" with $\varrho_A = 2$ and $\varphi_A = -60°$.

test of the QCD factorization approach, since it directly probes the magnitude of the dominant penguin-to-tree ratio in $B \to PP$ decays. With default parameters, QCD factorization predicts the values $|\alpha_1(\pi\pi) + \alpha_2(\pi\pi)| = 1.17$ and $|\alpha_4^c(\pi\bar{K}) + \beta_3^c(\pi\bar{K})| = |(-0.099 - 0.013i) - 0.009| = 0.108$, yielding 0.093 for the ratio of coefficients on the left-hand side, which is in excellent agreement with the data. Note that without the weak annihilation contribution from β_3^c we would obtain 0.085 for this ratio, which is still in good agreement with the data. For comparison, this ratio equals 0.061 in naive factorization. It follows that the dominant penguin amplitude in $B \to PP$ decays is correctly predicted in QCD factorization without any adjustment of parameters, and that the (incalculable) penguin annihilation contribution to this amplitude is a small effect, which in fact is consistent with the magnitude expected for a power correction. Specifically, we find that $|\beta_3^c/\alpha_4^c| = 0.09^{+0.32}_{-0.09}$. At least for the case of $\bar{B} \to \pi\bar{K}$ modes there is thus very little room for large non-perturbative contributions to the dominant penguin amplitude besides those already included in QCD factorization.

This observation can be used to place a constraint on the quantity X_A in (63), which we use to parameterize our model estimate for the annihilation terms. In the first plot in

Figure 10 we compare our theoretical results for the ratio $\hat{\alpha}_4^c(\pi\bar{K})/(\alpha_1+\alpha_2)(\pi\pi)$ with the experimental value of its magnitude obtained from (75). The point with error bars gives our central value with errors from parameter variations (including X_A and X_H). The solid "onion-shaped" curve indicates the variation allowed with $\varrho_A = 1$ and arbitrary annihilation phase φ_A. This is the region allowed by the error analysis of [10]. The larger onion-shaped curves correspond to values of the annihilation parameters outside our usual error analysis, namely $\varrho_A = 2$ (dashed curve) and $\varrho_A = 3$ (dashed-dotted curve). They are included here to indicate that for such large values of ϱ_A agreement with the data requires fine-tuning of the annihilation phase φ_A. We will see below that such large ϱ_A values are all but excluded by current data. In fact, the $\bar{B} \to \pi\bar{K}$ decays alone (PP case) do not allow for values of ϱ_A above about 2.5 once data from direct CP asymmetries are included (triangular shape, see below).

The penguin coefficients in the $B \to PV$ modes $B \to \pi K^*$ and $B \to K\rho$ can be probed via relations analogous to (75). For the case of $B^- \to \pi^-\bar{K}^{*0}$ data exist, and the corresponding result is shown in the second plot in Figure 10. In that case the ratio f_π/f_K in (75) must be replaced by f_π/f_{K^*}, but there is still no dependence on hadronic form factors. We observe that the central value for the magnitude of the penguin coefficient $\hat{\alpha}_4^c(\pi\bar{K}^*)$ obtained in QCD factorization is significantly smaller than the experimental value, and the two barely overlap when theoretical uncertainties are taken into account. Unfortunately, the branching fraction for the decay $B^- \to \rho^-\bar{K}^0$ has not yet been measured. We therefore cannot test whether the penguin coefficient in the $B \to VP$ modes $\bar{B} \to \rho\bar{K}$ is correctly predicted in QCD factorization.

It is also instructive to determine ratios of penguin coefficients that are independent of $|V_{ub}/V_{cb}|$, using the relations

$$\begin{aligned}
\left|\frac{\hat{\alpha}_4^c(\pi\bar{K}^*)}{\hat{\alpha}_4^c(\pi\bar{K})}\right| &= \frac{f_K}{f_{K^*}}\left[\frac{\Gamma(B^-\to\pi^-\bar{K}^{*0})}{\Gamma(B^-\to\pi^-\bar{K}^0)}\right]^{1/2} = 0.58 \pm 0.07 \quad (\text{exp.})\,, \\
\left|\frac{\hat{\alpha}_4^c(\rho\bar{K})}{\hat{\alpha}_4^c(\pi\bar{K})}\right| &= \frac{F_0^{B\to\pi}(0)}{A_0^{B\to\rho}(0)}\left[\frac{\Gamma(B^-\to\rho^-\bar{K}^0)}{\Gamma(B^-\to\pi^-\bar{K}^0)}\right]^{1/2} \qquad (\text{not yet observed})\,,
\end{aligned} \tag{76}$$

which can be used to relate the dominant penguin coefficients $\hat{\alpha}_4^c$ in the PV modes $\bar{B} \to \pi\bar{K}^*$ and $\bar{B} \to \rho\bar{K}$ to the corresponding coefficient in the PP mode $\bar{B} \to \pi\bar{K}$. While unfortunately no data are available yet that would allow us to deduce the relative magnitude of the penguin coefficients in the $B \to PV$ and $B \to VP$ modes, the first ratio above provides a first clue about the magnitude of the penguin coefficient in $B \to PV$ modes, which is seen to be significantly smaller than the corresponding coefficient in $B \to PP$ decays. Qualitatively, this reduction can be understood in terms of the fact that the quantity a_6^p in the relation $\alpha_4^p = a_4^p + r_\chi\, a_6^p$ in (31) vanishes at tree level for the case where M_2 is a vector meson. In fact, using default parameters we predict an even more drastic reduction of the penguin coefficient, $|\alpha_4^c(\pi\bar{K}^*) + \beta_3^c(\pi\bar{K}^*)| = |(-0.030 - 0.002i) - 0.005| = 0.035$, where the power-suppressed twist-3 term in the projector (29) contributes about 10% to the result for α_4^c. This leads to a ratio $|\hat{\alpha}_4^c(\pi\bar{K}^*)/\hat{\alpha}_4^c(\pi\bar{K})| = 0.32$. Note that the annihilation contribution is now potentially much bigger, $|\beta_3^c/\alpha_4^c| = 0.16\,^{+0.89}_{-0.14}$, and also much more uncertain. The main reason for the enhancement of this ratio is the reduction of α_4^c compared with the case of $B \to PP$ decays. We expect a similar situation to hold in the case of VP modes, for which we expect $|\alpha_4^c(\rho\bar{K}) + \beta_3^c(\rho\bar{K})| = |(0.037 + 0.003i) + 0.007| = 0.044$ and $|\beta_3^c/\alpha_4^c| = 0.18\,^{+0.83}_{-0.18}$.

Additional information can be obtained by combining the observables for the decays $\bar{B}^0 \to \pi^+ K^-$ and $B^- \to \pi^- \bar{K}^0$, as well as for the corresponding $B \to PV$ modes [46, 48]. Neglecting the small parameter $\hat{\alpha}_4^u$ (which is justified at the level of a few percent) and introducing the tree-to-penguin ratio $r_{\rm FM} = |\lambda_u^{(s)}/\lambda_c^{(s)}| \cdot (-\alpha_1(\pi\bar{K})/\hat{\alpha}_4^c(\pi\bar{K})) \approx 0.2$, we obtain

$$
\begin{aligned}
R_{\rm FM} &= \frac{\Gamma(\bar{B}^0 \to \pi^+ K^-)}{\Gamma(B^- \to \pi^- \bar{K}^0)} = 1 - 2\cos\gamma\,\mathrm{Re}\,r_{\rm FM} + |r_{\rm FM}|^2\,, \\
R_{\rm FM} \cdot A_{\rm CP}(\bar{B}^0 \to \pi^+ K^-) &= -2\sin\gamma\,\mathrm{Im}\,r_{\rm FM}\,.
\end{aligned}
\tag{77}
$$

In the $\bar{B} \to \pi\bar{K}$ sector the experimental values of these ratios are $R_{\rm FM} = 0.96 \pm 0.07$ and $R_{\rm FM} \cdot A_{\rm CP}(\bar{B}^0 \to \pi^+ K^-) = -(8.2 \pm 3.8)\%$. The second relation in (77) provides useful information on the relative strong-interaction phase of the ratio $\alpha_1(\pi\bar{K})/\hat{\alpha}_4^c(\pi\bar{K})$. Assuming that $\alpha_1(\pi\bar{K})$ has about the same phase as $\alpha_1(\pi\pi)$ (both are expected to be almost real and close to 1), we can then extract an estimate for the strong phase of the penguin coefficient $\hat{\alpha}_4^c(\pi\bar{K})$. The result is illustrated by the triangular-shaped area in the first plot in Figure 10.

We stress at this point that, in the future, the analogous ratios in the $\bar{B} \to \pi\bar{K}^*$ and $\bar{B} \to \rho\bar{K}$ systems will provide interesting information about tree–penguin interference in PV and VP modes. The corresponding ratios $r_{\rm FM}$ in these two systems are expected to be larger than $r_{\rm FM}(\pi\bar{K})$ by roughly a factor of 2, thereby enhancing significantly the interference terms in (77) and the sensitivity to γ. Note that the sign of the interference term is expected to be different in the $\rho\bar{K}$ modes ($\mathrm{Re}(r_{\rm FM}) < 0$) as compared with the $\pi\bar{K}^{(*)}$ modes ($\mathrm{Re}(r_{\rm FM}) > 0$).

The results for the penguin coefficients illustrated in Figure 10 motivated our scenarios S3 to S4 explained earlier. The values of the penguin-to-tree ratios obtained in these scenarios are indicated by the dots on the solid contours (S3) and by the squares (S4). From Tables 2 and 3 we observe that these scenarios are rather consistent with the data within errors. The best match is obtained for scenario S4. A notable exception is the decay $\bar{B}^0 \to \pi^0 \bar{K}^0$, whose measured branching fraction exceeds the values obtained using QCD factorization. We will discuss below that this fact cannot be attributed to uncertainties of the factorization approach.

5.1.2 Other decays

Within the approximations described earlier the amplitudes for the decays $B^- \to K^-\phi$ and $\bar{B}^0 \to \bar{K}^0\phi$ coincide and are determined in terms of the combination $\alpha_3^c + \hat{\alpha}_4^c - \frac{1}{2}\alpha_{3,\rm EW}^c$, where once again the terms with $p = u$ can be neglected to a good approximation. The experimental value of the ratio

$$\frac{\Gamma(B^- \to K^-\phi)}{\Gamma(\bar{B}^0 \to \bar{K}^0\phi)} = 1.10 \pm 0.18\,, \tag{78}$$

is indeed consistent with unity. In QCD factorization we find the central values $\alpha_3^c \approx 0.002$, $\hat{\alpha}_4^c \approx -0.038$, and $-\frac{1}{2}\alpha_{3,\mathrm{EW}}^c \approx 0.004$, suggesting that the amplitude is dominated by the penguin coefficient $\hat{\alpha}_4^c$. Under this assumption, and using the average of these two decay rates, we then obtain

$$\frac{F_0^{B\to K}(0)}{F_0^{B\to\pi}(0)} \left| \frac{\hat{\alpha}_4^c(\bar{K}\phi)}{\hat{\alpha}_4^c(\pi\bar{K}^*)} \right| \simeq \frac{f_{K^*}}{f_\phi} \left[\frac{\Gamma(\bar{B} \to \bar{K}\phi)}{\Gamma(B^- \to \pi^-\bar{K}^{*0})} \right]^{1/2} = 0.82 \pm 0.10\,. \tag{79}$$

Our theoretical value $1.33^{+0.43}_{-0.36}$ for the left-hand side of this equation is in marginal agreement with the data. Leaving aside the possibility that the $B \to K$ form factor is much smaller than assumed in our analysis, this might indicate a more modest penguin enhancement in the PV modes $\bar{B} \to \bar{K}\phi$ than in $\bar{B} \to \pi\bar{K}^*$.

5.2 Hints of departures from the Standard Model

Some measurements related to the penguin-dominated $\Delta S = 1$ transitions are difficult to explain theoretically. We will now study the corresponding observables. The quantities we will focus on are the mixing-induced CP asymmetries in the decays $B \to \phi K_S$ and $B \to \eta' K_S$, and the CP-averaged $\bar{B}^0 \to \pi^0\bar{K}^0$ branching ratio.

5.2.1 Mixing-induced CP asymmetries in $B \to \phi K_S$ and $B \to \eta' K_S$ decays

In neutral B-meson decays into a CP eigenstate f, one can define a time-dependent CP asymmetry

$$\frac{\mathrm{Br}(\bar{B}^0(t) \to f) - \mathrm{Br}(B^0(t) \to f)}{\mathrm{Br}(\bar{B}^0(t) \to f) + \mathrm{Br}(B^0(t) \to f)} \equiv S_f \sin(\Delta m_B\, t) - C_f \cos(\Delta m_B\, t)\,, \tag{80}$$

where $\Delta m_B > 0$ denotes the mass difference of the two neutral B eigenstates. The notation $B^0(t)$ refers to a state that was B^0 at time $t = 0$, and $\bar{B}^0(t)$ refers to a state that was $\bar{B}^0$ at time $t = 0$. The identity of these states at $t = 0$ is determined by tagging the "other B", using the fact that B^0 and $\bar{B}^0$ are produced in a coherent state at the $\Upsilon(4S)$. The quantity S_f is referred to as "mixing-induced CP asymmetry", while $-C_f$ is the direct CP asymmetry.

If all subdominant amplitudes are neglected, the mixing-induced CP asymmetries S_f for the three final states $J/\psi K_S$, ϕK_S, and $\eta' K_S$ all equal $\sin\phi_d$, where $\phi_d = 2\beta$ is the B_d–$\bar{B}_d$ mixing phase. As is well-known the correction to this result is smallest for the final state $J/\psi K_S$, since the subleading amplitude is CKM-suppressed and suppressed by a penguin-to-tree ratio. The correction is somewhat larger for the other two final states, where one can rely only on CKM suppression. The measurements of S_f for $f = \phi K_S$

and $\eta' K_S$ will become more accurate during the coming years, so that it is interesting to quantify the correction.

We can parameterize the $\bar{B}_d$ decay amplitude such that it is proportional to $1 + e^{-i\gamma}\, d_f\, e^{i\theta_f}$, where $d_f \geq 0$ includes the small ratio $|V_{ud}V_{ub}| \,/\, |V_{cd}V_{cb}|$ of CKM elements, and θ_f is the strong-interaction phase difference between the two amplitudes with different weak phases. The CP-asymmetry S_f is then given by

$$\begin{aligned} S_f &= \frac{\sin\phi_d + 2d_f\cos\theta_f\sin(\phi_d+\gamma) + d_f^2\sin(\phi_d+2\gamma)}{1 + 2d_f\cos\theta_f\cos\gamma + d_f^2} \\ &= \sin\phi_d + 2d_f\cos\theta_f\cos\phi_d\sin\gamma + O(d_f^2)\,. \end{aligned} \tag{81}$$

For the two modes of interest we obtain

$$2d_f\cos\theta_f = \begin{cases} 3.9 \pm 0.9\,{}^{+0.2}_{-0.1}\,{}^{+0.3}_{-0.2}\,{}^{+1.4}_{-1.6}\,\%\,; & f = \phi K_S\,, \\ 1.8 \pm 0.4 \pm 0.4\,{}^{+0.8}_{-1.2}\,{}^{+0.9}_{-0.8}\,\%\,; & f = \eta' K_S\,. \end{cases} \tag{82}$$

where the errors have the same meaning as in previous sections. The various scenarios give very similar values, ranging from 3.2–3.5% for ϕK_S and 0.5–1.7% for $\eta' K_S$.

As expected the correction is very small, since the QCD factorization approach does not contain any large enhancement mechanism that could compensate the CKM suppression. The theoretical uncertainties are under control in both cases, including those due to the power corrections parameterized by the quantities X_A and X_H. Using that $\cos\phi_d\sin\gamma = 0.64\,{}^{+0.04}_{-0.12}$ for $\gamma = (70\pm 20)^\circ$, we conclude that in the Standard Model

$$\begin{aligned} S_{\phi K_S} - S_{J/\psi K_S} &= 0.025 \pm 0.012 \pm 0.010\,, \\ S_{\eta' K_S} - S_{J/\psi K_S} &= 0.011 \pm 0.009 \pm 0.010\,, \end{aligned} \tag{83}$$

where the second error estimates the uncertainty in $S_{J/\psi K_S}$. Our theoretical results obtained using QCD factorization agree with simple model estimates obtained in [51]. The correction for $\eta' K_S$ is smaller than for ϕK_S since the color-suppressed tree and penguin amplitudes partially cancel each other. The precision of the predictions (83) is higher than in a scheme where only SU(3) flavor symmetry is employed [52], in which case the two differences above can only be bound to be less than about 30%. The present experimental values of the two differences are

$$\begin{aligned} S_{\phi K_S} - S_{J/\psi K_S} &= -1.11 \pm 0.41\,, \\ S_{\eta' K_S} - S_{J/\psi K_S} &= -0.40 \pm 0.34\,. \end{aligned} \tag{84}$$

In the first case there is a 2.8σ discrepancy between the data and the theoretical prediction obtained in the Standard Model. If confirmed with more data, this would be a clean signal of physics beyond the Standard Model.

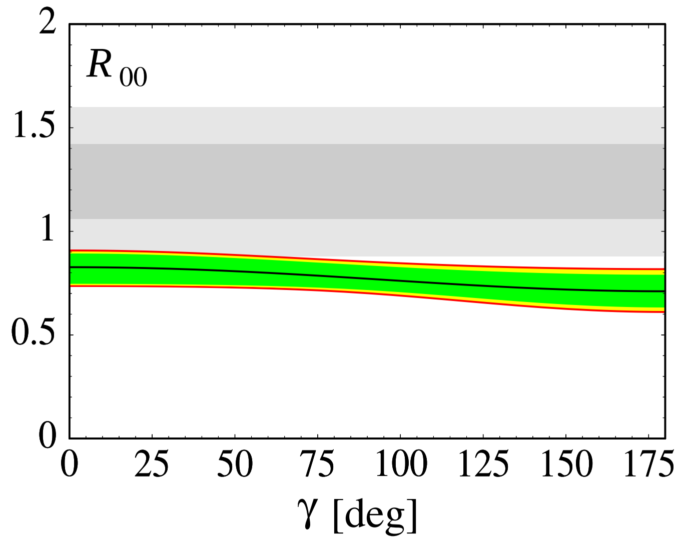

Figure 11: Theoretical prediction for the ratio R_{00} as a function of γ. The central value is shown by the solid line. The inner (dark) band corresponds to the variation of the theory input parameters, while the outer (light) band includes in addition the uncertainty from weak annihilation and twist-3 hard-spectator contributions parameterized by X_A and X_H. The gray bands show the experimental result for R_{00} with its 1σ (dark) and 2σ (light) errors.

5.2.2 The large $\bar{B}^0 \to \pi^0 \bar{K}^0$ decay rate

The experimental data for the $\bar{B}^0 \to \pi^0 \bar{K}^0$ decay rate are significantly larger than predictions obtained using QCD factorization. Sometimes this is interpreted as evidence for large rescattering effects. The purpose of this section is to point out that rescattering (or, more generally, any other source of hadronic uncertainty) cannot be invoked to explain the data.

In many analyses the $\bar{B}^0 \to \pi^0 \bar{K}^0$ decay rate is normalized to the rate for $\bar{B}^0 \to \pi^+ K^-$ in order to eliminate the dependence on the form factor [10, 48]. The resulting ratio is a strong function of γ, and in fact its high value can be explained by choosing a low value of γ. Here we propose to consider instead the ratio

$$R_{00} = \frac{2\Gamma(\bar{B}^0 \to \pi^0 \bar{K}^0)}{\Gamma(B^- \to \pi^- \bar{K}^0)} \tag{85}$$

of CP-averaged rates. The experimental value of this ratio is $R_{00}^{\rm exp} = 1.18 \pm 0.17$. The theoretical prediction obtained using QCD factorization is $R_{00}^{\rm th} = 0.79 \pm 0.02 \pm 0.06\,^{+0.03}_{-0.01} \pm 0.04$, essentially independent of γ. The largest uncertainties are due to the strange-quark mass, the $B \to \pi$ and $B \to K$ form factors, and X_A. The very weak dependence of this result on γ is illustrated in Figure 11. The results obtained in the various scenarios are: $R_{00}^{\rm th} = 0.75$ (S1), 0.87 (S2), 0.81 (S3), and 0.86 (S4). Even the largest theoretical values are about 2 standard deviations away from the central experimental result.

The theoretical interpretation of the ratio R_{00} in the Standard Model is very clean. Based on the amplitude parameterizations in (73) we define the ratios

$$\begin{aligned}
r_{\rm EW} &= \frac{3}{2}\,R_{\pi K}\,\frac{\alpha_{3,\rm EW}^c(\pi\bar K)}{\hat\alpha_4^c(\pi\bar K)} \approx 0.12-0.01i\,,\\
r_C &= -R_{\pi K}\left|\frac{\lambda_u^{(s)}}{\lambda_c^{(s)}}\right|\,\frac{\alpha_2(\pi\bar K)}{\hat\alpha_4^c(\pi\bar K)} \approx 0.03-0.02i\,,\\
r_P &= \left|\frac{\lambda_u^{(s)}}{\lambda_c^{(s)}}\right|\,\frac{\hat\alpha_4^u(\pi\bar K)}{\hat\alpha_4^c(\pi\bar K)} \approx 0.02-0.01i\,,
\end{aligned} \tag{86}$$

where $R_{\pi K}=(f_\pi/f_K)\cdot(F_0^{B\to K}/F_0^{B\to\pi})\approx 1$. The numerical values correspond to the central results obtained in QCD factorization and are meant only to illustrate the smallness of the various ratios. The ratio $r_{\rm EW}$ determines the relative magnitude of electroweak to QCD penguin contributions. In the Standard Model, the theoretical prediction for this quantity is to a large extent free of hadronic uncertainties. To see this, note that $r_{\rm EW}$ can be written as the product of the two ratios $\frac{3}{2}\,R_{\pi K}\,\alpha_{3,\rm EW}^c/(\alpha_1+\alpha_2)$ and $(\alpha_1+\alpha_2)/\hat\alpha_4^c$. Using Fierz identities and top-quark dominance in the electroweak penguin diagrams the first of these ratios can be calculated in a model-independent way up to corrections that break V-spin ($s\leftrightarrow u$) symmetry [47]. The second ratio can be determined experimentally using the strategies described in Section 5.1.1. Next, the quantity r_C determines the ratio of the color-suppressed tree amplitude to the dominant penguin amplitude. This ratio is doubly CKM suppressed. The magnitude of the penguin coefficient $\hat\alpha_4^c(\pi\bar K)$ is determined by data, and the magnitude of the tree coefficient α_2 is expected to be of order 0.2 (though it is larger in the scenarios S2 and S4). It then follows that r_C cannot be larger than a few percent in magnitude. Finally, the ratio r_P determines the relative magnitude of up and charm-penguin contributions weighted by their CKM factors. Being again doubly CKM suppressed, this ratio is bound to be of order a few percent. Moreover, to first order this ratio cancels between numerator and denominator in the ratio R_{00}.

It is then justified to work to first order in the small ratios r_C and r_P and to neglect cross terms of order $r_{\rm EW}r_C$ and $r_{\rm EW}r_P$. Parametrically, this amounts to neglecting terms of $O(\lambda^4,\alpha\lambda^2,\alpha^2)$, where $\lambda\approx 0.22$ is the Cabbibo angle and α the electromagnetic coupling. This gives

$$R_{00} = |1-r_{\rm EW}|^2 + 2\cos\gamma\,{\rm Re}\,r_C + \dots\,, \tag{87}$$

where the neglected terms are safely below 1% in magnitude. For $\gamma\approx 70^\circ$ the $\cos\gamma$-dependent term is about $+0.02$, which is negligible in view of the present experimental error in R_{00}. The fact that $R_{00}^{\rm th}<1$ can be understood in terms of a negative interference between QCD and electroweak penguin contributions. The value $r_{\rm EW}\approx 0.12$ predicted by QCD factorization indeed leads to $R_{00}^{\rm th}\approx 0.79$ in (87), which explains our numerical result. In the Standard Model the result $R_{00}<1$ is a practically model-independent prediction. In this regard the theoretical analysis of the observable R_{00} is almost as clean as that of the CP asymmetry $S(\phi K_S)$ discussed in the previous section. If the experimental finding of $R_{00} > 1$ is confirmed, this would be a clean signal of physics beyond the Standard Model.[4]

The concerned reader may ask whether the conclusion just obtained could be affected by contributions to the decay amplitudes neglected in our approximation scheme. Using the exact expressions for the amplitudes collected in Appendix A but dropping again terms of $O(\lambda^4, \alpha\lambda^2, \alpha^2)$, we find that the above analysis remains valid provided the ratios $r_{\rm EW}$ and r_C are redefined as

$$\begin{aligned} r_{\rm EW} &= \frac{3}{2}\,\frac{R_{\pi K}\,\alpha_{3,\rm EW}^c(\pi\bar K) + \beta_{3,\rm EW}^c(\pi\bar K)}{\hat\alpha_4^c(\pi\bar K)}\,, \\ r_C &= -\left|\frac{\lambda_u^{(s)}}{\lambda_c^{(s)}}\right|\,\frac{R_{\pi K}\,\alpha_2(\pi\bar K) + \beta_2(\pi\bar K)}{\hat\alpha_4^c(\pi\bar K)}\,. \end{aligned} \tag{88}$$

The additional annihilation and electroweak annihilation contributions are so small that they cannot affect the analysis presented above.

Since (87) contains a term linear in the parameter $r_{\rm EW}$, one might try to increase the value of R_{00} (without changing much the decay rates for other $B\to\pi K$ modes) by adding an O(1) New Physics contribution to the electroweak penguin coefficient $\alpha_{3,\rm EW}^c(\pi\bar K)$. Such large non-standard effects with the flavor structure of electroweak penguins can indeed arise in a large class of extensions of the Standard Model [54]. However, there is an alternative way of displaying the "$\pi^0 K^0$ anomaly" which points in a different direction. Using the isospin properties of the effective weak Hamiltonian and the (πK) final states it can be shown that the ratio

$$R_L = \frac{2\Gamma(\bar B^0\to\pi^0\bar K^0) + 2\Gamma(B^-\to\pi^0 K^-)}{\Gamma(B^-\to\pi^-\bar K^0) + \Gamma(\bar B^0\to\pi^+ K^-)} \tag{89}$$

equals 1 up to corrections that are at least quadratic in small amplitude ratios [55, 56]. In terms of the amplitude ratio $r_{\rm EW}$ defined in (86) and a new ratio

$$r_T = -\left|\frac{\lambda_u^{(s)}}{\lambda_c^{(s)}}\right|\,\frac{\alpha_1(\pi\bar K)}{\hat\alpha_4^c(\pi\bar K)} \approx 0.18 - 0.02i\,, \tag{90}$$

we find

$$R_L = 1 + |r_{\rm EW}|^2 - \cos\gamma\,{\rm Re}(r_T\,r_{\rm EW}^*) + \dots\,, \tag{91}$$

where we have neglected smaller second-order terms involving the ratios r_C and r_P. Because the corrections are of second order in small ratios the theoretical expectation for R_L lies very close to 1. We find $R_L^{\rm th} = 1.01 \pm 0.01 \pm 0.01\,{}^{+0.01}_{-0.00} \pm 0.01$ using our default

[4]The conclusion that the current πK data may point to an electroweak penguin contribution at variance with the Standard Model value of $\alpha_{3,\rm EW}^c$ has been reached independently in [53] through an analysis of a larger set of ratios.

error analysis, while the different scenarios predict: $R_L^{\rm th} = 1.03$ (S1), 1.02 (S2), 1.01 (S3), and 1.02 (S4). The current experimental result, $R_L^{\rm exp} = 1.24 \pm 0.10$, deviates from the theoretical expectation by about 2σ, as recently emphasized in [57]. To account for the experimental value requires that the magnitude of $r_{\rm EW}$ be many times larger than in the Standard Model (since r_T is restricted by data to lie close to its theoretical value). Specifically, from (87) and (91) it follows that in order to reproduce the central experimental data one needs $r_{\rm EW} \approx \pm 0.5i$ with a large (weak or strong) phase.

Before proceeding, we stress that ratios analogous to R_{00} and R_L can also be considered for vector–pseudoscalar final states, for which the final states $\pi\bar K$ are replaced by $\rho\bar K$ or $\pi\bar K^*$. Let us briefly consider the case of R_{00} in more detail. To leading order in small quantities relation (87) holds also in these cases once the ratio $R_{\pi K} \approx 1.0$ is replaced by corresponding ratios $R_{\rho K} = (f_\rho/f_K)\cdot(F_+^{B\to K}/A_0^{B\to\rho}) \approx 1.2$ and $R_{\pi K^*} = (f_\pi/f_{K^*})\cdot(A_0^{B\to K^*}/F_+^{B\to\pi}) \approx 1.0$. Due to the suppression of the penguin coefficient $\hat\alpha_4^c$ the values of the ratios $r_{\rm EW}$ and r_C are larger for the PV modes than for the PP modes. In addition, the sign of $r_{\rm EW}$ in the $\rho\bar K$ modes is negative and opposite to the case of $\pi\bar K$ and $\pi\bar K^*$. This qualitatively explains our results $R_{00}^{\rm th}(\rho\bar K) = 1.73\,^{+0.62}_{-0.48}$ and $R_{00}^{\rm th}(\pi\bar K^*) = 0.41\,^{+0.25}_{-0.26}$. Obviously the uncertainties are significantly larger than in the $\pi\bar K$ case, but nevertheless it would be interesting to probe the qualitative features of these predictions. Unfortunately, the neutral B decays into $\rho^0\bar K^0$ and $\pi^0\bar K^{*0}$ have not been seen yet experimentally. However, in the case of $\pi\bar K^*$ we may derive the experimental upper bound $R_L^{\rm exp}(\pi\bar K^*) < 0.9$ at 90% confidence level, which agrees with the prediction that this ratio should be smaller than 1.

5.3 Penguin and annihilation-dominated $\Delta D = 1$ decays

The last set of decays from which interesting information on penguin and annihilation terms can be deduced is $\bar B \to \bar K K$ and the corresponding PV modes. The decay amplitudes for $\bar B^0 \to K^- K^+$, $\bar B^0 \to K^- K^{*+}$, and $\bar B^0 \to K^{*-} K^+$ are particularly interesting, since they are the only decay modes that receive only weak annihilation contributions. The corresponding simplified amplitudes are given by

$$\begin{aligned}
\mathcal{A}_{B^-\to K^- K^0} &= A_{\bar K K}\Big[\delta_{pu}\,\beta_2 + \hat\alpha_4^p\Big]\,, \\
\mathcal{A}_{\bar B^0\to K^- K^+} &= A_{\bar K K}\Big[\delta_{pu}\,\beta_1 + \beta_4^p\Big] + B_{K\bar K}\,b_4^p\,, \\
\mathcal{A}_{\bar B^0\to \bar K^0 K^0} &= A_{\bar K K}\Big[\hat\alpha_4^p + \beta_4^p\Big] + B_{K\bar K}\,b_4^p\,,
\end{aligned} \tag{92}$$

where it is understood that each term must be multiplied with $\lambda_p^{(d)}$ and summed over $p = u, c$. The expressions for the $\bar B \to \bar K K^*$ and $\bar B \to \bar K^* K$ amplitudes are obtained by replacing $(\bar K K) \to (\bar K K^*)$ and $(\bar K^* K)$, respectively. We will also consider the modes $\bar B \to \pi\phi$, whose amplitudes are extremely simple and given by

$$\mathcal{A}_{B^-\to\pi^-\phi} = -\sqrt{2}\,\mathcal{A}_{\bar B^0\to\pi^0\phi} = A_{\pi\phi}\,\alpha_3^p\,. \tag{93}$$

Table 4: CP-averaged branching ratios (in units of 10^{-6}) of penguin-dominated $\bar{B} \to PP$ decays (top) and $\bar{B} \to PV$ decays (bottom) with $\Delta D = 1$.

Mode	Theory	S1	S2	S3	S4	Experiment
$B^- \to K^- K^0$	$1.36^{+0.45+0.72+0.14+0.91}_{-0.39-0.49-0.15-0.40}$	2.20	1.52	1.71	1.46	< 2.2
$\bar{B}^0 \to \bar{K}^0 K^0$	$1.35^{+0.41+0.71+0.13+1.09}_{-0.36-0.48-0.15-0.45}$	2.12	1.53	1.83	1.58	< 1.6
$B^- \to K^- K^{*0}$	$0.30^{+0.11+0.12+0.09+0.57}_{-0.09-0.10-0.09-0.19}$	0.50	0.21	0.54	0.66	< 5.3
$\bar{B}^0 \to \bar{K}^0 K^{*0}$	$0.26^{+0.08+0.10+0.08+0.46}_{-0.07-0.09-0.08-0.15}$	0.41	0.18	0.45	0.56	—
$B^- \to K^0 K^{*-}$	$0.30^{+0.08+0.41+0.08+0.58}_{-0.07-0.18-0.07-0.17}$	0.45	0.75	0.61	0.55	—
$\bar{B}^0 \to K^0 \bar{K}^{*0}$	$0.29^{+0.10+0.39+0.08+0.60}_{-0.09-0.17-0.07-0.17}$	0.47	0.71	0.61	0.54	—
$B^- \to \pi^- \phi$	≈ 0.005	0.008	0.010	0.005	0.009	< 0.4
$\bar{B}^0 \to \pi^0 \phi$	≈ 0.002	0.004	0.005	0.002	0.004	< 5.0

Table 5: Direct CP asymmetries (in units of 10^{-2}) of penguin-dominated $\bar{B} \to PP$ decays (top) and $\bar{B} \to PV$ decays (bottom) with $\Delta D = 1$. We only consider modes with branching fractions larger than 10^{-7}.

Mode	Theory	S1	S2	S3	S4	Experiment
$B^- \to K^- K^0$	$-16.3^{+4.7+5.0+1.6+11.3}_{-3.7-5.7-1.7-13.3}$	-10.0	-14.7	-6.5	-4.3	—
$\bar{B}^0 \to \bar{K}^0 K^0$	$-16.7^{+4.7+4.5+1.5+4.6}_{-3.7-5.1-1.7-3.6}$	-10.6	-15.0	-12.7	-11.5	—
$B^- \to K^- K^{*0}$	$-23.5^{+6.9+7.8+5.5+25.2}_{-5.7-9.0-6.5-36.8}$	-13.9	-22.5	-7.7	-9.6	—
$\bar{B}^0 \to \bar{K}^0 K^{*0}$	$-26.7^{+7.4+7.2+5.7+10.9}_{-5.7-9.0-6.9-13.4}$	-16.9	-26.0	-16.8	-13.6	—
$B^- \to K^0 K^{*-}$	$-13.4^{+3.7+7.8+4.2+27.4}_{-3.0-3.5-4.7-36.7}$	-8.9	-12.7	-13.9	-21.1	—
$\bar{B}^0 \to K^0 \bar{K}^{*0}$	$-13.1^{+3.8+5.4+4.5+5.8}_{-3.0-2.9-5.2-7.4}$	-8.0	-12.2	-8.8	-10.0	—

Table 6: CP-averaged branching ratios (in units of 10^{-6}) of annihilation-dominated $\bar{B} \to PP$ decays (top) and $\bar{B} \to PV$ decays (bottom) with $\Delta D = 1$.

Mode	Theory	S1	S2	S3	S4	Experiment
$\bar{B}^0 \to K^- K^+$	$0.013^{+0.005+0.008+0.000+0.087}_{-0.005-0.005-0.000-0.011}$	0.007	0.014	0.079	0.070	< 0.6
$\bar{B}^0 \to K^- K^{*+}$	$0.014^{+0.007+0.010+0.000+0.106}_{-0.006-0.006-0.000-0.012}$	0.016	0.011	0.095	0.094	—
$\bar{B}^0 \to K^+ K^{*-}$	$0.014^{+0.007+0.010+0.000+0.106}_{-0.006-0.006-0.000-0.012}$	0.016	0.011	0.095	0.056	—

Our default theoretical predictions for these modes are shown in Tables 4, 5 and 6.

In principle, the modes $\bar{B}^0 \to K^- K^+$ (and the corresponding PV modes) can provide interesting information about the weak annihilation amplitudes. Unfortunately, however, their branching fractions are too small to be observed in the near future. The other decay modes are penguin dominated. Using this information we predict

$$\frac{\Gamma(B^- \to K^- K^0)}{\Gamma(\bar{B}^0 \to \bar{K}^0 K^0)} \approx 1\,, \quad \frac{\Gamma(B^- \to K^- K^{*0})}{\Gamma(\bar{B}^0 \to \bar{K}^0 K^{*0})} \approx 1\,, \quad \frac{\Gamma(B^- \to K^0 K^{*-})}{\Gamma(\bar{B}^0 \to K^0 \bar{K}^{*0})} \approx 1\,. \tag{94}$$

The relevant branching fractions are found to be of order few times 10^{-7}, which should be within the long-term reach of the B factories. If these equalities could be established, this would be another indication that annihilation contributions are suppressed with respect to the dominant penguin amplitudes governed by α_4^p.

In the approximations described above, the decays $B^- \to \pi^- \phi$ and $\bar{B}^0 \to \pi^0 \phi$ are determined by the singlet penguin coefficients α_3^p, which are predicted to be highly suppressed in the QCD factorization approach. In addition these modes are CKM suppressed. An experimental upper bounds exists for $B^- \to \pi^- \phi$, which however lies two orders of magnitude above the theoretical predictions. It will therefore not be possible to extract useful information from these modes is the foreseeable future.

5.4 Bounds on large annihilation contributions

Our discussion in this section was confined to the treatment of annihilation effects suggested in [10], in which the value of the model parameter ϱ_A is limited to $\varrho_A \leq 1$, corresponding to a 100% uncertainty on the default value for the quantity X_A. While we still believe that this is a reasonable assumption, which so far has not been invalidated by the data, one might ask what would happen if larger values of ϱ_A were considered. Note that the annihilation kernels in (57) and (58) are quadratically dependent on the quantity X_A, so that increasing the value of ϱ_A can have a dramatic effect on the relative strength of annihilation terms as compared with the leading penguin amplitude.

It is apparent from Figure 10 that for values of ϱ_A significantly larger than 1 a fine-tuning of the phase φ_A is required so as not to be in conflict with the experimental constraints on the magnitudes of the $\hat{\alpha}_4^c$ parameters in the $\pi\bar{K}$ and $\pi\bar{K}^*$ systems. Let us assume for a moment that this fine-tuning is indeed realized in nature. To be specific, we set $\varrho_A = 2$ and adjust the phase $\varphi_A = -60^\circ$ such that the resulting $\hat{\alpha}_4^c$ values fall in the center of the dark rings in Figure 10 (see the dots on the dashed curves). All other parameters are set to their default values. We might then ask whether such a scenario is consistent with the experimental data.

Interestingly, we find that for several decay channels the results obtained with such large annihilation contributions are already in conflict with the data. In the upper part of Table 7 we collect results for branching ratios where significant discrepancies appear. In the lower portion of the table we give results for $K^{(*)}\bar{K}^{(*)}$ modes, some of which are also very sensitive to annihilation effects. We conclude that the data support the assumption that a reasonable estimate of weak annihilation effects can be obtained by

Table 7: CP-averaged branching ratios (in units of 10^{-6}) of some decays that imply bounds on the weak annihilation parameter X_A. The theoretical results refer to the choice $\varrho_A = 2$ with strong phase $\varphi_A = -60°$.

Mode	Default	Large Annihilation	Experiment
$\bar{B}^0 \to \pi^0 \bar{K}^{*0}$	0.7	6.0	< 3.6
$B^- \to K^- \rho^0$	2.6	9.0	< 6.2
$\bar{B}^0 \to K^- \rho^+$	7.4	19.3	8.5 ± 2.1
$B^- \to K^- \phi$	4.5	22.4	9.2 ± 0.7
$\bar{B}^0 \to \bar{K}^0 \phi$	4.1	20.2	7.7 ± 1.1
$B^- \to K^- K^0$	1.36	1.65	< 2.2
$B^- \to K^{*-} K^0$	0.30	1.14	—
$B^- \to K^- K^{*0}$	0.30	0.95	< 5.3
$\bar{B}^0 \to K^- K^+$	0.01	0.21	< 0.6
$\bar{B}^0 \to K^{*-} K^+$	0.01	0.26	—
$\bar{B}^0 \to K^- K^{*+}$	0.01	0.26	—

varying the parameter ϱ_A between 0 and 1, allowing for an arbitrary strong phase φ_A. Values of ϱ_A larger than 1 are strongly disfavored by the data, and values $\varrho_A \geq 2$ can already be excluded, at least if universal annihilation is a reasonable approximation. It has occasionally been argued that one should allow for much larger values of $\varrho_A < 8$ to account for the theoretical uncertainties related to power corrections [58]. Table 7 shows that such large weak annihilation effects cannot be tolerated by the data.

6 Tree-dominated decays

Many of the decays with $\Delta D = 1$ are dominated by tree amplitudes and do not suffer from a large sensitivity to light quark masses or chirally-enhanced power corrections. We now analyze this class of decays, including the time evolution of the $\pi\rho$ final states.

We first summarize the decay amplitudes simplified according to the discussion of Section 4.2. There are three independent amplitudes for the decays $\bar{B} \to \pi\rho$ given by

$$\begin{aligned}
\sqrt{2}\,\mathcal{A}_{B^-\to\pi^-\rho^0} &= A_{\pi\rho}\Big[\delta_{pu}\,(\alpha_2 - \beta_2) - \hat{\alpha}_4^p\Big] + A_{\rho\pi}\Big[\delta_{pu}\,(\alpha_1 + \beta_2) + \hat{\alpha}_4^p\Big]\,, \\
\mathcal{A}_{\bar{B}^0\to\pi^+\rho^-} &= A_{\pi\rho}\Big[\delta_{pu}\,\alpha_1 + \hat{\alpha}_4^p + \beta_4^p\Big] + A_{\rho\pi}\Big[\delta_{pu}\,\beta_1 + \beta_4^p\Big]\,, \qquad (95) \\
-2\,\mathcal{A}_{\bar{B}^0\to\pi^0\rho^0} &= A_{\pi\rho}\Big[\delta_{pu}\,(\alpha_2 - \beta_1) - \hat{\alpha}_4^p - 2\beta_4^p\Big] + A_{\rho\pi}\Big[\delta_{pu}\,(\alpha_2 - \beta_1) - \hat{\alpha}_4^p - 2\beta_4^p\Big]\,.
\end{aligned}$$

Table 8: Magnitudes of the amplitude parameters for $\pi\pi$ and $\pi\rho$ final states in the different scenarios. "Default" refers to the default input parameters. Scenarios not shown agree with the default. A minus sign indicates that a parameter is negative in naive factorization or (in case of the annihilation parameters) if $\varrho_A = 0$. Theoretical errors are added in quadrature.

	Default	S2	S4		Default	S2	S3	S4
$\alpha_1(\pi\pi)$	$0.99^{+0.04}_{-0.07}$	0.84	0.88	$\beta_1(\pi\pi)$	$0.025^{+0.046}_{-0.018}$	0.032	0.062	0.071
$\alpha_1(\pi\rho)$	$0.99^{+0.04}_{-0.06}$	0.89	0.90	$\beta_1(\pi\rho)$	$0.020^{+0.037}_{-0.013}$	0.023	0.051	0.063
$\alpha_1(\rho\pi)$	$1.01^{+0.04}_{-0.05}$	0.94	0.95	$\beta_1(\rho\pi)$	$0.024^{+0.045}_{-0.015}$	0.024	0.061	0.053
$\alpha_2(\pi\pi)$	$0.20^{+0.17}_{-0.11}$	0.57	0.48	$-\beta_2(\pi\pi)$	$0.010^{+0.018}_{-0.007}$	0.012	0.024	0.027
$\alpha_2(\pi\rho)$	$0.20^{+0.16}_{-0.10}$	0.45	0.41	$-\beta_2(\pi\rho)$	$0.008^{+0.015}_{-0.005}$	0.009	0.019	0.024
$\alpha_2(\rho\pi)$	$0.16^{+0.13}_{-0.09}$	0.31	0.30	$-\beta_2(\rho\pi)$	$0.009^{+0.018}_{-0.006}$	0.009	0.023	0.020
$-\alpha_4^c(\pi\pi)$	$0.102^{+0.020}_{-0.014}$	0.110	0.102	$-\beta_3(\pi\pi)$	$0.009^{+0.032}_{-0.009}$	0.013	0.035	0.041
$-\alpha_4^c(\pi\rho)$	$0.032^{+0.006}_{-0.006}$	0.027	0.028	$-\beta_3(\pi\rho)$	$0.005^{+0.024}_{-0.004}$	0.007	0.025	0.034
$\alpha_4^c(\rho\pi)$	$0.035^{+0.020}_{-0.013}$	0.062	0.049	$\beta_3(\rho\pi)$	$0.007^{+0.031}_{-0.007}$	0.008	0.032	0.028

These expressions must be multiplied with $\lambda_p^{(d)}$ and summed over $p = u, c$. The order of the arguments of the coefficients $\alpha_i^p(M_1M_2)$ and $\beta_i^p(M_1M_2)$ is determined by the order of the arguments of the $A_{M_1M_2}$ prefactors. The amplitudes for $B^- \to \pi^0\rho^-$ and $\bar{B}^0 \to \pi^-\rho^+$ are obtained from the first two expressions by interchanging $\pi \leftrightarrow \rho$ everywhere, including the arguments of the amplitude parameters. The expressions for the $\bar{B} \to \pi\pi$ amplitudes are obtained by setting $\rho \to \pi$, in which case they simplify to

$$\begin{aligned} \sqrt{2}\,\mathcal{A}_{B^-\to\pi^-\pi^0} &= A_{\pi\pi}\,\delta_{pu}\,(\alpha_1 + \alpha_2)\,, \\ \mathcal{A}_{\bar{B}^0\to\pi^+\pi^-} &= A_{\pi\pi}\Big[\delta_{pu}\,(\alpha_1 + \beta_1) + \hat{\alpha}_4^p + 2\beta_4^p\Big]\,, \\ -\mathcal{A}_{\bar{B}^0\to\pi^0\pi^0} &= A_{\pi\pi}\Big[\delta_{pu}\,(\alpha_2 - \beta_1) - \hat{\alpha}_4^p - 2\beta_4^p\Big]\,. \end{aligned} \tag{96}$$

Bose symmetry implies that the two-pion final state must have isospin $I = 0, 2$ but not $I = 1$, which is the reason why the $\bar{B} \to \pi\pi$ decay amplitudes are simpler than those for $\bar{B} \to \pi\rho$. Finally,

$$\begin{aligned} \sqrt{2}\,\mathcal{A}_{B^-\to\pi^-\omega} &= A_{\pi\omega}\Big[\delta_{pu}\,(\alpha_2 + \beta_2) + 2\alpha_3^p + \hat{\alpha}_4^p\Big] + A_{\omega\pi}\Big[\delta_{pu}\,(\alpha_1 + \beta_2) + \hat{\alpha}_4^p\Big]\,, \\ -2\,\mathcal{A}_{\bar{B}^0\to\pi^0\omega} &= A_{\pi\omega}\Big[\delta_{pu}\,(\alpha_2 - \beta_1) + 2\alpha_3^p + \hat{\alpha}_4^p\Big] + A_{\omega\pi}\Big[\delta_{pu}\,(-\alpha_2 - \beta_1) + \hat{\alpha}_4^p\Big]\,. \end{aligned} \tag{97}$$

To understand the pattern of branching fractions and asymmetries it is useful to bear in mind the magnitudes of the amplitude parameters as given in Table 8. The table also shows the values of the parameters in the four scenarios defined in Section 5. Generically α_2 is large in scenarios S2 and S4 (and α_1 is somewhat reduced), while the annihilation coefficients are increased in S3 and S4. Because of the cancellation of vector and scalar penguin contributions, the combination $\alpha_4^p(\rho\pi) = a_4^p(\rho\pi) - r_\chi^\pi a_6^p(\rho\pi)$ is very sensitive to the strange-quark mass. Except for the purely neutral final states the most important interference of amplitudes with different weak phases occurs between the tree coefficient α_1 and the effective penguin amplitude $\hat{\alpha}_4^c$. Comparing the $\pi\rho$ final states to $\pi\pi$ we note two important differences: first, the penguin amplitudes are smaller for $\pi\rho$. This implies reduced sensitivity to the angle γ in CP-averaged branching fractions and smaller direct CP violation, but it also implies a reduced "penguin pollution" in time-dependent studies of CP violation. Second, while $\hat{\alpha}_4^c(\pi\pi)$ and $\alpha_1(\pi\pi)$ have opposite signs (always assuming small relative phases), which implies constructive tree-penguin interference for $\gamma < 90^\circ$, both relative signs occur for $\pi\rho$.

6.1 Branching fractions and direct CP asymmetries

Our results for the $\pi\pi$, $\pi\rho$, and $\pi\omega$ branching fractions and direct CP asymmetries are shown in Tables 9 and 10. In many cases the dominant theoretical uncertainty arises from the variation of CKM parameters or form factors. The latter source of uncertainty can be reduced once better data on semileptonic or leptonic B decays become available. The sensitivity to CKM parameters is not a theoretical limitation but rather provides access to $|V_{ub}|$ and γ.

From the numbers shown in the tables one observes reasonable global agreement between theory and data within their respective error ranges. Since many of the theoretical errors are correlated among the various final states we shall consider below certain ratios of observables, which provide more sensitive probes of the underlying hadronic amplitudes. With default parameters the decay rates to the charged final states $\pi^+\pi^-$ and $\pi^\pm\rho^\mp$ are predicted to be significantly larger than the data. The discrepancy disappears for the two-pion final state if γ is large (scenario S1) or α_2 is large (scenario S2). However, the table shows that the $\pi\rho$ modes do not favor the large-γ scenario. Both S2 and S4, which combines elements of the large-α_2 scenarios with a moderate increase of weak annihilation, describe the branching fractions very well, but S4 is singled out if we add the information from penguin-dominated decays discussed in the previous section.

The data on direct CP asymmetries are still too uncertain to draw conclusions from the comparison. We note a 2–3 standard deviation discrepancy for the $\pi^+\pi^-$ final state. The current central value 0.51 of the CP asymmetry is certainly too large to be understood in the QCD factorization framework, and appears even more puzzling in view of the small asymmetries for the πK final states. Unless we allow for very large SU(3)-breaking effects the only difference between $\pi^+\pi^-$ and π^+K^- occurs in the annihilation term $\delta_{pu}\beta_1 + 2\beta_4^p$, but it is hard to see how this could cause such a dramatic effect on the CP asymmetry, since β_4^p is always very small in our framework and never exceeds a quarter (and often less) of the other penguin annihilation coefficient β_3^p. In the future this combination of annihilation amplitudes can be constrained independently

Table 9: CP-averaged branching ratios (in units of 10^{-6}) of tree-dominated $\bar{B} \to PP$ decays (top) and $\bar{B} \to PV$ decays (bottom) with $\Delta D = 1$. The errors and scenarios have the same meaning as explained in Section 5.

Mode	Theory	S1	S2	S3	S4	Experiment
$B^- \to \pi^-\pi^0$	$6.0^{+3.0+2.1+1.0+0.4}_{-2.4-1.8-0.5-0.4}$	5.8	5.5	6.0	5.1	5.3 ± 0.8
$\bar{B}^0 \to \pi^+\pi^-$	$8.9^{+4.0+3.6+0.6+1.2}_{-3.4-3.0-1.0-0.8}$	6.0	4.6	9.5	5.2	4.6 ± 0.4
$\bar{B}^0 \to \pi^0\pi^0$	$0.3^{+0.2+0.2+0.3+0.2}_{-0.2-0.1-0.1-0.1}$	0.7	0.9	0.4	0.7	1.6 ± 0.7 (< 3.6)
$B^- \to \pi^-\rho^0$	$11.9^{+6.3+3.6+2.5+1.3}_{-5.0-3.1-1.2-1.1}$	14.2	12.6	12.2	12.3	9.4 ± 1.6
$B^- \to \pi^0\rho^-$	$14.0^{+6.5+5.1+1.0+0.8}_{-5.5-4.3-0.6-0.7}$	10.7	10.4	14.2	10.3	9.3 ± 1.3
$\bar{B}^0 \to \pi^+\rho^-$	$21.2^{+10.3+8.7+1.3+2.0}_{-8.4-7.2-2.3-1.6}$	18.6	11.0	22.2	11.8	13.9 ± 2.7
$\bar{B}^0 \to \pi^-\rho^+$	$15.4^{+8.0+5.5+0.7+1.9}_{-6.4-4.7-1.3-1.3}$	17.5	10.8	16.4	11.8	8.9 ± 2.5
$\bar{B}^0 \to \pi^\pm\rho^\mp$	$36.5^{+18.2+10.3+2.0+3.9}_{-14.7-8.6-3.5-2.9}$	36.1	21.8	38.6	23.6	24.0 ± 2.5
$\bar{B}^0 \to \pi^0\rho^0$	$0.4^{+0.2+0.2+0.9+0.5}_{-0.2-0.1-0.3-0.3}$	0.3	1.7	0.3	1.1	< 2.5
$B^- \to \pi^-\omega$	$8.8^{+4.4+2.6+1.8+0.8}_{-3.5-2.2-0.9-0.9}$	8.6	9.1	8.4	8.4	5.9 ± 0.9
$\bar{B}^0 \to \pi^0\omega$	$0.01^{+0.00+0.02+0.02+0.03}_{-0.00-0.00-0.00-0.00}$	0.01	0.07	0.01	0.01	< 1.9

Table 10: Direct CP asymmetries (in units of 10^{-2}) of tree-dominated $\bar{B} \to PP$ decays (top) and $\bar{B} \to PV$ decays (bottom) with $\Delta D = 1$. We only consider modes with branching fractions larger than 10^{-7}.

Mode	Theory	S1	S2	S3	S4	Experiment
$B^- \to \pi^-\pi^0$	$-0.02^{+0.01+0.05+0.00+0.01}_{-0.01-0.05-0.00-0.01}$	-0.02	-0.02	-0.02	-0.02	-7 ± 14
$\bar{B}^0 \to \pi^+\pi^-$	$-6.5^{+2.1+3.0+0.1+13.2}_{-2.1-2.8-0.3-12.8}$	-9.6	-9.1	5.6	10.3	51 ± 23
$\bar{B}^0 \to \pi^0\pi^0$	$45.1^{+18.4+15.1+4.3+46.5}_{-12.8-13.8-14.1-61.6}$	23.0	21.7	5.6	-19.0	—
$B^- \to \pi^-\rho^0$	$4.1^{+1.3+2.2+0.6+19.0}_{-0.9-2.0-0.7-18.8}$	3.4	4.6	-13.3	-11.0	—
$B^- \to \pi^0\rho^-$	$-4.0^{+1.2+1.8+0.4+17.5}_{-1.2-2.2-0.4-17.7}$	-5.3	-6.3	12.2	9.9	—
$\bar{B}^0 \to \pi^+\rho^-$	$-1.5^{+0.4+1.2+0.2+8.5}_{-0.4-1.3-0.3-8.4}$	-1.7	-1.8	6.6	3.9	-11 ± 17
$\bar{B}^0 \to \pi^-\rho^+$	$0.6^{+0.2+1.3+0.1+11.5}_{-0.1-1.6-0.1-11.7}$	0.5	1.7	-10.3	-12.9	-62 ± 27
$\bar{B}^0 \to \pi^0\rho^0$	$-15.7^{+4.8+12.3+11.0+19.8}_{-4.7-14.0-12.9-25.8}$	-20.9	-9.5	-10.6	10.7	—
$B^- \to \pi^-\omega$	$-1.8^{+0.5+2.7+0.8+2.1}_{-0.5-3.3-0.7-2.2}$	-1.8	0.6	-2.1	-6.0	-20 ± 17

using $\bar{B}^0 \to K^- K^+$ decays (up to SU(3)-breaking effects).

With the exception of the neutral final states the direct CP asymmetries are all predicted to be small, although with large uncertainties due to weak annihilation that affect even the signs of the asymmetries. However, the analysis of Section 5 has shown that for the largest values of weak annihilation allowed by our error definition not all values of the annihilation phase are compatible with data on branching fractions and CP asymmetries of penguin-dominated decays (see Figure 10). This might favor the signs displayed in scenario S3 and S4, although this conclusion must be regarded with great caution since it is mainly based on the direct CP asymmetry in the $\pi^\mp K^\pm$ mode.

It is worth emphasizing that the correlations between various asymmetries are predicted more reliably in the factorization framework than the asymmetries themselves, at least if the annihilation parameter ϱ_A is not too different for the PP, PV, and VP amplitudes, or if annihilation is a small effect altogether. Table 10 shows that this is the case for all our scenarios. Since in the case of a small penguin-to-tree ratio the direct CP asymmetry is approximately given by $2\sin\gamma\,|\lambda_c^{(d)}/\lambda_u^{(d)}|\,\mathrm{Im}(\hat{\alpha}_4^c/\alpha_1)$, the relative magnitudes of the CP asymmetries in $\pi^+\pi^-$, $\pi^-\rho^0$, $\pi^0\rho^-$, $\pi^-\rho^+$, and $\pi^+\rho^-$ provide direct access to the magnitudes and signs (phases) of the penguin amplitudes $\hat{\alpha}_4^c$ for $\pi\pi$, $\pi\rho$, and $\rho\pi$, which are predicted to be rather different (see Table 8). We note specifically the case of the $B^- \to \pi^-\rho^0$ and $B^- \to \pi^0\rho^-$ amplitudes, where according to (95) the PV and VP penguin amplitudes appear as $A_{\rho\pi}\,\hat{\alpha}_4^c - A_{\pi\rho}\,\hat{\alpha}_4^c$ but with opposite sign relative to α_1, and the charged final states, which probe the magnitude and sign of the PV and VP penguin amplitudes independently. A verification of these sign patterns alone would provide an impressive confirmation of the relevance of factorization to the calculation of direct CP asymmetries.

6.2 Ratios of decay rates

We now discuss a number of ratios of CP-averaged $\pi\pi$ and $\pi\rho$ decay rates, which are either sensitive to the CKM angle γ or to particular aspects of the hadronic amplitudes. In addition to $R_{\pi\pi} = \Gamma(\bar{B}^0 \to \pi^+\pi^-)/(2\Gamma(B^- \to \pi^-\pi^0))$ we consider the ratios:

$$
\begin{aligned}
R_1 &\equiv \frac{\Gamma(\bar{B}^0 \to \pi^+\rho^-)}{\Gamma(\bar{B}^0 \to \pi^+\pi^-)}\,, \qquad R_2 \equiv \frac{\Gamma(\bar{B}^0 \to \pi^+\rho^-) + \Gamma(\bar{B}^0 \to \pi^-\rho^+)}{2\Gamma(\bar{B}^0 \to \pi^+\pi^-)}\,, \\
R_3 &\equiv \frac{\Gamma(\bar{B}^0 \to \pi^+\rho^-)}{\Gamma(\bar{B}^0 \to \pi^-\rho^+)}\,, \\
R_4 &\equiv \frac{2\,\Gamma(B^- \to \pi^-\rho^0)}{\Gamma(\bar{B}^0 \to \pi^-\rho^+)} - 1\,, \qquad R_5 \equiv \frac{2\,\Gamma(B^- \to \pi^0\rho^-)}{\Gamma(\bar{B}^0 \to \pi^+\rho^-)} - 1\,.
\end{aligned}
\tag{98}
$$

The theoretical and experimental results for these ratios are summarized in Table 11. The ratio $R_{\pi\pi}$ has already been discussed in part in Section 4.3 as one of the motivations for exploring a scenario with large α_2. Since QCD factorization does not contain a mechanism to generate a large strong phase between the two amplitudes with different

Table 11: Results for the ratios $R_{\pi\pi}$ and R_{1-5}.

	Theory	S1	S2	S3	S4	Experiment
$R_{\pi\pi}$	$0.80^{+0.12\,+0.05\,+0.13\,+0.14}_{-0.12\,-0.06\,-0.20\,-0.11}$	0.56	0.45	0.85	0.55	0.47 ± 0.08
R_1	$2.39^{+0.31\,+0.04\,+0.15\,+0.05}_{-0.25\,-0.08\,-0.12\,-0.11}$	3.11	2.39	2.33	2.28	3.02 ± 0.64
R_2	$2.06^{+0.40\,+0.53\,+0.12\,+0.03}_{-0.30\,-0.36\,-0.09\,-0.06}$	3.02	2.37	2.03	2.28	2.61 ± 0.35
R_3	$1.38^{+0.18\,+0.82\,+0.03\,+0.02}_{-0.17\,-0.59\,-0.04\,-0.05}$	1.06	1.01	1.35	0.99	1.56 ± 0.53
R_4	$0.42^{+0.04\,+0.15\,+0.45\,+0.23}_{-0.04\,-0.11\,-0.21\,-0.20}$	0.49	1.14	0.37	0.92	0.95 ± 0.64
R_5	$0.22^{+0.07\,+0.08\,+0.23\,+0.14}_{-0.08\,-0.06\,-0.12\,-0.12}$	0.06	0.75	0.18	0.61	0.23 ± 0.30

weak phases contributing to $\bar{B}^0 \to \pi^+\pi^-$, $R_{\pi\pi}$ is described well only if γ is significantly larger than 100°, or if α_2 is large and $A_{\pi\pi}|\lambda_u^{(d)}|$ is small.

We find that the ratio R_1 is theoretically rather clean and yet sensitive to γ, because it is almost independent of the B-meson form factors, and it is independent of the uncertain color-suppressed tree coefficient α_2 as seen from (95). In fact, if the tree coefficient α_1 dominated the amplitude and were universal, R_1 would equal $(f_\rho/f_\pi)^2 = 2.55$, which is not far from the complete result. In our framework the largest theoretical uncertainty comes from the pion and ρ-meson light-cone distribution amplitudes, since these cause the largest non-universality of the amplitude parameters. From Table 11 we see that R_1 is nearly constant, except in the scenario where $\gamma = 110^\circ$. The sensitivity to γ arises from the fact that while in both cases the penguin–tree interference is constructive for $\gamma < 90^\circ$, the effect is more pronounced for $\pi\pi$ than for $\pi\rho$ due to the larger penguin amplitude in the former case. We should note, however, that the conclusion that R_1 is theoretically clean hinges on the assumption that the phase of the penguin annihilation amplitude is not very different for the PP and PV amplitudes, or, if it is different, that the magnitude of penguin annihilation is not too large. The current experimental value of R_1 is somewhat higher than the theoretical prediction for $\gamma = 70^\circ$, but the difference is only one standard deviation.

Since the sum of the $\pi^+\rho^-$ and $\pi^-\rho^+$ decay rates is measured more accurately than the individual rates, we also consider the second ratio R_2. In this case there is a substantial uncertainty from the ratio of form factors, $A_0^{B\to\rho}(0)/F_0^{B\to\pi}(0)$, evidenced by the second error of the "Theory" column in Table 11. Perhaps the only thing that can be said at present is that theory and experiment agree within their respective errors, which can be taken as a qualitative argument in favor of factorization.

The ratio R_3 of $\bar{B}^0 \to \pi^+\rho^-$ to $\bar{B}^0 \to \pi^-\rho^+$ is mainly sensitive to the form-factor ratio $A_0^{B\to\rho}(0)/F_0^{B\to\pi}(0)$, and to a lesser extent to γ. Since the information provided by R_3 is largely equivalent to the one from the parameter ΔC in the time-dependent analysis of the $\pi^\mp\rho^\pm$ final states (see Section 6.3 below), we do not discuss R_3 further here. The experimental result is again in good agreement with factorization.

Finally, the quantities R_4 and R_5 are constructed such that the dominant tree amplitude cancels out in the numerator. This leaves as the leading term

$$R_4 = 2\,\frac{A_{\pi\rho}}{A_{\rho\pi}}\,\mathrm{Re}\left(\frac{\alpha_2(\pi\rho)}{\alpha_1(\rho\pi)}\right) + \dots\,, \tag{99}$$

where the dots denote the interference terms with the penguin amplitude and other smaller contributions. For R_5 a similar approximation (with somewhat larger corrections) holds with $\pi \leftrightarrow \rho$ exchanged everywhere. Hence $R_{4,5}$ are expected to be nearly independent of γ, and in first approximation they access the real part of the color-suppressed tree amplitude. These observables may therefore be interesting for assessing the viability of the large-α_2 scenarios S2 and S4. However, the current experimental values of R_4 and R_5 are not sufficiently precise to support or disfavor these scenarios.

6.3 Time-dependent analysis of the $\pi^\mp\rho^\pm$ system

We now analyze the asymmetries in time-dependent measurements of B^0 and $\bar{B}^0$ decays into the $\pi^\mp\rho^\pm$ final states. We begin with setting up conventions and notation for a general final state f and its CP conjugate $\bar{f}$ [59].

We define $\mathcal{A}_f$, $\bar{\mathcal{A}}_f$, $\mathcal{A}_{\bar{f}}$, and $\bar{\mathcal{A}}_{\bar{f}}$ to be the amplitudes for the four decay modes, where the bar on $\mathcal{A}$ refers to the decay of the $\bar{B}^0$ meson. In the standard approximation, which neglects CP violation in the B^0–$\bar{B}^0$ mixing matrix and the width difference of the two mass eigenstates, the decay amplitude squared at time t of the state that was a pure B^0 at time $t=0$ can be parameterized by

$$|\mathcal{A}_f(t)|^2 \equiv |\langle f|B(t)\rangle|^2 = \frac{e^{-\Gamma t}}{2}\big(|\mathcal{A}_f|^2 + |\bar{\mathcal{A}}_f|^2\big)\Big\{1 + C_f\cos(\Delta m_B\,t) - S_f\sin(\Delta m_B\,t)\Big\}\,, \tag{100}$$

where $\Delta m_B > 0$ denotes the mass difference, and Γ the common total width of the B-meson eigenstates. For an initial $\bar{B}^0$ the signs of the cos and sin terms are reversed. For decays to the CP conjugate final state one replaces f by $\bar{f}$.

For the following discussion we adopt the phase convention $\mathrm{CP}|B^0\rangle = -|\bar{B}^0\rangle$ and define the amplitude ratios

$$\rho_f = \frac{\bar{\mathcal{A}}_f}{\mathcal{A}_f}\,, \qquad \rho_{\bar{f}} = \frac{\bar{\mathcal{A}}_{\bar{f}}}{\mathcal{A}_{\bar{f}}}\,. \tag{101}$$

In terms of these

$$C_f = \frac{1-|\rho_f|^2}{1+|\rho_f|^2}\,, \qquad S_f = -2\,\frac{\mathrm{Im}\,(e^{-2i\beta}\rho_f)}{1+|\rho_f|^2}\,, \tag{102}$$

which are phase-convention independent. (The CKM angle β is defined according to the convention of the Particle Data Group.) The system of four decay modes defines five asymmetries, C_f, S_f, $C_{\bar{f}}$, $S_{\bar{f}}$ – alternatively parametrized as $C \equiv \frac{1}{2}(C_f + C_{\bar{f}})$, $S \equiv \frac{1}{2}(S_f + S_{\bar{f}})$, $\Delta C \equiv \frac{1}{2}(C_f - C_{\bar{f}})$ and $\Delta S \equiv \frac{1}{2}(S_f - S_{\bar{f}})$ – together with the global charge asymmetry related to the overall normalization of (100):

$$\frac{1+A_{\mathrm{CP}}}{1-A_{\mathrm{CP}}} \equiv \frac{|\mathcal{A}_f|^2 + |\bar{\mathcal{A}}_f|^2}{|\mathcal{A}_{\bar{f}}|^2 + |\bar{\mathcal{A}}_{\bar{f}}|^2}\,, \tag{103}$$

or

$$A_{\rm CP} = \frac{|\mathcal{A}_f|^2 + |\bar{\mathcal{A}}_f|^2 - |\mathcal{A}_{\bar f}|^2 - |\bar{\mathcal{A}}_{\bar f}|^2}{|\mathcal{A}_f|^2 + |\bar{\mathcal{A}}_f|^2 + |\mathcal{A}_{\bar f}|^2 + |\bar{\mathcal{A}}_{\bar f}|^2} \,. \tag{104}$$

Under a CP transformation ρ_f goes into $1/\rho_{\bar f}$; hence ΔC and ΔS are CP-even, but $A_{\rm CP}$, C, and S are CP-odd. For the special case that f is a CP eigenstate there are only two different amplitudes since $f=\bar f$, and $A_{\rm CP}$, ΔC and ΔS vanish.

For the $\pi\rho$ system we identify $f=\pi^-\rho^+$. We write the amplitudes as

$$\begin{aligned}
\bar{\mathcal{A}}_f = \bar{\mathcal{A}}_{\pi^-\rho^+} &= A_{\rho\pi}\,|\lambda_u^{(d)}|\,T_{\rho\pi}\left(e^{-i\gamma}+\frac{P_{\rho\pi}}{T_{\rho\pi}}\right), \\
\mathcal{A}_f = \mathcal{A}_{\pi^-\rho^+} &= -\,A_{\pi\rho}\,|\lambda_u^{(d)}|\,T_{\pi\rho}\left(e^{i\gamma}+\frac{P_{\pi\rho}}{T_{\pi\rho}}\right).
\end{aligned} \tag{105}$$

For $\bar f=\pi^+\rho^-$ one must exchange $\pi\leftrightarrow\rho$ on A, T, and P. These equations define the "tree" amplitudes T and the "penguin-to-tree" ratios, while the factors $A_{\pi\rho}$ and $A_{\rho\pi}$ are given by (11). From (95) we see that $\bar{\mathcal{A}}_{\pi^-\rho^+}$ is proportional to $A_{\rho\pi}$ up to the small weak annihilation contribution $\delta_{pu}\beta_1+\beta_4^p$, which suggests to extract this factor as we have done. The sign in the last amplitude is related to the CP convention for the B-meson state and the convention that all decay constants and form factors are taken to be positive.[5]

[5]The phases of the B-meson decay amplitudes are obtained as follows. Let $\mathrm{C}\,|\pi^-\rangle=\xi_\pi|\pi^+\rangle$ and $\mathrm{C}\,|\rho^-\rangle=\xi_\rho|\rho^+\rangle$. Our CP convention for the B meson implies $\mathrm{C}|\bar B^0\rangle=|B^0\rangle$, i.e., $\xi_B=1$. Isospin invariance suggests to choose $\xi_\pi=1$ and $\xi_\rho=-1$, since π^0 is C-even and ρ^0 is C-odd, but in the following we shall keep the charge-conjugation phases for the charged pions and ρ mesons arbitrary. It follows from this that $|\pi^-\pi^+\rangle$ is CP-even, but $\mathrm{CP}\,|\pi^-(\vec p)\rho^+(-\vec p)\rangle=\xi_\pi\xi_\rho^*|\pi^+(-\vec p)\rho^-(\vec p)\rangle=-\xi_\pi\xi_\rho^*|\pi^+(\vec p)\rho^-(-\vec p)\rangle$. The second equality assumes that we form a wave-packet state by integrating over the relative momentum $\vec p$ and uses that the $\pi^-\rho^+$ is in a P-wave state. Using $\mathrm{CP}\,\mathcal{O}\,(\mathrm{CP})^\dagger=\mathcal{O}^\dagger$ for the operators in the effective weak Hamiltonian and dropping the momentum labels that are understood to be equal on the left and right-hand sides, we obtain

$$\langle\pi^-\pi^+|\mathcal{O}^\dagger|B^0\rangle=-\langle\pi^-\pi^+|\mathcal{O}|\bar B^0\rangle\,,\qquad \langle\pi^-\rho^+|\mathcal{O}^\dagger|B^0\rangle=\xi_\pi\xi_\rho^*\,\langle\pi^+\rho^-|\mathcal{O}|\bar B^0\rangle\,.$$

This can be used to show that $\rho_{\pi^+\pi^-}=-e^{-2i\gamma}$, and hence $S_{\pi\pi}=\sin 2\alpha$ in the absence of the penguin contribution. Similarly, one finds $S_{\pi^0\rho^0}=\sin 2\alpha$ for the neutral $\pi\rho$ final state.

The conclusion is more subtle in the case of a non-CP eigenstate such as $\pi^\mp\rho^\pm$, since after applying the CP transformation $\rho_{\pi^-\rho^+}$ involves the $\bar B$ matrix elements of two different final states. To clarify the issue we evaluate the matrix elements in naive factorization before and after applying the CP transformation, neglecting in addition the penguin contribution. This gives

$$\rho_{\pi^-\rho^+}=e^{-2i\gamma}\,\frac{f_{\pi^-}A_0^{\bar B\to\rho^+}}{f_{\rho^+}F_0^{B\to\pi^-}}=e^{-2i\gamma}\,\xi_\pi\xi_\rho^*\,\frac{f_{\pi^-}A_0^{\bar B\to\rho^+}}{f_{\rho^-}F_0^{\bar B\to\pi^+}}\,.$$

The standard C and P transformations of the vector and axial-vector currents together with the CP convention for the B meson imply $f_{\pi^+}=\xi_\pi f_{\pi^-}$, $f_{\rho^+}=-\xi_\rho f_{\rho^-}$, $F_0^{B\to\pi^-}=-\xi_\pi^* F_0^{\bar B\to\pi^+}$, and $A_0^{B\to\rho^-}=\xi_\rho^* A_0^{\bar B\to\rho^+}$. The previous equation is consistent with this. However, the relative phase (actually, only a sign) of f_B times the form factor to the light-meson decay constant cannot be inferred from symmetry considerations alone. Neither can it be determined from the semileptonic decay rates, which provide

Table 12: Magnitudes of the amplitude parameters in $B \to \pi\pi$ and $B \to \pi\rho$ decays.

	Theory	S2	S3	S4
$\lvert T_{\pi\pi}\rvert$	$0.91^{+0.05}_{-0.07}$	0.75	0.92	0.81
$\lvert P_{\pi\pi}/T_{\pi\pi}\rvert$	$0.32^{+0.16}_{-0.09}$	0.49	0.37	0.48
$\lvert T_{\pi\rho}\rvert$	$0.98^{+0.04}_{-0.07}$	0.88	0.99	0.88
$\lvert P_{\pi\rho}/T_{\pi\rho}\rvert$	$0.10^{+0.06}_{-0.04}$	0.12	0.12	0.20
$\lvert T_{\rho\pi}\rvert$	$1.07^{+0.09}_{-0.07}$	1.03	1.11	1.07
$\lvert P_{\rho\pi}/T_{\rho\pi}\rvert$	$0.10^{+0.09}_{-0.05}$	0.19	0.14	0.15

The magnitudes of the "tree" and "penguin-to-tree" parameters in QCD factorization are given in Table 12, where we also show the corresponding quantities for the $\pi\pi$ case. Note that the sign of $P_{\rho\pi}/T_{\rho\pi}$ is negative in naive factorization, where all amplitudes are real, while the other two penguin-to-tree ratios are positive. The largest uncertainty on the penguin-to-tree ratios is caused by $|V_{ub}|$, m_s, and weak annihilation. The important point is that the penguin amplitudes are smaller for the $\pi\rho$ final states compared to $\pi\pi$. Furthermore, $|P_{\pi\rho}/T_{\pi\rho}|$ and $|P_{\rho\pi}/T_{\rho\pi}|$ are similar in magnitude and interfere with an opposite sign with the tree amplitude. We should note that the near equality of the two penguin-to-tree ratios is the result of intricate dynamics specific to factorization. $|P_{\pi\rho}/T_{\pi\rho}|$ is explained by the fact that $a_4^c(\pi\rho) + r_\chi^\rho a_6^c(\pi\rho) \approx a_4^c(\pi\rho)$, since the scalar penguins have a small effect on PV amplitudes. On the other hand, for $|P_{\rho\pi}/T_{\rho\pi}|$ the scalar penguin amplitude $a_6^c(\rho\pi)$ is large and changes the sign of $a_4^c(\rho\pi) - r_\chi^\pi a_6^c(\rho\pi)$, such that the PV and VP amplitudes have similar magnitude but opposite sign.

The results for the time-dependent asymmetry parameters are given in Table 13 including again our default prediction with errors and the four standard scenarios to exhibit possible correlations. Since the penguin-to-tree ratios are small, it is instructive to compare the complete results with an expansion of the asymmetries in these ratios.

---

access only to the magnitudes of these quantities. The expression after the second equality makes it clear that we cannot simply assume all decay constants and form factors to be positive numbers.

To fix the sign we have to resort to theoretical input such as lattice calculations or QCD sum rules. We then find that the (re-phasing invariant) ratios $f_B F_0^{\bar{B}\to\pi^+}/f_{\pi^+}$, $f_B A_0^{\bar{B}\to\rho^+}/f_{\rho^+}$ are positive (see, for instance, [60]), hence $f_B F_0^{B\to\pi^-}/f_{\pi^-}$ and the ratio of form factors and decay constants in $\rho_{\pi^-\rho^+}$ is negative. However, in this paper we have ignored the possible phase and sign conventions for the decay constants and form factors, always assuming them positive. Hence, we must write

$$\rho_{\pi^-\rho^+} = -e^{-2i\gamma}\,\frac{A_{\rho\pi}}{A_{\pi\rho}}$$

in the naive factorization approximation. In QCD factorization these considerations carry over to the full amplitude. This explains the minus sign in the B-meson decay amplitude of (105).

Table 13: Parameters of the time-dependent $B \to \pi^\mp \rho^\pm$ decay rate asymmetries as defined in the text. S and ΔS are computed for $\beta = 23.6°$, corresponding to $\sin(2\beta) = 0.734$.

	Theory	S1	S2	S3	S4	Experiment
$A_{\rm CP}$	$0.01\,{}^{+0.00\,+0.01\,+0.00\,+0.10}_{-0.00\,-0.01\,-0.00\,-0.10}$	0.01	0.02	-0.08	-0.08	-0.21 ± 0.08
C	$0.00\,{}^{+0.00\,+0.01\,+0.00\,+0.02}_{-0.00\,-0.01\,-0.00\,-0.02}$	0.01	0.00	0.02	0.05	0.36 ± 0.18
S	$0.13\,{}^{+0.60\,+0.04\,+0.02\,+0.02}_{-0.65\,-0.03\,-0.01\,-0.01}$	1.00	0.20	0.14	0.09	0.19 ± 0.24
ΔC	$0.16\,{}^{+0.06\,+0.23\,+0.01\,+0.01}_{-0.07\,-0.26\,-0.02\,-0.02}$	0.03	0.01	0.15	0.00	0.28 ± 0.19
ΔS	$-0.02\,{}^{+0.01\,+0.00\,+0.00\,+0.01}_{-0.00\,-0.01\,-0.00\,-0.01}$	0.00	-0.02	0.00	-0.03	0.15 ± 0.25

Defining $P_{\pi\rho}/T_{\pi\rho} = a\, e^{i\delta_a}$, $P_{\rho\pi}/T_{\rho\pi} = -b\, e^{i\delta_b}$ (such that δ_a, δ_b are small and a, b are positive), and $A_{\rho\pi}T_{\rho\pi}/(A_{\pi\rho}T_{\pi\rho}) = R\, e^{i\delta_T}$, and treating a, b, and δ_T as small, the leading terms read

$$\begin{aligned}
A_{\rm CP} &= \frac{2}{1+R^2}\,\left(a\sin\delta_a + R^2\, b\sin\delta_b\right)\sin\gamma + \dots\,,\\
C &= \frac{4R^2}{(1+R^2)^2}\,(a\sin\delta_a - b\sin\delta_b)\sin\gamma + \dots\,,\\
\Delta C &= \frac{1-R^2}{1+R^2} + \frac{4R^2}{(1+R^2)^2}\,(a\cos\delta_a + b\cos\delta_b)\cos\gamma + \dots\,,\\
S &= \frac{2R}{1+R^2}\,\sin 2\alpha - \frac{2R}{1+R^2}\left\{a\cos\delta_a\left(\frac{2\sin 2\alpha}{1+R^2}\cos\gamma + \sin(2\beta+\gamma)\right)\right.\\
&\quad\left. -\; b\cos\delta_b\left(\frac{2R^2\sin 2\alpha}{1+R^2}\cos\gamma + \sin(2\beta+\gamma)\right)\right\} + \dots\,,\\
\Delta S &= \frac{2R}{1+R^2}\,\cos 2\alpha\sin\delta_T - \frac{2R}{1+R^2}\left\{a\sin\delta_a\left(\frac{2\sin 2\alpha}{1+R^2}\sin\gamma + \cos(2\beta+\gamma)\right)\right.\\
&\quad\left. +\; b\sin\delta_b\left(\frac{2R^2\sin 2\alpha}{1+R^2}\sin\gamma + \cos(2\beta+\gamma)\right)\right\} + \dots\,,
\end{aligned} \tag{106}$$

with $\alpha = \pi - \beta - \gamma$. The numerical values of a and b are given in Table 12. With our input parameters the tree-to-tree ratio is given by $R = 0.91\,{}^{+0.26}_{-0.21}$ with phase $\delta_T = (1{\pm}3)°$, where the sizable error on R is entirely due to the form factors.

The asymmetries $A_{\rm CP}$, C, and ΔS are suppressed by the penguin-to-tree ratios and the sin of a strong phase, hence they are always small in QCD factorization. This can be seen explicitly in Table 13. Note that ΔS has a potentially large coefficient in front of $\sin\delta_T$, however a large relative phase of the PV and VP tree amplitudes would constitute

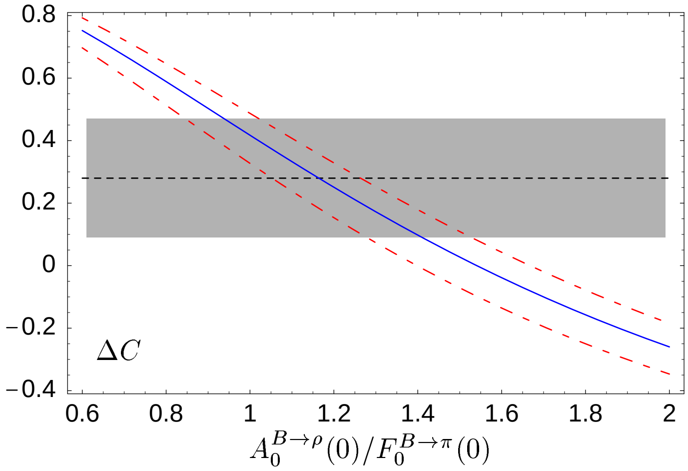

Figure 12: Dependence of ΔC on the ratio of B-meson form factors (for fixed $F^{B\to\pi}(0) = 0.28$) for $\gamma = 70^\circ$ (center solid), $\gamma = 40^\circ$ (upper dashed) and $\gamma = 100^\circ$ (lower dashed). The experimental value with its 1σ error is also shown. Our central input value for the form-factor ratio is 1.32.

a rather unexpected failure of QCD factorization. The data show a large value of C, which is related to the large direct CP asymmetry in $\bar{B} \to \pi^-\rho^+$, since

$$A_{\rm CP}(\pi^-\rho^+) = \frac{A_{\rm CP}\,(1-\Delta C) - C}{1-\Delta C - A_{\rm CP}\,C}\,, \qquad A_{\rm CP}(\pi^\mp\rho^\pm) = -\frac{A_{\rm CP}\,(1+\Delta C) + C}{1+\Delta C + A_{\rm CP}\,C}\,. \tag{107}$$

It seems impossible to accommodate a penguin–tree interference as large as needed to reproduce the central experimental values of $A_{\rm CP}$ and C within QCD factorization.

In first approximation ΔC is determined by the ratio R alone, with the largest uncertainty due to the form factor ratio $A_0^{B\to\rho}(0)/F_0^{B\to\pi}(0)$. Since R is close to 1, the second term in the expansion in the penguin-to-tree ratios is also important and introduces some dependence on γ. This ratio is graphically displayed in Figure 12.

The most interesting asymmetry is S. The numerical values of the parameters R, a, b, δ_a, and δ_b are such that the first correction to S in (106) nearly cancels, hence S is nearly proportional to $\sin(2\alpha)$. Furthermore, the expression $2R/(1+R^2)$ is not very sensitive to R near $R=1$, leaving little uncertainty from the B-meson form factors. This suggests that α or, more precisely, γ (given the B–$\bar{B}$ mixing phase) can be accurately determined from this asymmetry. In the upper panel of Figure 13 we overlay the experimental 1σ band for S to the theoretical prediction given as a function of γ for $\beta = 23.6^\circ$, which (up to a discrete ambiguity) corresponds to the current measurement of the B–$\bar{B}$ mixing phase. The figure also contains two further curves, which define the theory error band, including the error $\pm 2.4^\circ$ on β. Since this observable might be used to put a constraint on γ, we adopt an estimate of the theoretical error where the parameters ϱ_A that model the size of weak annihilation are allowed to vary independently for the PV and VP annihilation coefficients. This is more conservative than the standard error estimate, since it allows for a significant difference in the magnitudes of $P_{\pi\rho}/T_{\pi\rho}$ and $P_{\rho\pi}/T_{\rho\pi}$,

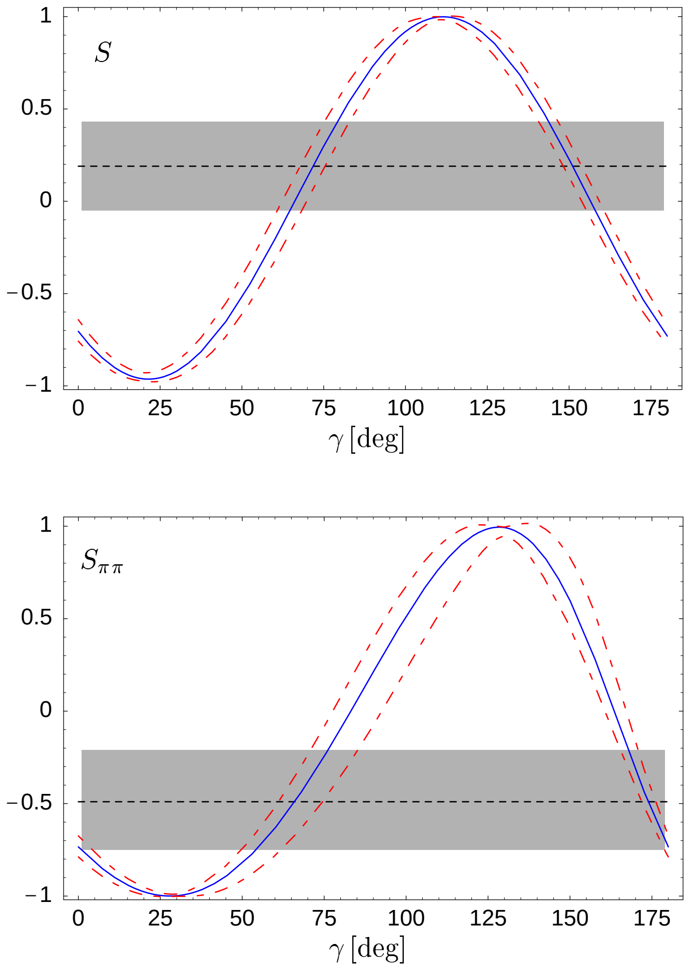

Figure 13: Dependence of S on the γ for $\beta = (23.6 \pm 2.4)^\circ$. Upper panel: S from the $\pi^\mp \rho^\pm$ final states. Lower panel: $S_{\pi\pi}$ from the $\pi^-\pi^+$ final state. The experimental values of S and $S_{\pi\pi}$ with their 1σ errors are overlaid. The dashed curves specify the theoretical error.

which breaks the near cancellation in the correction term to S in (106). The figure shows that the theoretical error remains small even with this conservative estimate. Using $S_{\rm exp} = 0.19 \pm 0.24$ we obtain the allowed ranges

$$\gamma = (72 \pm 11)^\circ \quad \text{or} \quad \gamma = (151 \pm 10)^\circ \qquad (\text{from } S)\,, \tag{108}$$

where the limiting values are defined by the intersection of the theory error band with the 1σ experimental error band. The error given is dominated by the experimental error. The first range is in reasonable agreement with the standard unitarity-triangle fit. Note that if we allow for the second solution for β, given by $\beta \to \pi/2 - \beta$, we obtain the above ranges with $\gamma \to 180^\circ - \gamma$ to a very good approximation.

It is interesting to compare the constraint on γ from S with the constraint obtained from the analogous asymmetry in the decay to the $\pi^-\pi^+$ final state. Here the correction due to the penguin amplitude is larger. The current average experimental value $S_{\pi\pi} = -0.49 \pm 0.27$ yields

$$\gamma = (66\,^{+19}_{-16})^\circ \quad \text{or} \quad \gamma = (174\,^{+9}_{-8})^\circ \qquad (\text{from } S_{\pi\pi})\,, \tag{109}$$

as shown in the lower panel of Figure 13. Despite the rather different values of the asymmetry, the allowed values of γ are consistent with each other, in particular for the first range that is also compatible with the standard unitarity-triangle fit. This provides a strong argument for the validity of the theoretical framework underlying the computation of the hadronic amplitudes. While this is reassuring, one should keep in mind that there are several aspects of the current $\pi\pi$ and $\pi\rho$ data that cannot be accommodated in QCD factorization, in particular the large direct CP asymmetries for $\pi^-\pi^+$ and $\pi^-\rho^+$. Other pieces of data, such as the measurements of $S_{\pi\pi}$, are not compatible between the BaBar and Belle experiments. It remains to be seen whether these anomalies disappear without affecting the apparent consistency of the remaining data.

The analysis of the $\pi\rho$ final states has been performed under the assumption that the ρ-meson width is negligible. The experimental error from the quasi two-body assumption on the extraction of the parameters of the time-evolution of $B, \bar{B} \to \pi^\mp\rho^\pm$ decays has been estimated as 0.08 for the CP-violating parameters $A_{\rm CP}$, C, and S, and as 0.03 for ΔC and ΔS [61]. This leaves enough room for an improvement of the experimental error, so that we can look forward to more comprehensive unitarity-triangle constraints from the $\pi\rho$ system once higher statistics data samples become available.

7 Final states containing η or η'

In this section we give results for the 23 B^- and $\bar{B}^0$ decays into final states containing the mesons η or η'. A dedicated investigation of the $\Delta S = 1$ decays in QCD factorization has already been performed in [18]. For comparison of the different scenarios that we defined in the present paper we repeat the results for these decays in Tables 14 and 15. Small differences in the "Theory" column relative to the "Default" in [18] result from slight changes in the input parameters as mentioned in Section 3.

We shall not repeat here the discussion of the complex dynamics of decays to mesons with flavor-singlet components that is particularly important for the penguin-dominated $\Delta S = 1$ decays. Let us briefly summarize the conclusions reached in [18]. The singlet penguin amplitude is presumably small and plays no important role in the enhancement of the $\bar{B} \to \eta' \bar{K}$ branching fractions. Rather, the particular pattern of the $\bar{B} \to \eta^{(\prime)} \bar{K}^{(*)}$ decay rates is caused by the interference of different non-singlet penguin amplitudes. In particular, the large $\bar{B} \to \eta' \bar{K}$ branching fractions are obtained naturally in QCD factorization. There are, however, large uncertainties in applying QCD factorization to $\eta^{(\prime)}$ final states related to η–η' mixing, a possible singlet contribution to the $B \to \eta^{(\prime)}$ form factors, and a novel, soft spectator-scattering term. The numerical results given in the tables and their errors corroborate these findings.

The $\Delta D = 1$ decay modes all have small branching fractions (and, perhaps, large CP asymmetries) unless they involve the color-favored tree coefficient α_1. The corresponding

Table 14: CP-averaged branching ratios (in units of 10^{-6}) of penguin-dominated $\bar{B} \to PP$ decays (top) and $\bar{B} \to PV$ decays (bottom) with $\Delta S = 1$. The errors and scenarios have the same meaning as explained in Section 5.

Mode	Theory	S1	S2	S3	S4	Experiment
$B^- \to \eta K^-$	$1.9^{+0.5}_{-0.5}{}^{+2.4}_{-1.6}{}^{+0.5}_{-0.6}{}^{+1.6}_{-0.7}$	1.1	1.6	2.4	1.6	3.1 ± 0.7
$\bar{B}^0 \to \eta \bar{K}^0$	$1.1^{+0.1}_{-0.1}{}^{+2.0}_{-1.3}{}^{+0.4}_{-0.5}{}^{+1.3}_{-0.5}$	1.0	1.1	1.6	1.1	< 4.6
$B^- \to \eta' K^-$	$49.1^{+5.1}_{-4.9}{}^{+26.5}_{-16.3}{}^{+13.6}_{-7.4}{}^{+33.6}_{-14.6}$	52.1	78.3	64.6	76.1	77.6 ± 4.6
$\bar{B}^0 \to \eta' \bar{K}^0$	$46.5^{+4.7}_{-4.4}{}^{+24.9}_{-15.4}{}^{+12.3}_{-6.8}{}^{+31.0}_{-13.5}$	46.0	72.8	60.7	70.3	60.6 ± 7.0
$B^- \to \eta K^{*-}$	$10.8^{+1.9}_{-1.7}{}^{+8.1}_{-4.4}{}^{+1.8}_{-1.3}{}^{+16.5}_{-5.5}$	14.0	19.4	19.1	19.9	25.4 ± 5.3
$\bar{B}^0 \to \eta \bar{K}^{*0}$	$10.7^{+1.1}_{-1.0}{}^{+7.8}_{-4.3}{}^{+1.4}_{-1.2}{}^{+16.2}_{-5.5}$	10.7	18.2	18.6	18.6	16.4 ± 3.0
$B^- \to \eta' K^{*-}$	$5.1^{+0.9}_{-1.0}{}^{+7.5}_{-3.8}{}^{+2.1}_{-3.0}{}^{+6.7}_{-3.3}$	3.5	7.6	7.1	2.2	< 35
$\bar{B}^0 \to \eta' \bar{K}^{*0}$	$3.9^{+0.4}_{-0.4}{}^{+6.6}_{-3.3}{}^{+1.8}_{-2.5}{}^{+6.2}_{-2.9}$	3.7	6.7	6.0	1.9	< 13

results are summarized in Tables 16 and 17. We discuss specifically here only the $\Delta D = 1$ decays to final states with one pion or ρ meson. The two independent decay amplitudes, simplified according to Section 4.2, are given by

$$\begin{aligned}
\sqrt{2}\,\mathcal{A}_{B^-\to\pi^-\eta} &= A_{\pi\eta_q}\Big[\delta_{pu}\,(\alpha_2+\beta_2)+2\hat{\alpha}_3^p+\hat{\alpha}_4^p\Big]+\sqrt{2}A_{\pi\eta_s}\hat{\alpha}_3^p+\sqrt{2}A_{\pi\eta_c}\delta_{pc}\,\alpha_2 \\
&\quad + A_{\eta_q\pi}\Big[\delta_{pu}\,(\alpha_1+\beta_2)+\hat{\alpha}_4^p\Big], \\
-2\,\mathcal{A}_{\bar{B}^0\to\pi^0\eta} &= A_{\pi\eta_q}\Big[\delta_{pu}\,(\alpha_2-\beta_1)+2\hat{\alpha}_3^p+\hat{\alpha}_4^p\Big]+\sqrt{2}A_{\pi\eta_s}\hat{\alpha}_3^p+\sqrt{2}A_{\pi\eta_c}\delta_{pc}\,\alpha_2 \\
&\quad + A_{\eta_q\pi}\Big[\delta_{pu}\,(-\alpha_2-\beta_1)+\hat{\alpha}_4^p\Big], \qquad (110)
\end{aligned}$$

where $\hat{\alpha}_3^p \equiv \alpha_3^p + \beta_{S3}^p$. The amplitudes for $\bar{B} \to \pi\eta'$ and $\bar{B} \to \rho\eta^{(\prime)}$ are obtained from these results by replacing $(\pi,\eta) \to (\pi,\eta')$ and $(\pi,\eta) \to (\rho,\eta^{(\prime)})$, respectively. We find that the singlet coefficient $\hat{\alpha}_3^p$ and the "charm content" in the $\eta^{(\prime)}$ are small. The amplitudes can then be further approximated by setting $\hat{\alpha}_3^p$ and $A_{M_1\eta_c'}$ to zero.

The neutral B-meson decays to $\pi^0\eta^{(\prime)}$ and $\rho^0\eta^{(\prime)}$ have small branching fractions, because the color-suppressed tree amplitudes proportional to α_2 tend to cancel each other. A consequence of this is that the $\bar{B}^0 \to \rho^0\eta^{(\prime)}$ decay rates are predicted to be much smaller than the $\bar{B}^0 \to \pi^0\eta^{(\prime)}$ rates, because the residual PV and VP penguin amplitudes are smaller. The charged decays have branching fractions of a few times 10^{-6}. We note from (110) that the penguin coefficient $\hat{\alpha}_4^p$ enters both parts of the amplitude with equal sign. We should therefore expect larger penguin–tree interference in $\bar{B}^0 \to \pi^-\eta$ than in $\bar{B}^0 \to \pi^-\pi^+$. Data are available only for $B^- \to \pi^-\eta$, whose branching fraction

Table 15: Direct CP asymmetries (in units of 10^{-2}) of penguin-dominated $\bar{B} \to PP$ decays (top) and $\bar{B} \to PV$ decays (bottom) with $\Delta S = 1$.

Mode	Theory	S1	S2	S3	S4	Experiment
$B^- \to \eta K^-$	$-18.9^{+6.4+11.7+4.8+25.3}_{-6.9-17.5-8.5-21.8}$	-33.3	-19.6	2.7	9.6	-32 ± 20
$\bar{B}^0 \to \eta \bar{K}^0$	$-9.0^{+2.8+5.4+2.8+8.2}_{-2.1-12.6-6.2-7.8}$	-10.2	-10.3	-3.5	0.5	—
$B^- \to \eta' K^-$	$2.4^{+0.6+0.6+0.3+3.4}_{-0.7-0.8-0.4-3.5}$	2.3	1.6	-0.6	-0.8	2 ± 4
$\bar{B}^0 \to \eta' \bar{K}^0$	$1.8^{+0.4+0.3+0.1+0.8}_{-0.5-0.3-0.2-0.8}$	1.9	1.4	1.2	0.7	8 ± 18
$B^- \to \eta K^{*-}$	$3.5^{+0.9+1.9+0.8+20.7}_{-0.9-2.7-0.8-20.5}$	2.7	3.0	-9.2	-5.7	-5 ± 28
$\bar{B}^0 \to \eta \bar{K}^{*0}$	$3.8^{+0.9+1.1+0.2+3.8}_{-1.1-0.8-0.2-3.5}$	3.8	2.9	1.5	0.8	17 ± 27
$B^- \to \eta' K^{*-}$	$-14.2^{+4.7+8.5+4.9+27.5}_{-4.2-13.8-14.6-26.1}$	-20.8	-9.8	4.5	22.1	—
$\bar{B}^0 \to \eta' \bar{K}^{*0}$	$-5.5^{+1.6+3.1+1.8+6.2}_{-1.3-5.1-5.9-7.0}$	-5.8	-4.1	-2.4	1.7	—

Table 16: CP-averaged branching ratios (in units of 10^{-6}) of tree-dominated $\bar{B} \to PP$ decays (top) and $\bar{B} \to PV$ decays (bottom) with $\Delta D = 1$.

Mode	Theory	S1	S2	S3	S4	Experiment
$B^- \to \pi^- \eta$	$4.7^{+1.9+1.8+0.6+0.4}_{-1.7-1.5-0.3-0.3}$	2.7	4.1	4.7	3.8	3.9 ± 0.9
$\bar{B}^0 \to \pi^0 \eta$	$0.28^{+0.09+0.43+0.02+0.19}_{-0.08-0.26-0.02-0.08}$	0.45	0.31	0.35	0.30	< 2.9
$B^- \to \pi^- \eta'$	$3.1^{+1.3+1.2+0.6+0.3}_{-1.2-1.0-0.3-0.3}$	1.8	3.1	3.1	2.9	< 7
$\bar{B}^0 \to \pi^0 \eta'$	$0.17^{+0.05+0.28+0.10+0.14}_{-0.05-0.16-0.05-0.06}$	0.27	0.36	0.24	0.35	< 5.7
$\bar{B}^0 \to \eta\eta$	$0.16^{+0.03+0.43+0.09+0.10}_{-0.03-0.18-0.03-0.05}$	0.13	0.24	0.23	0.27	—
$\bar{B}^0 \to \eta\eta'$	$0.16^{+0.04+0.59+0.14+0.07}_{-0.04-0.16-0.06-0.05}$	0.10	0.30	0.20	0.31	—
$\bar{B}^0 \to \eta'\eta'$	$0.06^{+0.01+0.23+0.07+0.06}_{-0.01-0.05-0.03-0.03}$	0.03	0.13	0.10	0.16	—
$B^- \to \eta\rho^-$	$9.4^{+4.6+3.6+0.7+0.7}_{-3.7-3.0-0.4-0.7}$	8.3	6.3	9.1	6.3	< 6.2
$\bar{B}^0 \to \eta\rho^0$	$0.03^{+0.02+0.16+0.02+0.05}_{-0.01-0.10-0.01-0.02}$	0.05	0.04	0.06	0.09	< 5.5
$B^- \to \eta'\rho^-$	$6.3^{+3.1+2.4+0.5+0.5}_{-2.5-2.0-0.3-0.5}$	6.0	4.3	6.1	4.2	< 33
$\bar{B}^0 \to \eta'\rho^0$	$0.01^{+0.01+0.11+0.02+0.03}_{-0.00-0.06-0.00-0.01}$	0.01	0.03	0.03	0.06	< 12
$\bar{B}^0 \to \eta\omega$	$0.31^{+0.14+0.16+0.35+0.22}_{-0.12-0.11-0.14-0.16}$	0.23	0.53	0.44	0.65	—
$\bar{B}^0 \to \eta'\omega$	$0.20^{+0.10+0.15+0.25+0.15}_{-0.08-0.05-0.10-0.11}$	0.17	0.36	0.29	0.44	—
$\bar{B}^0 \to \eta\phi$	≈ 0.001	0.001	0.001	0.000	0.001	—
$\bar{B}^0 \to \eta'\phi$	≈ 0.001	0.002	0.002	0.002	0.003	—

Table 17: Direct CP asymmetries (in units of 10^{-2}) of tree-dominated $\bar{B} \to PP$ decays (top) and $\bar{B} \to PV$ decays (bottom) with $\Delta D = 1$. We only consider modes with branching fractions larger than 10^{-7}.

Mode	Theory	S1	S2	S3	S4	Experiment
$B^- \to \pi^- \eta$	$-14.9^{+4.9+8.3+1.3+17.4}_{-5.4-7.4-0.8-17.3}$	-25.9	-15.4	0.7	5.6	-51 ± 19
$\bar{B}^0 \to \pi^0 \eta$	$-17.9^{+5.2+7.9+1.2+33.4}_{-4.1-14.1-1.4-32.9}$	-11.0	-15.8	3.8	8.5	—
$B^- \to \pi^- \eta'$	$-8.6^{+2.8+10.5+0.7+20.4}_{-3.1-9.0-0.7-20.4}$	-14.9	-10.5	8.6	11.1	—
$\bar{B}^0 \to \pi^0 \eta'$	$-19.2^{+5.5+7.7+4.1+35.7}_{-4.3-7.8-3.3-35.8}$	-11.9	-12.1	1.9	6.1	—
$\bar{B}^0 \to \eta\eta$	$-62.8^{+18.1+65.6+19.0+23.4}_{-13.1-22.2-9.5-16.2}$	-79.1	-41.3	-45.1	-20.1	—
$\bar{B}^0 \to \eta\eta'$	$-56.3^{+17.1+141.0+20.7+13.7}_{-16.6-16.1-15.8-16.3}$	-87.2	-34.3	-46.8	-28.0	—
$\bar{B}^0 \to \eta'\eta'$	$-46.0^{+14.6+138.4+22.0+40.2}_{-14.9-11.0-17.5-34.0}$	-75.3	-27.8	-18.4	-3.5	—
$B^- \to \eta\rho^-$	$-2.4^{+0.7+6.3+0.4+0.2}_{-0.7-6.3-0.4-0.2}$	-2.7	-1.9	-2.4	-6.0	—
$B^- \to \eta'\rho^-$	$4.1^{+1.2+7.9+0.5+7.0}_{-1.1-6.9-0.8-7.0}$	4.3	5.2	4.1	1.1	—
$\bar{B}^0 \to \eta\omega$	$-33.4^{+10.0+65.3+20.9+19.2}_{-9.5-55.8-21.4-20.8}$	-44.9	-10.5	-31.4	-27.5	—
$\bar{B}^0 \to \eta'\omega$	$0.2^{+0.1+53.0+11.6+20.4}_{-0.1-76.5-11.5-20.1}$	0.2	3.7	-1.9	-15.2	—

is in good agreement with our result. The upper limit on the $\eta\rho^-$ final state is already below or near our prediction, and hence we expect this decay to be discovered soon.

It should be noted that some of the decay rates for final states containing an η' meson, in particular the modes $B^- \to \pi^-\eta'$, $\rho^-\eta'$, are very sensitive to the singlet contribution to the $B \to \eta'$ form factor in (62), which we simply put to zero. For instance, setting $F_2 = 0.1$ increases $\mathrm{Br}(B^- \to \eta'\pi^-)$ to about 7×10^{-6}, and $\mathrm{Br}(B^- \to \eta'\rho^-)$ to 16×10^{-6}.

The direct CP asymmetries in Table 17 confirm the possibility of significant penguin–tree interference in the decays $B^- \to \pi^-\eta^{(\prime)}$. However, the measurement of $A_{\mathrm{CP}}(\pi^-\eta) = (-51 \pm 19)\%$, together with a large CP asymmetry $A_{\mathrm{CP}}(\pi^-\pi^+) = (51 \pm 23)\%$ of opposite sign and a large asymmetry $A_{\mathrm{CP}}(\eta K^-) = (-32 \pm 20)\%$ of the same sign, is difficult to understand in QCD factorization and presumably in any framework (see, for instance, the comments in [62]), unless one can accommodate very large SU(3) flavor-symmetry breaking in the amplitudes pertaining to the $\pi\pi$, $\pi\eta^{(\prime)}$, and $\bar{K}\eta^{(\prime)}$ final states. Indeed, if the dominant interference is between $\hat{\alpha}_4^c$ and α_1, then the two CP asymmetries must have the same sign, barring very large final-state dependence of these coefficients. Possible corrections could come from the singlet penguin amplitude $\hat{\alpha}_3^c$, but for this amplitude to have an effect as significant as indicated by the data, the estimates in [18] or [62] would have to be grossly in error. This leaves α_2, which if large could affect the phase of the penguin-to-tree ratio by a noticeable amount. However, for this to reverse the sign of a large CP asymmetry the color-suppressed tree coefficient would have to exceed the color-allowed one (α_1), which would affect all the color-suppressed B decays.

8 Results for $\bar{B}_s$ decays

8.1 Simplified expressions for the decay amplitudes

So far we have focused our attention on the decays of B^- and $\bar{B}^0$ mesons, which are currently under investigation at the B factories. Our formalism applies equally to the decays of B_s mesons, which cannot be studied at these facilities. These decay modes will soon become accessible at hadronic B factories operated at the Tevatron Run-II, and in the longer term at LHC-b and BTeV. In this section we present results for the branching ratios and CP asymmetries of B_s decays into PP and PV final states. Our predictions are collected in Tables 18–24.

8.1.1 Decays with $\Delta S = 1$

Tables 18 and 19 contain results for penguin-dominated B_s decays with $\Delta S = 1$. The modes with two pseudoscalars in the final state have large branching fractions, which in fact are among the largest of all rare B decays studied in this work. The expressions for the $\bar{B}_s \to \bar{K}K$ amplitudes, simplified according to the approximations described in Section 4.2, are given by

$$\begin{aligned}
\mathcal{A}_{\bar{B}_s\to\bar{K}^0K^0} &= B_{\bar{K}K}\,\delta_{pc}\,b_4^c + A_{K\bar{K}}\Big[\hat{\alpha}_4^p + \delta_{pc}\,\beta_4^c\Big]\,, \\
\mathcal{A}_{\bar{B}_s\to K^-K^+} &= B_{\bar{K}K}\,\delta_{pc}\,b_4^c + A_{K\bar{K}}\Big[\delta_{pu}\,\alpha_1 + \hat{\alpha}_4^p + \delta_{pc}\,\beta_4^c\Big]\,.
\end{aligned} \tag{111}$$

The expressions on the right-hand side must be multiplied with $\lambda_p^{(s)}$ and summed over $p = u, c$. The amplitudes for $\bar{B}_s \to \bar{K}K^*$ and $\bar{B}_s \to \bar{K}^*K$ are obtained from these expressions by interchanging $K \leftrightarrow K^*$ or $\bar{K} \leftrightarrow \bar{K}^*$ everywhere. Apart from the small annihilation terms parameterized by β_4^c these modes are characterized by a simple pattern of tree–penguin interference, which resembles that in the decays $B^- \to \pi^-\bar{K}^0$ and $\bar{B}^0 \to \pi^+K^-$ in (73). This means that many of the analysis strategies discussed in Section 5.1.1 can be applied also here, once experimental data on the decays $\bar{B}_s \to \bar{K}K$ (and the corresponding PV modes) will become available. The expressions for modes involving η or η' are more complicated and will not be given here. The exact decay amplitudes for these modes can be found in Appendix A. Note from Table 18 that the branching fractions for the decays $\bar{B}_s \to \eta^{(\prime)}\omega$ and $\bar{B}_s \to \eta^{(\prime)}\phi$ are several orders of magnitude smaller than the corresponding branching fractions for the decays $\bar{B}_s \to \eta^{(\prime)}\eta^{(\prime)}$. For the $\eta^{(\prime)}\omega$ final states this occurs because the ω meson is assumed to have no strange component. For the case of the $\eta^{(\prime)}\phi$ final states there is a strong cancellation between the PV and VP penguin amplitudes $\hat{\alpha}_4^c(\eta^{(\prime)}\phi)$ and $\hat{\alpha}_4^c(\phi\eta^{(\prime)})$. The corresponding branching fractions can be enhanced by an order of magnitude by choosing a different value for m_s or giving up the assumption of universal annihilation. The direct CP asymmetries of the penguin-dominated B_s decays with $\Delta S = 1$ are predicted to be small except for the modes with very small branching fractions.

Table 18: CP-averaged branching ratios (in units of 10^{-6}) of penguin-dominated $\bar{B}_s \to PP$ decays (top) and $\bar{B}_s \to PV$ decays (bottom) with $\Delta S = 1$. The errors and scenarios have the same meaning as in Section 5.

Mode	Theory	S1	S2	S3	S4
$\bar{B}_s \to K^+K^-$	$22.7^{+3.5\,+12.7\,+2.0\,+24.1}_{-3.2\,-\ 8.4\,-2.0\,-\ 9.1}$	28.0	33.4	34.3	36.1
$\bar{B}_s \to K^0\bar{K}^0$	$24.7^{+2.5\,+13.7\,+2.6\,+25.6}_{-2.4\,-\ 9.2\,-2.9\,-\ 9.8}$	24.0	35.6	36.7	38.3
$\bar{B}_s \to \eta\eta$	$15.6^{+1.6\,+9.9\,+2.2\,+13.5}_{-1.5\,-6.8\,-2.5\,-\ 5.5}$	14.9	22.7	21.4	22.5
$\bar{B}_s \to \eta\eta'$	$54.0^{+5.5\,+32.4\,+8.3\,+40.5}_{-5.2\,-22.4\,-6.4\,-16.7}$	52.4	79.5	72.3	77.7
$\bar{B}_s \to \eta'\eta'$	$41.7^{+4.2\,+26.3\,+15.2\,+36.6}_{-4.0\,-17.2\,-\ 8.5\,-15.4}$	41.4	63.4	60.2	65.5
$\bar{B}_s \to K^+K^{*-}$	$4.1^{+1.7\,+1.5\,+1.0\,+9.2}_{-1.5\,-1.3\,-0.9\,-2.3}$	7.4	4.3	9.0	13.7
$\bar{B}_s \to K^0\bar{K}^{*0}$	$3.9^{+0.4\,+1.5\,+1.3\,+10.4}_{-0.4\,-1.4\,-1.4\,-\ 2.8}$	3.8	4.2	9.1	14.3
$\bar{B}_s \to K^-K^{*+}$	$5.5^{+1.3\,+5.0\,+0.8\,+14.2}_{-1.4\,-2.6\,-0.7\,-\ 3.6}$	3.3	9.9	13.0	9.0
$\bar{B}_s \to \bar{K}^0K^{*0}$	$4.2^{+0.4\,+4.6\,+1.1\,+13.2}_{-0.4\,-2.2\,-0.9\,-\ 3.2}$	4.1	8.7	11.4	7.9
$\bar{B}_s \to \eta\omega$	$0.012^{+0.005\,+0.010\,+0.028\,+0.025}_{-0.004\,-0.003\,-0.006\,-0.006}$	0.017	0.011	0.010	0.009
$\bar{B}_s \to \eta'\omega$	$0.024^{+0.011\,+0.028\,+0.077\,+0.042}_{-0.009\,-0.006\,-0.010\,-0.015}$	0.024	0.024	0.039	0.033
$\bar{B}_s \to \eta\phi$	$0.12^{+0.02\,+0.95\,+0.54\,+0.32}_{-0.02\,-0.14\,-0.12\,-0.13}$	0.15	1.02	0.24	1.47
$\bar{B}_s \to \eta'\phi$	$0.05^{+0.01\,+1.10\,+0.18\,+0.40}_{-0.01\,-0.17\,-0.08\,-0.04}$	0.05	1.08	0.07	2.10

Table 19: Direct CP asymmetries (in units of 10^{-2}) of penguin-dominated $\bar{B}_s \to PP$ decays (top) and $\bar{B}_s \to PV$ decays (bottom) with $\Delta S = 1$. We only consider modes with branching fractions larger than 10^{-7}.

Mode	Theory	S1	S2	S3	S4
$\bar{B}_s \to K^+K^-$	$4.0^{+1.0\,+2.0\,+0.5\,+10.4}_{-1.0\,-2.3\,-0.5\,-11.3}$	3.2	3.0	-4.5	-4.7
$\bar{B}_s \to K^0\bar{K}^0$	$0.9^{+0.2\,+0.2\,+0.1\,+0.2}_{-0.2\,-0.2\,-0.1\,-0.3}$	0.9	0.7	0.6	0.6
$\bar{B}_s \to \eta\eta$	$-1.6^{+0.5\,+0.6\,+0.4\,+2.2}_{-0.4\,-0.6\,-0.7\,-2.2}$	-1.7	-1.1	-0.4	-0.1
$\bar{B}_s \to \eta\eta'$	$0.4^{+0.1\,+0.3\,+0.1\,+0.4}_{-0.1\,-0.3\,-0.1\,-0.3}$	0.4	0.4	0.3	0.2
$\bar{B}_s \to \eta'\eta'$	$2.1^{+0.5\,+0.4\,+0.2\,+1.1}_{-0.6\,-0.4\,-0.3\,-1.2}$	2.1	1.7	1.3	1.0
$\bar{B}_s \to K^+K^{*-}$	$2.2^{+0.6\,+8.4\,+5.1\,+68.6}_{-0.7\,-8.0\,-5.9\,-71.0}$	1.2	1.8	-34.8	-10.0
$\bar{B}_s \to K^0\bar{K}^{*0}$	$1.7^{+0.4\,+0.6\,+0.5\,+1.4}_{-0.5\,-0.5\,-0.4\,-0.8}$	1.7	1.5	1.0	0.8
$\bar{B}_s \to K^-K^{*+}$	$-3.1^{+1.0\,+3.8\,+1.6\,+47.5}_{-1.1\,-2.6\,-1.3\,-45.0}$	-5.2	-2.4	18.8	26.6
$\bar{B}_s \to \bar{K}^0K^{*0}$	$0.2^{+0.0\,+0.2\,+0.1\,+0.2}_{-0.1\,-0.3\,-0.1\,-0.1}$	0.2	0.3	0.1	0.1
$\bar{B}_s \to \eta\phi$	$-8.4^{+2.0\,+30.1\,+14.6\,+36.3}_{-2.1\,-71.2\,-44.7\,-59.7}$	-6.5	3.8	-8.7	-9.5
$\bar{B}_s \to \eta'\phi$	$-62.2^{+15.9\,+132.3\,+80.8\,+122.4}_{-10.2\,-\ 84.2\,-46.8\,-\ 49.9}$	-61.1	-8.9	-34.0	7.5

Table 20: CP-averaged branching ratios (in units of 10^{-6}) of tree-dominated $\bar{B}_s \to PP$ decays (top) and $\bar{B}_s \to PV$ decays (bottom) with $\Delta S = 1$.

Mode	Theory	S1	S2	S3	S4
$\bar{B}_s \to \pi^0\eta$	$0.075\,^{+0.013}_{-0.012}\,^{+0.030}_{-0.025}\,^{+0.008}_{-0.010}\,^{+0.010}_{-0.007}$	0.097	0.069	0.077	0.073
$\bar{B}_s \to \pi^0\eta'$	$0.11\,^{+0.02}_{-0.02}\,^{+0.04}_{-0.04}\,^{+0.01}_{-0.01}\,^{+0.01}_{-0.01}$	0.15	0.10	0.10	0.10
$\bar{B}_s \to \pi^0\omega$	≈ 0.0005	0.0004	0.0004	0.0033	0.0024
$\bar{B}_s \to \pi^0\phi$	$0.12\,^{+0.03}_{-0.02}\,^{+0.04}_{-0.04}\,^{+0.01}_{-0.01}\,^{+0.02}_{-0.01}$	0.16	0.12	0.12	0.12
$\bar{B}_s \to \rho^0\eta$	$0.17\,^{+0.03}_{-0.03}\,^{+0.07}_{-0.06}\,^{+0.02}_{-0.02}\,^{+0.02}_{-0.01}$	0.23	0.17	0.18	0.17
$\bar{B}_s \to \rho^0\eta'$	$0.25\,^{+0.06}_{-0.05}\,^{+0.10}_{-0.08}\,^{+0.02}_{-0.02}\,^{+0.02}_{-0.02}$	0.35	0.24	0.24	0.24

Table 21: Direct CP asymmetries (in units of 10^{-2}) of tree-dominated $\bar{B}_s \to PP$ decays (top) and $\bar{B}_s \to PV$ decays (bottom) with $\Delta S = 1$. We only consider modes with branching fractions larger than 10^{-7}.

Mode	Theory	S1	S2	S3	S4
$\bar{B}_s \to \pi^0\eta'$	$27.8\,^{+6.0}_{-7.1}\,^{+9.6}_{-5.7}\,^{+2.0}_{-2.0}\,^{+24.7}_{-27.2}$	19.5	26.1	36.6	35.3
$\bar{B}_s \to \pi^0\phi$	$27.2\,^{+6.1}_{-6.8}\,^{+9.8}_{-5.6}\,^{+2.7}_{-2.4}\,^{+32.0}_{-37.1}$	20.0	25.2	27.2	24.8
$\bar{B}_s \to \rho^0\eta$	$27.8\,^{+6.4}_{-6.7}\,^{+9.1}_{-5.7}\,^{+2.6}_{-2.2}\,^{+25.9}_{-28.4}$	21.0	25.1	16.4	15.6
$\bar{B}_s \to \rho^0\eta'$	$28.9\,^{+6.1}_{-7.5}\,^{+10.3}_{-\ 6.3}\,^{+1.5}_{-1.8}\,^{+24.8}_{-27.5}$	20.0	26.1	36.7	32.2

Tables 20 and 21 contain results for tree-dominated B_s decays with $\Delta S = 1$. The corresponding branching fractions are very small, typically of order few times 10^{-7}. Accordingly, the direct CP asymmetries can be large in all cases but will hardly be observable in the near future. As an example we quote the simplified amplitude expressions $\mathcal{A}_{\bar{B}_s\to\pi^0\omega} = 0$ and

$$\sqrt{2}\,\mathcal{A}_{\bar{B}_s\to\pi^0\phi} = A_{\phi\pi}\Big[\delta_{pu}\,\alpha_2 + \delta_{pc}\,\tfrac{3}{2}\alpha^c_{3,\mathrm{EW}}\Big]\,. \tag{112}$$

The amplitudes for modes with η or η' are given in Appendix A.

Some of the B_s decays with $\Delta S = 1$ receive only annihilation contributions. As shown in Table 22 these modes have tiny branching fractions of order few times 10^{-9} to few times 10^{-8}. The simplified expressions for the corresponding decay amplitudes are

$$\mathcal{A}_{\bar{B}_s\to\pi^+\rho^-} = \mathcal{A}_{\bar{B}_s\to\pi^0\rho^0} = \delta_{pc}\Big[B_{\pi\rho}\,b^c_4 + B_{\rho\pi}\,b^c_4\Big]\,. \tag{113}$$

The amplitude for $\bar{B}_s \to \pi^-\rho^+$ is obtained from the first expression by interchanging $\pi \leftrightarrow \rho$ everywhere. The expressions for the $\bar{B}_s \to \pi\pi$ amplitudes are obtained by setting $\rho \to \pi$.

Table 22: CP-averaged branching ratios (in units of 10^{-6}) of annihilation-dominated $\bar{B}_s \to PP$ decays (top) and $\bar{B}_s \to PV$ decays (bottom) with $\Delta S = 1$.

Mode	Theory	S1	S2	S3	S4
$\bar{B}_s \to \pi^+\pi^-$	$0.024\,^{+0.003}_{-0.003}\,^{+0.025}_{-0.012}\,^{+0.000}_{-0.000}\,^{+0.163}_{-0.021}$	0.027	0.032	0.149	0.155
$\bar{B}_s \to \pi^0\pi^0$	$0.012\,^{+0.001}_{-0.001}\,^{+0.013}_{-0.006}\,^{+0.000}_{-0.000}\,^{+0.082}_{-0.011}$	0.014	0.016	0.075	0.078
$\bar{B}_s \to \pi^+\rho^-$	≈ 0.003	0.002	0.003	0.019	0.014
$\bar{B}_s \to \pi^0\rho^0$	≈ 0.003	0.002	0.003	0.019	0.017
$\bar{B}_s \to \pi^-\rho^+$	≈ 0.003	0.002	0.003	0.019	0.015

8.1.2 Decays with $\Delta D = 1$

Most B_s decays with $\Delta D = 1$ are dominated by tree topologies. The branching fractions and direct CP asymmetries of these decays are given in Tables 23 and 24. The decays $\bar{B}_s \to \pi^- K^+$, $\pi^- K^{*+}$, and $\rho^- K^+$ have large branching fractions of order $(1–2)\cdot 10^{-5}$. The corresponding neutral modes have much smaller rates. The direct CP asymmetries are predicted to be of moderate, sometimes even large magnitude, ranging from order 10% for the charged modes to significantly larger values for the neutral modes. The simplified expressions for the corresponding decay amplitudes are

$$
\begin{aligned}
\mathcal{A}_{\bar{B}_s\to\pi^- K^+} &= A_{K\pi}\Big[\delta_{pu}\,\alpha_1 + \hat{\alpha}_4^p\Big]\,, \\
\sqrt{2}\,\mathcal{A}_{\bar{B}_s\to\pi^0 K^0} &= A_{K\pi}\Big[\delta_{pu}\,\alpha_2 - \hat{\alpha}_4^p\Big]\,.
\end{aligned}
\tag{114}
$$

The right-hand sides of the expressions must be multiplied with $\lambda_p^{(d)}$ and summed over $p = u, c$. The amplitudes for $\bar{B}_s \to \pi K^*$ and $\bar{B}_s \to \rho K$ are obtained from these expressions by interchanging $(\pi, K) \leftrightarrow (\pi, K^*)$ or $(\pi, K) \leftrightarrow (\rho, K)$ everywhere. Note that these decays are governed by a relatively simple pattern of tree–penguin interference, which allows extractions of the penguin coefficients $\hat{\alpha}_4^c$ and gives sensitivity to γ.

The branching fractions for the remaining B_s decays with $\Delta D = 1$ are smaller, typically of order few times 10^{-7} (except for $\bar{B}_s \to K^0\eta'$). The simplified expressions for the $\bar{B}_s \to K^0\omega$, $K^0\phi$ decay amplitudes are

$$
\begin{aligned}
\sqrt{2}\,\mathcal{A}_{\bar{B}_s\to K^0\omega} &= A_{K\omega}\Big[\delta_{pu}\,\alpha_2 + 2\alpha_3^p + \hat{\alpha}_4^p\Big]\,, \\
\mathcal{A}_{\bar{B}_s\to K^0\phi} &= A_{K\phi}\,\alpha_3^p + A_{\phi K}\,\hat{\alpha}_4^p\,.
\end{aligned}
\tag{115}
$$

The amplitudes for modes with η or η' are given in Appendix A. In the first case the tree contribution is color suppressed, while the second process is a pure penguin decay. This explains the small branching fractions. Correspondingly, we predict generically large direct CP asymmetries for these modes.

Table 23: CP-averaged branching ratios (in units of 10^{-6}) of $\bar{B}_s \to PP$ decays (top) and $\bar{B}_s \to PV$ decays (bottom) with $\Delta D = 1$.

Mode	Theory	S1	S2	S3	S4
$\bar{B}_s \to \pi^- K^+$	$10.2^{+4.5+3.8+0.7+0.8}_{-3.9-3.2-1.2-0.7}$	6.8	8.1	10.4	8.3
$\bar{B}_s \to \pi^0 K^0$	$0.49^{+0.28+0.22+0.40+0.33}_{-0.24-0.14-0.14-0.17}$	0.95	0.68	0.60	0.61
$\bar{B}_s \to K^0 \eta$	$0.34^{+0.19+0.64+0.21+0.16}_{-0.16-0.27-0.07-0.08}$	0.65	0.42	0.38	0.37
$\bar{B}_s \to K^0 \eta'$	$2.0^{+0.3+1.5+0.6+1.5}_{-0.3-1.1-0.3-0.6}$	2.6	3.0	2.7	2.9
$\bar{B}_s \to \pi^- K^{*+}$	$8.7^{+4.6+3.5+0.7+0.8}_{-3.7-2.9-1.0-0.7}$	10.1	6.7	9.0	6.8
$\bar{B}_s \to \pi^0 K^{*0}$	$0.25^{+0.08+0.10+0.32+0.30}_{-0.08-0.06-0.14-0.14}$	0.15	0.39	0.36	0.33
$\bar{B}_s \to K^+ \rho^-$	$24.5^{+11.9+9.2+1.8+1.6}_{-9.7-7.8-3.0-1.6}$	21.3	19.2	24.6	19.8
$\bar{B}_s \to K^0 \rho^0$	$0.61^{+0.33+0.21+1.06+0.56}_{-0.26-0.15-0.38-0.36}$	0.82	0.58	0.70	0.68
$\bar{B}_s \to K^0 \omega$	$0.51^{+0.20+0.15+0.68+0.40}_{-0.18-0.11-0.23-0.25}$	0.33	0.50	0.58	0.63
$\bar{B}_s \to K^0 \phi$	$0.27^{+0.09+0.28+0.09+0.67}_{-0.08-0.14-0.06-0.18}$	0.43	0.54	0.64	0.46
$\bar{B}_s \to \eta K^{*0}$	$0.26^{+0.15+0.49+0.15+0.57}_{-0.13-0.22-0.05-0.15}$	0.52	0.29	0.54	0.57
$\bar{B}_s \to \eta' K^{*0}$	$0.28^{+0.04+0.46+0.23+0.29}_{-0.04-0.24-0.10-0.15}$	0.23	0.24	0.39	0.67

Table 24: Direct CP asymmetries (in units of 10^{-2}) of $\bar{B}_s \to PP$ decays (top) and $\bar{B}_s \to PV$ decays (bottom) with $\Delta D = 1$.

Mode	Theory	S1	S2	S3	S4
$\bar{B}_s \to \pi^- K^+$	$-6.7^{+2.1+3.1+0.2+15.5}_{-2.2-2.9-0.4-15.2}$	-10.0	-8.5	7.7	10.9
$\bar{B}_s \to \pi^0 K^0$	$41.6^{+16.6+14.3+7.8+40.9}_{-12.0-13.3-14.5-51.0}$	21.4	33.6	14.3	4.6
$\bar{B}_s \to K^0 \eta$	$46.8^{+18.5+28.6+5.2+34.6}_{-13.2-32.2-12.5-45.6}$	24.1	39.3	28.6	24.2
$\bar{B}_s \to K^0 \eta'$	$-36.6^{+8.6+6.0+3.8+19.3}_{-8.2-7.4-2.5-17.3}$	-28.8	-29.5	-22.2	-18.2
$\bar{B}_s \to \pi^- K^{*+}$	$0.6^{+0.2+1.4+0.1+19.9}_{-0.1-1.7-0.1-20.1}$	0.5	1.6	-18.5	-22.0
$\bar{B}_s \to \pi^0 K^{*0}$	$-45.7^{+14.3+13.0+28.4+80.0}_{-16.0-11.6-28.0-59.7}$	-79.3	-41.9	0.3	15.4
$\bar{B}_s \to K^+ \rho^-$	$-1.5^{+0.4+1.2+0.2+12.1}_{-0.4-1.4-0.3-12.1}$	-1.7	-1.7	10.1	6.2
$\bar{B}_s \to K^0 \rho^0$	$24.7^{+7.1+14.0+22.8+51.3}_{-5.2-12.4-17.7-52.3}$	18.3	24.5	-11.8	11.6
$\bar{B}_s \to K^0 \omega$	$-43.9^{+13.6+18.0+30.6+57.7}_{-13.4-18.2-30.2-49.3}$	-67.5	-40.9	-9.6	-30.1
$\bar{B}_s \to K^0 \phi$	$-10.3^{+3.0+4.7+3.7+5.0}_{-2.4-3.0-4.1-7.5}$	-6.4	-10.5	-6.3	-7.4
$\bar{B}_s \to \eta K^{*0}$	$40.2^{+17.0+24.6+7.8+65.9}_{-11.5-30.8-14.0-96.3}$	20.4	36.3	-11.7	0.6
$\bar{B}_s \to \eta' K^{*0}$	$-58.6^{+16.9+41.4+19.9+44.9}_{-11.9-11.7-13.9-35.7}$	-70.8	-54.5	-24.9	-32.7

9 Conclusions

In this paper we extended our previous analysis [10] of B-meson decays to $\pi\pi$ and πK final states and to final states with $\eta^{(\prime)}$ mesons [18] within the QCD factorization approach to all two-body final states with pseudoscalar mesons or one pseudoscalar and one vector meson, including also decays of B_s mesons. The main motivation for performing a comprehensive analysis of all 96 final states is to obtain a global assessment of the phenomenology of QCD factorization with a consistent common input to all decay modes, and to display possible correlations between the various modes.

The theoretical analysis follows [10]. The computation is performed at next-to-leading order in α_s for the hard-scattering kernels at leading order in $1/m_b$, and similarly for the kernels that multiply the subleading twist-3 quark–antiquark distribution amplitudes. Spectator scattering effects at subleading power in $1/m_b$ (including weak annihilation), which do not generally factorize, are estimated by a phenomenological model and assigned a 100% uncertainty (including an arbitrary strong-interaction phase). On the technical side, the generalization of the decay amplitudes computed in [10] to pseudoscalar–vector final states is for most parts straightforward, involving only a few sign changes in the decay amplitudes and a few new hard-scattering kernels. For the analysis of this paper only the kernels for the twist-3 quark–antiquark amplitudes of vector mesons needed to be computed anew. We also discussed a new electroweak penguin effect that contributes only to neutral vector mesons.

We have taken this comprehensive analysis as the occasion to summarize in a unified notation all results available at next-to-leading order in QCD factorization. The matrix elements of the effective weak Hamiltonian are decomposed according to their flavor structure. A complete list of all decay amplitudes expressed in terms of the flavor coefficients (which generalizes and simplifies the more familiar a_i and b_i notation) is given in Appendix A. The next-to-leading order results for the coefficients are given in Section 2, including the results from [10] for completeness.

The comparison of theory with data shows many interesting effects, which we summarize here. We should note, however, that no experimental information exists to date for the majority of the 96 decay modes considered in this paper. This will allow further tests of the theory in the future. When passed successfully, this implies a rich source of information on flavor-changing transitions in the quark sector from purely hadronic decays.

Results related to the $\pi\pi$, πK final states

A detailed discussion of these modes can be found in [10]. Since 2001 the experimental errors have been reduced by almost a factor of two. QCD factorization continues to provide a natural explanation for the magnitudes of the tree and penguin amplitudes relevant to these decays. The theory with default input parameters does not fare well on the $\pi^-\pi^+$ decay mode, which it predicts too large, and on the $\pi^0\bar{K}^0$ mode, which it predicts too small. The former discrepancy is often interpreted as evidence of a large value of γ or large rescattering. We find that an alternative "hadronic physics" explanation is possible if the $B \to \pi$ form factor is about 15% smaller than usually assumed, the strange-quark mass is at the smaller end of the currently favored range, and if the color-suppressed tree amplitude is enhanced, for example by a sizable spectator-scattering effect. While the evidence for this scenario is not conclusive now, crucial input will be provided by a measurement of the semileptonic decay rate near $q^2 = 0$. Interestingly, this scenario is also favored by measurements of the decay rates for $\bar{B}^0 \to \pi^\mp \rho^\pm$. With regard to the "$\pi^0 \bar{K}^0$ anomaly", we find that the large experimental $\bar{B}^0 \to \pi^- \bar{K}^0$ rate cannot be explained by a different value of γ, and that "hadronic physics" explanations appear extremely unlikely. While a significant modification of the electroweak penguin amplitude due to "New Physics" may explain the effect, we consider it to be more likely a statistical fluctuation.

It will require more data to arrive at a conclusive picture for the direct CP asymmetries. While it appears now certain that the asymmetries are small for the πK modes, in agreement with the predictions of QCD factorization, a quantitative comparison needs better statistics and a more accurate theoretical computation. The experimental situation for the $\pi^-\pi^+$ final state is still unsettled. If a direct CP asymmetry of order 50% is confirmed in the future, the factorization framework would be in trouble. Similar comments apply to other observations of large direct CP asymmetries, which at present all have large experimental errors.

Results related to the $\pi\rho$ final states

The $\pi\rho$ system discussed in Section 6 exhibits some advantages for studies of CP violation that render it highly interesting even within the limitations of the quasi two-body assumption. We defined and discussed several ratios of $\pi\rho$ branching fractions that should shed light on the magnitudes of the hadronic amplitudes underlying this class of decays. The theoretical predictions for these ratios are in good agreement with the available data. In particular, QCD factorization predicts that the two distinct penguin-to-tree ratios in the $\pi\rho$ system are about a factor of three smaller than the corresponding ratio for $\pi\pi$, and have smaller errors. If this can be confirmed, it implies that γ can be determined relatively accurately from time-dependent CP violation measurements. We considered the five quantities that parameterize the time-dependent asymmetries in the decays $B^0, \bar{B}^0 \to \pi^\mp \rho^\pm$ in detail. If data and theory are taken at face value, we determine $\gamma \approx 70^\circ$ with an error of about 10° from the asymmetry S. This value is consistent with a less accurate result obtained from the corresponding quantity in the $\pi\pi$ system (if one takes the average of the two experiments, which are mutually incompatible). This appears intriguing but should be taken with some reservation, since the central values of the direct CP asymmetries $A_{\rm CP}$ and C are once more larger than theoretically expected. We anticipate that, with more data available soon, the $\pi\rho$ system will play an important role in the understanding of hadronic decays and CP violation.

Results related to the penguin-dominated $\boldsymbol{PV}$ final states

The comparison of the penguin-dominated final states πK, πK^* and ρK allows for crucial tests of the factorization framework, since the PP, PV, and VP penguin amplitudes take very different values for reasons specific to factorization. The πK^* data are indeed consistent with a smaller penguin amplitude; however, as has been noted before [20, 22, 23], the reduction is not as large as predicted by theory. With default parameters one underestimates the amplitude by about 40%, but the theoretical error on the penguin amplitude for vector-meson final states is large, in particular the one from weak annihilation. This taken into account, the prediction may be in agreement with the measured branching fractions within their errors. However, the situation is not satisfactory, since one would wish to have an explanation of the data that does not invoke weak annihilation.

The estimate of weak annihilation is necessarily model-dependent in the QCD factorization approach. In particular, the error range (technically implemented by requiring $\varrho_A < 1$) has to be specified as an "educated guess". It is therefore desirable to derive experimental constraints on weak annihilation. It was already found in [10] that the πK branching fractions do not favor a sizable annihilation amplitude, since this would require a fine-tuning of its strong phase to keep the branching fraction small enough. On the other hand, such a coincidence cannot be excluded. Assuming this to happen and further assuming universal annihilation amplitudes, we find that several branching fractions of pseudoscalar–vector final states, in particular $K\phi$, are much above the data for $\varrho_A \geq 2$. This, together with an estimate of the pure annihilation mode $\bar{B}_d \to D_s^+ K^-$ [63], seem to imply that weak annihilation cannot be much larger than the upper limit defined by the phenomenological treatment adopted in the present analysis and in [10].

As a by-product of the analysis of penguin-dominated PV modes, we also obtain an estimate of the difference of the time-dependent CP asymmetries in $J/\psi K_S$, ϕK_S, and $\eta' K_S$ decays. As may have been expected, the factorization approach does not contain any mechanism that could enhance the CKM-suppressed amplitudes with a different weak phase, limiting the CP-asymmetry differences to a few percent.

Acknowledgments

We would like to thank A. Höcker for correspondence and for making [61] accessible to us. We are grateful to M. Gronau, A. Kagan, U. Nierste, and J. Rosner for useful comments, and to J. Alexander, H. Jawahery, and H. Yamamoto for help with collecting the references to the experimental results compiled in Appendix C. We are grateful to the Aspen Center of Physics, where this work was completed. The work of M.B. is supported in part by the Bundesministerium für Bildung und Forschung, Project 05 HT1PAB/2, and by the DFG Sonderforschungsbereich/Transregio 9 "Computer-gestützte Theoretische Teilchenphysik". The research of M.N. is supported by the U.S. National Science Foundation under Grant PHY-0098631.

Appendix A: Explicit results for the decay amplitudes

The results for the large set of $\bar{B}_q \to PP, PV$ decay amplitudes can be expressed most concisely in terms of traces over flavor matrices. We collect the three B-meson states into a row vector $\boldsymbol{B} = (B^-, \bar{B}^0, \bar{B}_s)$ and represent the final-state pseudoscalar and vector mesons by matrices

$$\boldsymbol{P} = \begin{pmatrix} \frac{\pi^0}{\sqrt{2}} + \frac{\eta_q}{\sqrt{2}} + \frac{\eta_q'}{\sqrt{2}} & \pi^- & K^- \\ \pi^+ & -\frac{\pi^0}{\sqrt{2}} + \frac{\eta_q}{\sqrt{2}} + \frac{\eta_q'}{\sqrt{2}} & \bar{K}^0 \\ K^+ & K^0 & \eta_s + \eta_s' \end{pmatrix},$$
$$\boldsymbol{V} = \begin{pmatrix} \frac{\rho^0}{\sqrt{2}} + \frac{\omega_q}{\sqrt{2}} + \frac{\phi_q}{\sqrt{2}} & \rho^- & K^{*-} \\ \rho^+ & -\frac{\rho^0}{\sqrt{2}} + \frac{\omega_q}{\sqrt{2}} + \frac{\phi_q}{\sqrt{2}} & \bar{K}^{*0} \\ K^{*+} & K^{*0} & \omega_s + \phi_s \end{pmatrix}, \tag{116}$$

respectively. (One should also add a $\bar{c}c$ component for η and η', whose contribution is given by (51).) In addition, we define a column vector

$$\boldsymbol{\Lambda}_p = \begin{pmatrix} 0 \\ \lambda_p^{(d)} \\ \lambda_p^{(s)} \end{pmatrix} \tag{117}$$

containing CKM matrix elements, as well as matrices

$$\boldsymbol{U}_p = \begin{pmatrix} \delta_{pu} & 0 & 0 \\ 0 & 0 & 0 \\ 0 & 0 & 0 \end{pmatrix}, \qquad \hat{\boldsymbol{Q}} = \frac{3}{2}\,\boldsymbol{Q} = \begin{pmatrix} 1 & 0 & 0 \\ 0 & -\frac{1}{2} & 0 \\ 0 & 0 & -\frac{1}{2} \end{pmatrix}. \tag{118}$$

Finally, we use the definitions of the quantities $A_{M_1M_2}$, $\alpha_i(M_1M_2)$ and $\beta_i(M_1M_2)$ given in (11), (9) and (18). Then the entity of all decay amplitudes $\mathcal{A}_{\bar{B}\to M_1M_2}$ is reproduced by evaluating the master expression

$$\begin{aligned} \sum_{p=u,c} A_{M_1M_2} \Big\{ & \boldsymbol{BM_1} \left(\alpha_1\,\boldsymbol{U}_p + \alpha_4^p + \alpha_{4,\rm EW}^p\,\hat{\boldsymbol{Q}}\right) \boldsymbol{M_2}\,\boldsymbol{\Lambda}_p \\ & + \boldsymbol{BM_1\Lambda}_p \cdot \mathrm{Tr}\left[\left(\alpha_2\,\boldsymbol{U}_p + \alpha_3^p + \alpha_{3,\rm EW}^p\,\hat{\boldsymbol{Q}}\right) \boldsymbol{M_2}\right] \\ & + \boldsymbol{B} \left(\beta_2\,\boldsymbol{U}_p + \beta_3^p + \beta_{3,\rm EW}^p\,\hat{\boldsymbol{Q}}\right) \boldsymbol{M_1M_2\Lambda}_p \\ & + \boldsymbol{B\Lambda}_p \cdot \mathrm{Tr}\left[\left(\beta_1\,\boldsymbol{U}_p + \beta_4^p + b_{4,\rm EW}^p\,\hat{\boldsymbol{Q}}\right) \boldsymbol{M_1M_2}\right] \\ & + \boldsymbol{B} \left(\beta_{S2}\,\boldsymbol{U}_p + \beta_{S3}^p + \beta_{S3,\rm EW}^p\,\hat{\boldsymbol{Q}}\right) \boldsymbol{M_1\Lambda}_p \cdot \mathrm{Tr}\boldsymbol{M_2} \\ & + \boldsymbol{B\Lambda}_p \cdot \mathrm{Tr}\left[\left(\beta_{S1}\,\boldsymbol{U}_p + \beta_{S4}^p + b_{S4,\rm EW}^p\,\hat{\boldsymbol{Q}}\right) \boldsymbol{M_1}\right] \cdot \mathrm{Tr}\boldsymbol{M_2} \Big\}, \end{aligned} \tag{119}$$

where $\alpha_i \equiv \alpha_i(M_1M_2)$ and $\beta_i \equiv \beta_i(M_1M_2)$. We recall that the α_i terms include vertex, penguin and hard spectator contributions, whereas the β_i terms result from weak annihilation. Contributions proportional to $\boldsymbol{U}_p$ are from the current–current operators, those proportional to the unit matrix are from QCD penguins, and those proportional to the charge matrix are from electroweak penguins.

To determine the amplitude for a particular decay, for instance $\bar{B}^0 \to \pi^+K^-$, one inserts $\boldsymbol{P}$ for $\boldsymbol{M_1}$ and $\boldsymbol{M_2}$ and extracts the terms corresponding to π^+K^-. When π^+ comes from $\boldsymbol{M_1}$ the prefactor is $A_{\pi K}$, otherwise it is $A_{K\pi}$. For pseudoscalar–vector final states both possibilities, $\boldsymbol{M_1} = \boldsymbol{P}$, $\boldsymbol{M_2} = \boldsymbol{V}$ and $\boldsymbol{M_1} = \boldsymbol{V}$, $\boldsymbol{M_2} = \boldsymbol{P}$, must be summed and the $A_{M_1M_2}$ prefactor is determined as above. For some pure annihilation amplitudes the form factor $\bar{B} \to M_1$ does not exist, and $A_{M_1M_2}$ is not defined. In this case the expressions $A_{M_1M_2}\,\beta_i$ must be replaced by $B_{M_1M_2}\,b_i$. See Section 2.2 for the definition of the relevant quantities.

We now list our results for the various decay amplitudes expressed in terms of the α_i and β_i parameters. Several sets of amplitudes have the same representation in terms of flavor parameters, apart from obvious substitutions of labels.

A.1 Decays with $\Delta S = 1$

In this section the expressions for decay amplitudes must be multiplied with $\lambda_p^{(s)}$ and summed over $p = u, c$. Throughout, the order of the arguments of the $\alpha_i^p(M_1M_2)$ and $\beta_i^p(M_1M_2)$ coefficients is determined by the order of the arguments of the $A_{M_1M_2}$ prefactors. There is a total of 17 $\bar{B} \to PP$ and 31 $\bar{B} \to PV$ amplitudes, which split up as (4,4,9) and (8,8,15) into the flavor states $(B^-, \bar{B}^0, \bar{B}_s)$.

$\bar{B} \to \pi\bar{K}^{(*)}$ and $\bar{B} \to \rho\bar{K}$ decay amplitudes

There are four independent amplitudes, given by

$$\begin{aligned}
\mathcal{A}_{B^-\to\pi^-\bar{K}^0} &= A_{\pi\bar{K}}\left[\delta_{pu}\,\beta_2 + \alpha_4^p - \tfrac{1}{2}\alpha_{4,\mathrm{EW}}^p + \beta_3^p + \beta_{3,\mathrm{EW}}^p\right], \\
\sqrt{2}\,\mathcal{A}_{B^-\to\pi^0K^-} &= A_{\pi\bar{K}}\left[\delta_{pu}\,(\alpha_1 + \beta_2) + \alpha_4^p + \alpha_{4,\mathrm{EW}}^p + \beta_3^p + \beta_{3,\mathrm{EW}}^p\right] \\
&\quad + A_{\bar{K}\pi}\left[\delta_{pu}\,\alpha_2 + \tfrac{3}{2}\alpha_{3,\mathrm{EW}}^p\right], \\
\mathcal{A}_{\bar{B}^0\to\pi^+K^-} &= A_{\pi\bar{K}}\left[\delta_{pu}\,\alpha_1 + \alpha_4^p + \alpha_{4,\mathrm{EW}}^p + \beta_3^p - \tfrac{1}{2}\beta_{3,\mathrm{EW}}^p\right], \\
\sqrt{2}\,\mathcal{A}_{\bar{B}^0\to\pi^0\bar{K}^0} &= A_{\pi\bar{K}}\left[-\alpha_4^p + \tfrac{1}{2}\alpha_{4,\mathrm{EW}}^p - \beta_3^p + \tfrac{1}{2}\beta_{3,\mathrm{EW}}^p\right] \\
&\quad + A_{\bar{K}\pi}\left[\delta_{pu}\,\alpha_2 + \tfrac{3}{2}\alpha_{3,\mathrm{EW}}^p\right]. \qquad (120)
\end{aligned}$$

Isospin symmetry implies that

$$\sqrt{2}\,\mathcal{A}_{\bar{B}^0\to\pi^0\bar{K}^0} = -\mathcal{A}_{B^-\to\pi^-\bar{K}^0} + \sqrt{2}\,\mathcal{A}_{B^-\to\pi^0K^-} - \mathcal{A}_{\bar{B}^0\to\pi^+K^-}\,. \qquad (121)$$

The expressions for the $\bar{B} \to \pi\bar{K}^*$ and $\bar{B} \to \rho\bar{K}$ amplitudes are obtained by setting $(\pi\bar{K}) \to (\pi\bar{K}^*)$ and $(\pi\bar{K}) \to (\rho\bar{K})$, respectively.

$\bar{B} \to \bar{K}^{(*)}\eta^{(\prime)}$ and $\bar{B} \to \bar{K}\omega/\phi$ decay amplitudes

There are two independent amplitudes, given by

$$\begin{aligned}
\sqrt{2}\,\mathcal{A}_{B^-\to K^-\eta} &= A_{\bar{K}\eta_q}\left[\delta_{pu}\,(\alpha_2 + 2\beta_{S2}) + 2\alpha_3^p + \tfrac{1}{2}\alpha_{3,\rm EW}^p + 2\beta_{S3}^p + 2\beta_{S3,\rm EW}^p\right] \\
&\quad + \sqrt{2}A_{\bar{K}\eta_s}\Big[\delta_{pu}\,(\beta_2 + \beta_{S2}) + \alpha_3^p + \alpha_4^p - \tfrac{1}{2}\alpha_{3,\rm EW}^p - \tfrac{1}{2}\alpha_{4,\rm EW}^p + \beta_3^p + \beta_{3,\rm EW}^p \\
&\qquad\qquad + \beta_{S3}^p + \beta_{S3,\rm EW}^p\Big] \\
&\quad + \sqrt{2}A_{\bar{K}\eta_c}\left[\delta_{pc}\,\alpha_2 + \alpha_3^p\right] \\
&\quad + A_{\eta_q\bar{K}}\left[\delta_{pu}\,(\alpha_1 + \beta_2) + \alpha_4^p + \alpha_{4,\rm EW}^p + \beta_3^p + \beta_{3,\rm EW}^p\right], \\
\sqrt{2}\,\mathcal{A}_{\bar{B}^0\to\bar{K}^0\eta} &= A_{\bar{K}\eta_q}\left[\delta_{pu}\,\alpha_2 + 2\alpha_3^p + \tfrac{1}{2}\alpha_{3,\rm EW}^p + 2\beta_{S3}^p - \beta_{S3,\rm EW}^p\right] \\
&\quad + \sqrt{2}A_{\bar{K}\eta_s}\Big[\alpha_3^p + \alpha_4^p - \tfrac{1}{2}\alpha_{3,\rm EW}^p - \tfrac{1}{2}\alpha_{4,\rm EW}^p + \beta_3^p - \tfrac{1}{2}\beta_{3,\rm EW}^p + \beta_{S3}^p - \tfrac{1}{2}\beta_{S3,\rm EW}^p\Big] \\
&\quad + \sqrt{2}A_{\bar{K}\eta_c}\left[\delta_{pc}\,\alpha_2 + \alpha_3^p\right] \\
&\quad + A_{\eta_q\bar{K}}\left[\alpha_4^p - \tfrac{1}{2}\alpha_{4,\rm EW}^p + \beta_3^p - \tfrac{1}{2}\beta_{3,\rm EW}^p\right]. \qquad (122)
\end{aligned}$$

The amplitudes for $\bar{B}^0 \to \bar{K}\eta'$, $\bar{B}^0 \to \bar{K}^*\eta^{(\prime)}$, and $\bar{B}^0 \to \bar{K}\omega/\phi$ are obtained from this result by replacing $(\bar{K}\eta) \to (\bar{K}\eta')$, $(\bar{K}\eta) \to (\bar{K}^*\eta^{(\prime)})$, and $(\bar{K}\eta) \to (\bar{K}\omega/\phi)$, respectively. When ideal mixing for ω and ϕ is assumed, set $A_{\bar{K}\omega_s}$ and $A_{\bar{K}\phi_q}$ to zero. Furthermore, with our approximations $A_{\bar{K}\omega_c} = A_{\bar{K}\phi_c} = 0$.

$\bar{B}_s \to \pi\pi$ and $\bar{B}_s \to \pi\rho$ decay amplitudes

There are two independent amplitudes, given by

$$\begin{aligned}
\mathcal{A}_{\bar{B}_s\to\pi^+\rho^-} &= B_{\pi\rho}\left[b_4^p - \tfrac{1}{2}b_{4,\rm EW}^p\right] \\
&\quad + B_{\rho\pi}\left[\delta_{pu}\,b_1 + b_4^p + b_{4,\rm EW}^p\right], \\
2\,\mathcal{A}_{\bar{B}_s\to\pi^0\rho^0} &= B_{\pi\rho}\left[\delta_{pu}\,b_1 + 2b_4^p + \tfrac{1}{2}b_{4,\rm EW}^p\right] \\
&\quad + B_{\rho\pi}\left[\delta_{pu}\,b_1 + 2b_4^p + \tfrac{1}{2}b_{4,\rm EW}^p\right]. \qquad (123)
\end{aligned}$$

The amplitudes for $\bar{B}_s \to \pi^-\rho^+$ is obtained from the first expression by interchanging $\pi \leftrightarrow \rho$ everywhere. In the limit of isospin symmetry the following relation holds:

$$2\,\mathcal{A}_{\bar{B}_s\to\pi^0\rho^0} = \mathcal{A}_{\bar{B}_s\to\pi^+\rho^-} + \mathcal{A}_{\bar{B}_s\to\pi^-\rho^+}\,. \qquad (124)$$

The expressions for the $\bar{B}_s \to \pi\pi$ amplitudes are obtained by setting $\rho \to \pi$.

$\bar{B}_s \to \bar{K}^{(*)} K^{(*)}$ decay amplitudes

There are two independent amplitudes, given by

$$\begin{aligned}
\mathcal{A}_{\bar{B}_s \to \bar{K}^0 K^0} &= B_{\bar{K}K} \left[b_4^p - \tfrac{1}{2} b_{4,\mathrm{EW}}^p \right] \\
&\quad + A_{K\bar{K}} \left[\alpha_4^p - \tfrac{1}{2} \alpha_{4,\mathrm{EW}}^p + \beta_3^p + \beta_4^p - \tfrac{1}{2} \beta_{3,\mathrm{EW}}^p - \tfrac{1}{2} \beta_{4,\mathrm{EW}}^p \right] , \\
\mathcal{A}_{\bar{B}_s \to K^- K^+} &= B_{\bar{K}K} \left[\delta_{pu}\, b_1 + b_4^p + b_{4,\mathrm{EW}}^p \right] \\
&\quad + A_{K\bar{K}} \left[\delta_{pu}\, \alpha_1 + \alpha_4^p + \alpha_{4,\mathrm{EW}}^p + \beta_3^p + \beta_4^p - \tfrac{1}{2} \beta_{3,\mathrm{EW}}^p - \tfrac{1}{2} \beta_{4,\mathrm{EW}}^p \right] . \qquad (125)
\end{aligned}$$

The amplitudes for $\bar{B}_s \to \bar{K} K^*$ and $\bar{B}_s \to \bar{K}^* K$ are obtained from these expressions by replacing $(\bar{K}K) \to (\bar{K}K^*)$ and $(\bar{K}K) \to (\bar{K}^* K)$, respectively.

$\bar{B}_s \to \pi \eta^{(\prime)}$, $\bar{B}_s \to \pi \omega/\phi$, and $\bar{B}_s \to \rho \eta^{(\prime)}$ decay amplitudes

There is only one independent amplitude, given by

$$\begin{aligned}
2\, \mathcal{A}_{\bar{B}_s \to \pi^0 \eta} &= B_{\pi \eta_q} \left[\delta_{pu} \left(b_1 + 2 b_{S1} \right) + \tfrac{3}{2} b_{4,\mathrm{EW}}^p + 3 b_{4S,\mathrm{EW}}^p \right] \\
&\quad + \sqrt{2} B_{\pi \eta_s} \left[\delta_{pu}\, b_{S1} + \tfrac{3}{2} b_{4S,\mathrm{EW}}^p \right] \\
&\quad + B_{\eta_q \pi} \left[\delta_{pu}\, b_1 + \tfrac{3}{2} b_{4,\mathrm{EW}}^p \right] \\
&\quad + \sqrt{2} A_{\eta_s \pi} \left[\delta_{pu}\, \alpha_2 + \tfrac{3}{2} \alpha_{3,\mathrm{EW}}^p \right] . \qquad (126)
\end{aligned}$$

The amplitudes for $\bar{B}_s \to \pi \eta'$, $\bar{B}_s \to \pi \omega/\phi$, and $\bar{B}_s \to \rho \eta^{(\prime)}$ are obtained from these results by replacing $(\pi\eta) \to (\pi\eta')$, $(\pi\eta) \to (\pi\omega/\phi)$, and $(\pi\eta) \to (\rho\eta^{(\prime)})$, respectively. When ideal mixing for ω and ϕ is assumed, set $B_{\pi\omega_s}$ and $B_{\pi\phi_q}$ to zero.

$\bar{B}_s \to \eta^{(\prime)} \eta^{(\prime)}$ and $\bar{B}_s \to \eta^{(\prime)} \omega/\phi$ decay amplitudes

There is only one independent amplitude, given by

$$\begin{aligned}
2\, \mathcal{A}_{\bar{B}_s \to \eta\eta'} &= B_{\eta_q \eta_q'} \left[\delta_{pu} \left(b_1 + 2 b_{S1} \right) + 2 b_4^p + \tfrac{1}{2} b_{4,\mathrm{EW}}^p + 4 b_{S4}^p + b_{S4,\mathrm{EW}}^p \right] \\
&\quad + \sqrt{2} B_{\eta_q \eta_s'} \left[\delta_{pu}\, b_{S1} + 2 b_{S4}^p + \tfrac{1}{2} b_{S4,\mathrm{EW}}^p \right] \\
&\quad + \sqrt{2} A_{\eta_s \eta_q'} \left[\delta_{pu}\, \alpha_2 + 2 \alpha_3^p + \tfrac{1}{2} \alpha_{3,\mathrm{EW}}^p + 2 \beta_{S3}^p + 2 \beta_{S4}^p - \beta_{S3,\mathrm{EW}}^p - \beta_{S4,\mathrm{EW}}^p \right] \\
&\quad + 2 A_{\eta_s \eta_s'} \Big[\alpha_3^p + \alpha_4^p - \tfrac{1}{2} \alpha_{3,\mathrm{EW}}^p - \tfrac{1}{2} \alpha_{4,\mathrm{EW}}^p + \beta_3^p + \beta_4^p - \tfrac{1}{2} \beta_{3,\mathrm{EW}}^p - \tfrac{1}{2} \beta_{4,\mathrm{EW}}^p \\
&\qquad\qquad + \beta_{S3}^p + \beta_{S4}^p - \tfrac{1}{2} \beta_{S3,\mathrm{EW}}^p - \tfrac{1}{2} \beta_{S4,\mathrm{EW}}^p \Big] \\
&\quad + 2 A_{\eta_s \eta_c'} \left[\delta_{pc}\, \alpha_2 + \alpha_3^p \right]
\end{aligned}$$

$$
\begin{aligned}
&+\ B_{\eta_q'\eta_q}\left[\delta_{pu}\,(b_1+2b_{S1})+2b_4^p+\tfrac{1}{2}b_{4,\rm EW}^p+4b_{S4}^p+b_{S4,\rm EW}^p\right]\\
&+\ \sqrt{2}B_{\eta_q'\eta_s}\left[\delta_{pu}\,b_{S1}+2b_{S4}^p+\tfrac{1}{2}b_{S4,\rm EW}^p\right]\\
&+\ \sqrt{2}A_{\eta_s'\eta_q}\left[\delta_{pu}\,\alpha_2+2\alpha_3^p+\tfrac{1}{2}\alpha_{3,\rm EW}^p+2\beta_{S3}^p+2\beta_{S4}^p-\beta_{S3,\rm EW}^p-\beta_{S4,\rm EW}^p\right]\\
&+\ 2A_{\eta_s'\eta_s}\Big[\alpha_3^p+\alpha_4^p-\tfrac{1}{2}\alpha_{3,\rm EW}^p-\tfrac{1}{2}\alpha_{4,\rm EW}^p+\beta_3^p+\beta_4^p-\tfrac{1}{2}\beta_{3,\rm EW}^p-\tfrac{1}{2}\beta_{4,\rm EW}^p\\
&\qquad\qquad+\beta_{S3}^p+\beta_{S4}^p-\tfrac{1}{2}\beta_{S3,\rm EW}^p-\tfrac{1}{2}\beta_{S4,\rm EW}^p\Big]\\
&+\ 2A_{\eta_s'\eta_c}\left[\delta_{pc}\,\alpha_2+\alpha_3^p\right]. \qquad (127)
\end{aligned}
$$

The amplitudes for $\bar{B}_s\to\eta\eta$, $\bar{B}_s\to\eta'\eta'$, and $\bar{B}_s\to\eta^{(\prime)}\omega/\phi$ are obtained from this result by replacing $(\eta\eta')\to(\eta\eta)$, $(\eta\eta')\to(\eta'\eta')$, and $(\eta\eta')\to(\eta^{(\prime)}\omega/\phi)$, respectively. When ideal mixing for ω and ϕ is assumed, set $A_{\eta_s^{(\prime)}\omega_s}$, $A_{\eta_s^{(\prime)}\phi_q}$, $B_{\eta_q^{(\prime)}\omega_s}$, $B_{\eta_q^{(\prime)}\phi_q}$ to zero. Furthermore, with our approximations $A_{\eta_s^{(\prime)}\omega_c}=A_{\eta_s^{(\prime)}\phi_c}=0$.

A.2 Decays with $\Delta D = 1$

In this subsection the expressions for decay amplitudes must be multiplied with $\lambda_p^{(d)}$ and summed over $p=u,c$. Throughout, the order of the arguments of the $\alpha_i^p(M_1M_2)$ and $\beta_i^p(M_1M_2)$ coefficients is determined by the order of the arguments of the $A_{M_1M_2}$ prefactors. There is a total of 17 $\bar{B}\to PP$ and 31 $\bar{B}\to PV$ amplitudes, which split up as $(4,9,4)$ and $(8,15,8)$ into the flavor states $(B^-,\bar{B}^0,\bar{B}_s)$.

$\bar{B}\to\pi\pi$ and $\bar{B}\to\pi\rho$ decay amplitudes

There are three independent amplitudes, given by

$$
\begin{aligned}
\sqrt{2}\,\mathcal{A}_{B^-\to\pi^-\rho^0} &= A_{\pi\rho}\left[\delta_{pu}\,(\alpha_2-\beta_2)-\alpha_4^p+\tfrac{3}{2}\alpha_{3,\rm EW}^p+\tfrac{1}{2}\alpha_{4,\rm EW}^p-\beta_3^p-\beta_{3,\rm EW}^p\right]\\
&\quad+\ A_{\rho\pi}\left[\delta_{pu}\,(\alpha_1+\beta_2)+\alpha_4^p+\alpha_{4,\rm EW}^p+\beta_3^p+\beta_{3,\rm EW}^p\right],\\
\mathcal{A}_{\bar{B}^0\to\pi^+\rho^-} &= A_{\pi\rho}\left[\delta_{pu}\,\alpha_1+\alpha_4^p+\alpha_{4,\rm EW}^p+\beta_3^p+\beta_4^p-\tfrac{1}{2}\beta_{3,\rm EW}^p-\tfrac{1}{2}\beta_{4,\rm EW}^p\right]\\
&\quad+\ A_{\rho\pi}\left[\delta_{pu}\,\beta_1+\beta_4^p+\beta_{4,\rm EW}^p\right],\\
-2\,\mathcal{A}_{\bar{B}^0\to\pi^0\rho^0} &= A_{\pi\rho}\Big[\delta_{pu}\,(\alpha_2-\beta_1)-\alpha_4^p+\tfrac{3}{2}\alpha_{3,\rm EW}^p+\tfrac{1}{2}\alpha_{4,\rm EW}^p-\beta_3^p-2\beta_4^p\\
&\qquad\qquad+\tfrac{1}{2}\beta_{3,\rm EW}^p-\tfrac{1}{2}\beta_{4,\rm EW}^p\Big]\\
&\quad+\ A_{\rho\pi}\Big[\delta_{pu}\,(\alpha_2-\beta_1)-\alpha_4^p+\tfrac{3}{2}\alpha_{3,\rm EW}^p+\tfrac{1}{2}\alpha_{4,\rm EW}^p-\beta_3^p-2\beta_4^p\\
&\qquad\qquad+\tfrac{1}{2}\beta_{3,\rm EW}^p-\tfrac{1}{2}\beta_{4,\rm EW}^p\Big]. \qquad (128)
\end{aligned}
$$

The amplitudes for $B^-\to\pi^0\rho^-$ and $\bar{B}^0\to\pi^-\rho^+$ are obtained from the first two expressions by interchanging $\pi\leftrightarrow\rho$ everywhere. In the limit of isospin symmetry the following relation holds:

$$2\,\mathcal{A}_{\bar{B}^0\to\pi^0\rho^0} = \mathcal{A}_{\bar{B}^0\to\pi^+\rho^-} + \mathcal{A}_{\bar{B}^0\to\pi^-\rho^+} - \sqrt{2}\left(\mathcal{A}_{B^-\to\pi^-\rho^0} + \mathcal{A}_{B^-\to\pi^0\rho^-}\right). \tag{129}$$

The expressions for the $\bar{B}\to\pi\pi$ amplitudes are obtained by setting $\rho\to\pi$.

$\bar{B}\to\bar{K}^{(*)}K^{(*)}$ decay amplitudes

There are three independent amplitudes, given by

$$\begin{aligned}
\mathcal{A}_{B^-\to K^-K^0} &= A_{\bar{K}K}\left[\delta_{pu}\,\beta_2 + \alpha_4^p - \tfrac{1}{2}\alpha_{4,\rm EW}^p + \beta_3^p + \beta_{3,\rm EW}^p\right],\\
\mathcal{A}_{\bar{B}^0\to K^-K^+} &= A_{\bar{K}K}\left[\delta_{pu}\,\beta_1 + \beta_4^p + \beta_{4,\rm EW}^p\right]\\
&\quad + B_{K\bar{K}}\left[b_4^p - \tfrac{1}{2}b_{4,\rm EW}^p\right],\\
\mathcal{A}_{\bar{B}^0\to\bar{K}^0K^0} &= A_{\bar{K}K}\left[\alpha_4^p - \tfrac{1}{2}\alpha_{4,\rm EW}^p + \beta_3^p + \beta_4^p - \tfrac{1}{2}\beta_{3,\rm EW}^p - \tfrac{1}{2}\beta_{4,\rm EW}^p\right]\\
&\quad + B_{K\bar{K}}\left[b_4^p - \tfrac{1}{2}b_{4,\rm EW}^p\right].
\end{aligned} \tag{130}$$

The amplitudes for $\bar{B}\to\bar{K}K^*$ and $\bar{B}\to\bar{K}^*K$ are obtained from these by replacing $(\bar{K}K)\to(\bar{K}K^*)$ and $(\bar{K}K)\to(\bar{K}^*K)$, respectively.

$\bar{B}\to\pi\eta^{(\prime)}$, $\bar{B}\to\rho\eta^{(\prime)}$ and $\bar{B}\to\pi\omega/\phi$ decay amplitudes

There are two independent amplitudes, given by

$$\begin{aligned}
\sqrt{2}\,\mathcal{A}_{B^-\to\pi^-\eta} &= A_{\pi\eta_q}\Big[\delta_{pu}\,(\alpha_2+\beta_2+2\beta_{S2}) + 2\alpha_3^p + \alpha_4^p + \tfrac{1}{2}\alpha_{3,\rm EW}^p - \tfrac{1}{2}\alpha_{4,\rm EW}^p\\
&\qquad + \beta_3^p + \beta_{3,\rm EW}^p + 2\beta_{S3}^p + 2\beta_{S3,\rm EW}^p\Big]\\
&\quad + \sqrt{2}A_{\pi\eta_s}\left[\delta_{pu}\,\beta_{S2} + \alpha_3^p - \tfrac{1}{2}\alpha_{3,\rm EW}^p + \beta_{S3}^p + \beta_{S3,\rm EW}^p\right]\\
&\quad + \sqrt{2}A_{\pi\eta_c}\left[\delta_{pc}\,\alpha_2 + \alpha_3^p\right]\\
&\quad + A_{\eta_q\pi}\left[\delta_{pu}\,(\alpha_1+\beta_2) + \alpha_4^p + \alpha_{4,\rm EW}^p + \beta_3^p + \beta_{3,\rm EW}^p\right],\\
-2\,\mathcal{A}_{\bar{B}^0\to\pi^0\eta} &= A_{\pi\eta_q}\Big[\delta_{pu}\,(\alpha_2-\beta_1-2\beta_{S1}) + 2\alpha_3^p + \alpha_4^p + \tfrac{1}{2}\alpha_{3,\rm EW}^p - \tfrac{1}{2}\alpha_{4,\rm EW}^p\\
&\qquad + \beta_3^p - \tfrac{1}{2}\beta_{3,\rm EW}^p - \tfrac{3}{2}\beta_{4,\rm EW}^p + 2\beta_{S3}^p - \beta_{S3,\rm EW}^p - 3\beta_{S4,\rm EW}^p\Big]\\
&\quad + \sqrt{2}A_{\pi\eta_s}\left[-\delta_{pu}\,\beta_{S1} + \alpha_3^p - \tfrac{1}{2}\alpha_{3,\rm EW}^p + \beta_{S3}^p - \tfrac{1}{2}\beta_{S3,\rm EW}^p - \tfrac{3}{2}\beta_{S4,\rm EW}^p\right]\\
&\quad + \sqrt{2}A_{\pi\eta_c}\left[\delta_{pc}\,\alpha_2 + \alpha_3^p\right] \qquad\qquad (131)\\
&\quad + A_{\eta_q\pi}\left[\delta_{pu}\,(-\alpha_2-\beta_1) + \alpha_4^p - \tfrac{3}{2}\alpha_{3,\rm EW}^p - \tfrac{1}{2}\alpha_{4,\rm EW}^p + \beta_3^p - \tfrac{1}{2}\beta_{3,\rm EW}^p - \tfrac{3}{2}\beta_{4,\rm EW}^p\right].
\end{aligned}$$

The amplitudes for $\bar{B}\to\pi\eta'$, $\bar{B}\to\rho\eta^{(\prime)}$, and $\bar{B}\to\pi\omega/\phi$ are obtained from these results by replacing $(\pi\eta)\to(\pi\eta')$, $(\pi\eta)\to(\rho\eta^{(\prime)})$, and $(\pi\eta)\to(\pi\omega/\phi)$, respectively. When ideal mixing for ω and ϕ is assumed, set $A_{\pi\omega_s}$ and $A_{\pi\phi_q}$ to zero. Furthermore, with our approximations $A_{\pi\omega_c} = A_{\pi\phi_c} = 0$.

$\bar{B} \to \eta^{(\prime)}\eta^{(\prime)}$ and $\bar{B} \to \eta^{(\prime)}\omega/\phi$ decay amplitudes

There is only one independent amplitude, given by

$$\begin{aligned}
2\,\mathcal{A}_{\bar{B}^0\to\eta\eta'} = {} & A_{\eta_q\eta'_q}\Big[\delta_{pu}\,(\alpha_2+\beta_1+2\beta_{S1}) + 2\alpha_3^p + \alpha_4^p + \tfrac{1}{2}\alpha_{3,\mathrm{EW}}^p - \tfrac{1}{2}\alpha_{4,\mathrm{EW}}^p \\
& \qquad + \beta_3^p + 2\beta_4^p - \tfrac{1}{2}\beta_{3,\mathrm{EW}}^p + \tfrac{1}{2}\beta_{4,\mathrm{EW}}^p + 2\beta_{S3}^p + 4\beta_{S4}^p - \beta_{S3,\mathrm{EW}}^p + \beta_{S4,\mathrm{EW}}^p\Big] \\
& + \sqrt{2}A_{\eta_q\eta'_s}\left[\delta_{pu}\,\beta_{S1} + \alpha_3^p - \tfrac{1}{2}\alpha_{3,\mathrm{EW}}^p + \beta_{S3}^p + 2\beta_{S4}^p - \tfrac{1}{2}\beta_{S3,\mathrm{EW}}^p + \tfrac{1}{2}\beta_{S4,\mathrm{EW}}^p\right] \\
& + \sqrt{2}A_{\eta_q\eta'_c}\left[\delta_{pc}\,\alpha_2 + \alpha_3^p\right] \\
& + \sqrt{2}B_{\eta_s\eta'_q}\left[2b_{S4}^p - b_{S4,\mathrm{EW}}^p\right] \\
& + 2B_{\eta_s\eta'_s}\left[b_4^p - \tfrac{1}{2}b_{4,\mathrm{EW}}^p + b_{S4}^p - \tfrac{1}{2}b_{S4,\mathrm{EW}}^p\right] \\
& + A_{\eta'_q\eta_q}\Big[\delta_{pu}\,(\alpha_2+\beta_1+2\beta_{S1}) + 2\alpha_3^p + \alpha_4^p + \tfrac{1}{2}\alpha_{3,\mathrm{EW}}^p - \tfrac{1}{2}\alpha_{4,\mathrm{EW}}^p \\
& \qquad + \beta_3^p + 2\beta_4^p - \tfrac{1}{2}\beta_{3,\mathrm{EW}}^p + \tfrac{1}{2}\beta_{4,\mathrm{EW}}^p + 2\beta_{S3}^p + 4\beta_{S4}^p - \beta_{S3,\mathrm{EW}}^p + \beta_{S4,\mathrm{EW}}^p\Big] \\
& + \sqrt{2}A_{\eta'_q\eta_s}\left[\delta_{pu}\,\beta_{S1} + \alpha_3^p - \tfrac{1}{2}\alpha_{3,\mathrm{EW}}^p + \beta_{S3}^p + 2\beta_{S4}^p - \tfrac{1}{2}\beta_{S3,\mathrm{EW}}^p + \tfrac{1}{2}\beta_{S4,\mathrm{EW}}^p\right] \\
& + \sqrt{2}A_{\eta'_q\eta_c}\left[\delta_{pc}\,\alpha_2 + \alpha_3^p\right] \\
& + \sqrt{2}B_{\eta'_s\eta_q}\left[2b_{S4}^p - b_{S4,\mathrm{EW}}^p\right] \\
& + 2B_{\eta'_s\eta_s}\left[b_4^p - \tfrac{1}{2}b_{4,\mathrm{EW}}^p + b_{S4}^p - \tfrac{1}{2}b_{S4,\mathrm{EW}}^p\right]. \qquad (132)
\end{aligned}$$

The amplitudes for $\bar{B}^0 \to \eta\eta$, $\bar{B}^0 \to \eta'\eta'$, and $\bar{B}^0 \to \eta^{(\prime)}\omega/\phi$ are obtained from this result by replacing $(\eta\eta') \to (\eta\eta)$, $(\eta\eta') \to (\eta'\eta')$, and $(\eta\eta') \to (\eta^{(\prime)}\omega/\phi)$, respectively. When ideal mixing for ω and ϕ is assumed, set $A_{\eta_q^{(\prime)}\omega_s}$, $A_{\eta_q^{(\prime)}\phi_q}$, $B_{\eta_s^{(\prime)}\omega_s}$, $B_{\eta_s^{(\prime)}\phi_q}$ to zero. Furthermore, with our approximations $A_{\eta_q^{(\prime)}\omega_c} = A_{\eta_q^{(\prime)}\phi_c} = 0$.

$\bar{B}_s \to \pi K^{(*)}$ and $\bar{B}_s \to \rho K$ decay amplitudes

There are two independent amplitudes, given by

$$\begin{aligned}
\mathcal{A}_{\bar{B}_s\to\pi^-K^+} &= A_{K\pi}\left[\delta_{pu}\,\alpha_1 + \alpha_4^p + \alpha_{4,\mathrm{EW}}^p + \beta_3^p - \tfrac{1}{2}\beta_{3,\mathrm{EW}}^p\right], \\
\sqrt{2}\,\mathcal{A}_{\bar{B}_s\to\pi^0K^0} &= A_{K\pi}\left[\delta_{pu}\,\alpha_2 - \alpha_4^p + \tfrac{3}{2}\alpha_{3,\mathrm{EW}}^p + \tfrac{1}{2}\alpha_{4,\mathrm{EW}}^p - \beta_3^p + \tfrac{1}{2}\beta_{3,\mathrm{EW}}^p\right]. \qquad (133)
\end{aligned}$$

The expressions for the $\bar{B}_s \to \pi K^*$ and $\bar{B}_s \to \rho K$ amplitudes are obtained by setting $(\pi K) \to (\pi K^*)$ and $(\pi K) \to (\rho K)$, respectively.

$\bar{B}_s \to K^{(*)}\eta^{(\prime)}$ and $\bar{B}_s \to K\omega/\phi$ decay amplitudes

There is only one independent amplitude, given by

$$\begin{aligned}
\sqrt{2}\,\mathcal{A}_{\bar{B}_s\to K^0\eta} = A_{K\eta_q}\Big[&\delta_{pu}\,\alpha_2 + 2\alpha_3^p + \alpha_4^p + \tfrac{1}{2}\alpha_{3,\mathrm{EW}}^p - \tfrac{1}{2}\alpha_{4,\mathrm{EW}}^p + \beta_3^p - \tfrac{1}{2}\beta_{3,\mathrm{EW}}^p \\
&+ 2\beta_{S3}^p - \beta_{S3,\mathrm{EW}}^p\Big] \\
&+ \sqrt{2}A_{K\eta_s}\left[\alpha_3^p - \tfrac{1}{2}\alpha_{3,\mathrm{EW}}^p + \beta_{S3}^p - \tfrac{1}{2}\beta_{S3,\mathrm{EW}}^p\right] \\
&+ \sqrt{2}A_{K\eta_c}\left[\delta_{pc}\,\alpha_2 + \alpha_3^p\right] \\
&+ \sqrt{2}A_{\eta_s K}\left[\alpha_4^p - \tfrac{1}{2}\alpha_{4,\mathrm{EW}}^p + \beta_3^p - \tfrac{1}{2}\beta_{3,\mathrm{EW}}^p\right]. \qquad (134)
\end{aligned}$$

The amplitudes for $\bar{B}_s \to K\eta'$, $\bar{B}_s \to K^*\eta^{(\prime)}$, and $\bar{B}_s \to K\omega/\phi$ are obtained from this result by replacing $(K\eta) \to (K\eta')$, $(K\eta) \to (K^*\eta^{(\prime)})$, and $(K\eta) \to (K\omega/\phi)$, respectively. When ideal mixing for ω and ϕ is assumed, set $A_{K\omega_s}$ and $A_{K\phi_q}$ to zero. Furthermore, with our approximations $A_{K\omega_c} = A_{K\phi_c} = 0$.

Appendix B: Convolution integrals

The convolution integrals of the hard-scattering kernels with meson light-cone distribution amplitudes can be evaluated using expansions of the distribution amplitudes in terms of Gegenbauer polynomials. In [10] the corresponding expressions for final states containing two pseudoscalar mesons were given including the first three terms in this expansion. Here we list the corresponding results for the convolution integrals involving the twist-3 distribution amplitude $\Phi_v(x)$, which are needed for pseudoscalar–vector final states. We include the first three terms in the Gegenbauer expansion (27).

The convolution integral entering the vertex corrections for the coefficients $a^p_{6,8}$ is

$$\int_0^1 dx\, \Phi_v(x)\, h(x) = 9 - 6i\pi + \left(\frac{19}{6} - i\pi\right) \alpha^V_{2,\perp} + \dots\,, \tag{135}$$

with $h(x)$ as given in (38). The hard spectator contributions involve the divergent integral

$$\int_0^1 dx\, \frac{\Phi_v(x)}{1-x} = \Phi_v(1)\, X_H - (6 + 9\alpha^V_{1,\perp} + 11\alpha^V_{2,\perp} + \dots)\,, \tag{136}$$

where $\Phi_v(1) = 3\sum_n \alpha^V_{n,\perp}$. The penguin contributions involve the convolution

$$\widehat{G}_V(s) = \int_0^1 dx\, \Phi_v(x)\, G(s - i\epsilon, 1-x)\,, \tag{137}$$

where $G(s,x)$ is the penguin function defined in (40). We obtain

$$\begin{aligned}
\widehat{G}_V(s) = {} & \frac{1}{6}\,(6 + 2\alpha^V_{1,\perp} + \alpha^V_{2,\perp}) - 4s\,(9 + 12\alpha^V_{1,\perp} + 14\alpha^V_{2,\perp}) \\
& - 6s^2\,(8\alpha^V_{1,\perp} + 35\alpha^V_{2,\perp}) + 360 s^3\, \alpha^V_{2,\perp} \\
& + 12s\sqrt{1-4s}\,\left[1 + (1+4s)\,\alpha^V_{1,\perp} + (1 + 15s - 30s^2)\,\alpha^V_{2,\perp}\right] \\
& \quad \times \left(2\,\mathrm{arctanh}\sqrt{1-4s} - i\pi\right) \\
& - 12s^2\left[1 + (3-4s)\,\alpha^V_{1,\perp} + 2(3 - 10s + 15s^2)\,\alpha^V_{2,\perp}\right] \\
& \quad \times \left(2\,\mathrm{arctanh}\sqrt{1-4s} - i\pi\right)^2 + \dots\,.
\end{aligned} \tag{138}$$

For the special cases $s=0$ and $s=1$, this expression reduces to

$$\begin{aligned}
\widehat{G}_V(0) &= 1 + \frac{\alpha^V_{1,\perp}}{3} + \frac{\alpha^V_{2,\perp}}{6} + \dots\,, \\
\widehat{G}_V(1) &= -35 + 4\sqrt{3}\,\pi + \frac{4\pi^2}{3} + \left(-\frac{287}{3} + 20\sqrt{3}\,\pi - \frac{4\pi^2}{3}\right) \alpha^V_{1,\perp} \\
& \quad + \left(\frac{565}{6} - 56\sqrt{3}\,\pi + \frac{64\pi^2}{3}\right) \alpha^V_{2,\perp} + \dots\,.
\end{aligned} \tag{139}$$

Appendix C: Summary of experimental results

In Tables 25–28 we compile the available experimental data on the CP-averaged branching fractions and CP asymmetries in $B \to PP$ and $B \to PV$ decays, distinguishing the two classes of decays of the type $\Delta S = 1$ and $\Delta D = 1$. We also present our weighted averages of the data (ignoring correlated errors, which are small). Where measurements are inconsistent, the combined error is inflated by a factor of $\sqrt{S}$, and $S = \chi^2/(N-1)$ is shown seperately.

Table 25: CP-averaged branching ratios (top, in units of 10^{-6}) and CP asymmetries (bottom, in %) for $\bar{B} \to PP$ decays with $\Delta S = 1$. Upper limits are at 90% confidence level. We show $S = \chi^2/(N-1)$ in cases where $S > 1$.

Mode	BaBar	Belle	CLEO	Average
Penguin-dominated decays				
$B^- \to \pi^- \bar{K}^0$	$20.0 \pm 1.6 \pm 1.0$ [65]	$22.0 \pm 1.9 \pm 1.1$ [84]	$18.8^{+3.7}_{-3.3}{}^{+2.1}_{-1.8}$ [91]	20.6 ± 1.3
$B^- \to \pi^0 K^-$	$12.8^{+1.2}_{-1.1} \pm 1.0$ [73]	$12.8 \pm 1.4^{+1.4}_{-1.0}$ [84]	$12.9^{+2.4}_{-2.2}{}^{+1.2}_{-1.1}$ [91]	12.8 ± 1.1
$\bar{B}^0 \to \pi^+ K^-$	$17.9 \pm 0.9 \pm 0.7$ [73]	$18.5 \pm 1.0 \pm 0.7$ [84]	$18.0^{+2.3}_{-2.1}{}^{+1.2}_{-0.9}$ [91]	18.2 ± 0.8
$\bar{B}^0 \to \pi^0 \bar{K}^0$	$10.4 \pm 1.5 \pm 0.8$ [75]	$12.6 \pm 2.4 \pm 1.4$ [84]	$12.8^{+4.0}_{-3.3}{}^{+1.7}_{-1.4}$ [91]	11.2 ± 1.4
$B^- \to \eta K^-$	$2.8^{+0.8}_{-0.7} \pm 0.2$ [71]	$5.3^{+1.8}_{-1.5} \pm 0.6$ [84]	$2.2^{+2.8}_{-2.2}$ (< 6.9) [96]	3.1 ± 0.7
$\bar{B}^0 \to \eta \bar{K}^0$	$2.6^{+0.9}_{-0.8} \pm 0.2$ (< 4.6) [71]	< 12 [84]	< 9.3 [96]	< 4.6
$B^- \to \eta' K^-$	$76.9 \pm 3.5 \pm 4.4$ [69]	$78 \pm 6 \pm 9$ [84]	$80^{+10}_{-9} \pm 7$ [96]	77.6 ± 4.6
$\bar{B}^0 \to \eta' \bar{K}^0$	$55.4 \pm 5.2 \pm 4.0$ [69]	$68 \pm 10^{+9}_{-8}$ [84]	$89^{+18}_{-16} \pm 9$ [96]	60.6 ± 7.0 ($S = 1.6$)

Mode	BaBar	Belle	CLEO	Average
Penguin-dominated decays				
$B^- \to \pi^- \bar{K}^0$	$-17 \pm 10 \pm 2$ [77]	$7^{+9}_{-8}{}^{+1}_{-3}$ [84]	$18 \pm 24 \pm 2$ [95]	-2 ± 9 ($S = 2.0$)
$B^- \to \pi^0 K^-$	$-9 \pm 9 \pm 1$ [73]	$23 \pm 11^{+1}_{-4}$ [84]	$-29 \pm 23 \pm 2$ [95]	1 ± 12 ($S = 3.4$)
$\bar{B}^0 \to \pi^+ K^-$	$-10 \pm 5 \pm 2$ [76]	$-7 \pm 6 \pm 1$ [84]	$-4 \pm 16 \pm 2$ [95]	-9 ± 4
$\bar{B}^0 \to \pi^0 \bar{K}^0$	$3 \pm 36 \pm 9$ [75]	—	—	3 ± 37
$B^- \to \eta K^-$	$-32^{+22}_{-18} \pm 1$ [71]	—	—	-32 ± 20
$B^- \to \eta' K^-$	$3.7 \pm 4.5 \pm 1.1$ [69]	$-1 \pm 7 \pm 1$ [83]	$3 \pm 12 \pm 2$ [95]	2 ± 4
$\bar{B}^0 \to \eta' \bar{K}^0$	$-10 \pm 22 \pm 3$ [69]	$26 \pm 22 \pm 4$ [86]	—	8 ± 18 ($S = 1.3$)
$S_{\eta' K_S}$:	$2 \pm 34 \pm 3$ [69]	$71 \pm 37^{+5}_{-6}$ [86]	—	33 ± 34 ($S = 1.9$)

Table 26: CP-averaged branching ratios (top, in units of 10^{-6}) and CP asymmetries (bottom, in %) for $\bar{B} \to PV$ decays with $\Delta S = 1$. Upper limits are at 90% confidence level.

Mode	BaBar	Belle	CLEO	Average
Penguin-dominated decays				
$B^- \to \pi^- \bar{K}^{*0}$	$15.5 \pm 1.8^{+1.5}_{-3.2}$ [74]	$19.4^{+4.2}_{-3.9}{}^{+2.1}_{-2.1}{}^{+3.5}_{-6.8}$ [89]	$7.6^{+3.5}_{-3.0} \pm 1.6$ (< 16) [94]	13.0 ± 3.0 ($S = 1.9$)
$B^- \to \pi^0 K^{*-}$	—	—	< 31 [94]	< 31
$\bar{B}^0 \to \pi^+ K^{*-}$	—	$14.8^{+4.6}_{-4.4}{}^{+1.5}_{-1.0}{}^{+2.4}_{-0.9}$ [79]	$16^{+6}_{-5} \pm 2$ [92]	15.3 ± 3.8
$\bar{B}^0 \to \pi^0 \bar{K}^{*0}$	—	—	< 3.6 [94]	< 3.6
$B^- \to \bar{K}^0 \rho^-$	—	—	< 48 [65]	< 48
$B^- \to K^- \rho^0$	< 6.2 [74]	< 12 [89]	< 17 [94]	< 6.2
$\bar{B}^0 \to K^- \rho^+$	$7.3^{+1.3}_{-1.2} \pm 1.3$ [66]	$15.1^{+3.4}_{-3.3}{}^{+1.4}_{-1.5}{}^{+2.0}_{-2.1}$ [79]	$16.0^{+7.6}_{-6.4} \pm 2.8$ (< 32) [94]	8.9 ± 2.2 ($S = 1.9$)
$\bar{B}^0 \to \bar{K}^0 \rho^0$	—	< 12 [88]	< 39 [65]	< 12
$B^- \to \eta K^{*-}$	$22.1^{+11.1}_{-9.2} \pm 3.3$ [83]	$26.5^{+7.8}_{-7.0} \pm 3.0$ [83]	$26.4^{+9.6}_{-8.2} \pm 3.3$ [96]	25.4 ± 5.3
$\bar{B}^0 \to \eta \bar{K}^{*0}$	$19.8^{+6.5}_{-5.6} \pm 1.7$ [83]	$16.5^{+4.6}_{-4.2} \pm 1.2$ [83]	$13.8^{+5.5}_{-4.6} \pm 1.6$ [96]	16.4 ± 3.0
$B^- \to \eta' K^{*-}$	—	< 90 [83]	< 35 [96]	< 35
$\bar{B}^0 \to \eta' \bar{K}^{*0}$	< 13 [83]	< 20 [83]	< 24 [96]	< 13
$B^- \to K^- \omega$	$5.0 \pm 1.0 \pm 0.4$ [70]	$6.7^{+1.3}_{-1.2} \pm 0.6$ [80]	$3.2^{+2.4}_{-1.9} \pm 0.8$ (< 7.9) [94]	5.3 ± 0.8
$\bar{B}^0 \to \bar{K}^0 \omega$	$5.3^{+1.4}_{-1.2} \pm 0.5$ [70]	$4.0^{+1.9}_{-1.6} \pm 0.5$ (< 7.6) [80]	$10.0^{+5.4}_{-4.2} \pm 1.4$ (< 21) [94]	5.1 ± 1.1
$B^- \to K^- \phi$	$10.0^{+0.9}_{-0.8} \pm 0.5$ [72]	$9.4 \pm 1.1 \pm 0.7$ [82]	$5.5^{+2.1}_{-1.8} \pm 0.6$ [93]	9.2 ± 0.7 ($S = 2.0$)
$\bar{B}^0 \to \bar{K}^0 \phi$	$7.6^{+1.3}_{-1.2} \pm 0.5$ [72]	$9.0^{+2.2}_{-1.8} \pm 0.7$ [82]	$5.4^{+3.7}_{-2.7} \pm 0.7$ (< 12.3) [93]	7.7 ± 1.1

Mode	BaBar	Belle	CLEO	Average
Penguin-dominated decays				
$\bar{B}^0 \to \pi^+ K^{*-}$	—	—	$26^{+33}_{-34}{}^{+10}_{-8}$ [90]	26 ± 35
$\bar{B}^0 \to K^- \rho^+$	$28 \pm 17 \pm 8$ [66]	$22^{+22}_{-23}{}^{+6}_{-2}$ [79]	—	26 ± 15
$B^- \to K^- \omega$	$-5 \pm 16 \pm 1$ [70]	$-6^{+18}_{-20} \pm 1$ [80]	—	-5 ± 12
$B^- \to K^- \phi$	$3.9 \pm 8.6 \pm 1.1$ [72]	$1 \pm 12 \pm 5$ [83]	—	3 ± 7
$\bar{B}^0 \to \bar{K}^0 \phi$	$80 \pm 38 \pm 12$ [67]	$-56 \pm 41 \pm 16$ [86]	—	19 ± 68 ($S = 5.2$)
$S_{\phi K_S}$:	$-18 \pm 51 \pm 7$ [67]	$-73 \pm 64 \pm 22$ [86]	—	-38 ± 41

Table 27: CP-averaged branching ratios (top, in units of 10^{-6}) and CP asymmetries (bottom, in %) for $\bar{B} \to PP$ decays with $\Delta D = 1$. Upper limits are at 90% confidence level.

Mode	BaBar	Belle	CLEO	Average
Tree-dominated decays				
$B^- \to \pi^-\pi^0$	$5.5^{+1.0}_{-0.9} \pm 0.6$ [73]	$5.3 \pm 1.3 \pm 0.5$ [84]	$4.6^{+1.8}_{-1.6}{}^{+0.6}_{-0.7}$ [91]	5.3 ± 0.8
$\bar{B}^0 \to \pi^+\pi^-$	$4.7 \pm 0.6 \pm 0.2$ [76]	$4.4 \pm 0.6 \pm 0.3$ [84]	$4.5^{+1.4}_{-1.2}{}^{+0.5}_{-0.4}$ [91]	4.6 ± 0.4
$\bar{B}^0 \to \pi^0\pi^0$	$1.6^{+0.7}_{-0.6}{}^{+0.6}_{-0.3}$ [73] < 3.6 [73]	$1.8^{+1.4}_{-1.3}{}^{+0.5}_{-0.7}$ [84] < 4.4 [84]	— < 4.4 [91]	1.6 ± 0.7 (< 3.6)
$B^- \to \pi^-\eta$	$4.2^{+1.0}_{-0.9} \pm 0.3$ [71]	$5.2^{+2.0}_{-1.7} \pm 0.6$ [84]	$1.2^{+2.8}_{-1.2}$ (< 5.7) [96]	3.9 ± 0.9 $(S = 1.2)$
$\bar{B}^0 \to \pi^0\eta$	—	—	< 2.9 [96]	< 2.9
$B^- \to \pi^-\eta'$	< 12 [78]	< 7 [83]	< 12 [96]	< 7
$\bar{B}^0 \to \pi^0\eta'$	—	—	< 5.7 [96]	< 5.7
Penguin-dominated decays				
$B^- \to K^-K^0$	< 2.2 [65]	< 3.4 [84]	< 3.3 [91]	< 2.2
$\bar{B}^0 \to \bar{K}^0K^0$	< 1.6 [65]	< 3.2 [84]	< 3.3 [91]	< 1.6
Pure annihilation decays				
$\bar{B}^0 \to K^-K^+$	< 0.6 [76]	< 0.7 [84]	< 0.8 [91]	< 0.6

Mode	BaBar	Belle	Average
Tree-dominated decays			
$B^- \to \pi^-\pi^0$	$-3^{+18}_{-17} \pm 2$ [73]	$-14 \pm 24^{+5}_{-4}$ [84]	-7 ± 14
$\bar{B}^0 \to \pi^+\pi^-$	$30 \pm 25 \pm 4$ [76]	$77 \pm 27 \pm 8$ [85]	51 ± 23 $(S = 1.5)$
$S_{\pi^+\pi^-}$:	$2 \pm 34 \pm 5$ [76]	$-123 \pm 41^{+8}_{-7}$ [85]	-49 ± 61 $(S = 5.4)$
$B^- \to \pi^-\eta$	$-51^{+20}_{-18} \pm 1$ [71]	—	-51 ± 19

Table 28: CP-averaged branching ratios (top, in units of 10^{-6}) and CP asymmetries (bottom, in %) for $\bar{B} \to PV$ decays with $\Delta D = 1$. Upper limits are at 90% confidence level.

Mode	BaBar	Belle	CLEO	Average
Tree-dominated decays				
$B^- \to \pi^- \rho^0$	$11.0 \pm 1.9 \pm 1.9$ [64]	$8.0^{+2.3}_{-2.0} \pm 0.7$ [87]	$10.4^{+3.3}_{-3.4} \pm 2.1$ [94]	9.4 ± 1.6
$B^- \to \pi^0 \rho^-$	$9.3 \pm 1.0 \pm 0.8$ [64]	—	< 43 [94]	9.3 ± 1.3
$\bar{B}^0 \to \pi^+ \rho^-$	13.9 ± 2.7 [61]	—	—	13.9 ± 2.7
$\bar{B}^0 \to \pi^- \rho^+$	8.9 ± 2.5 [61]	—	—	8.9 ± 2.5
$\bar{B}^0 \to \pi^\pm \rho^\mp$	$22.6 \pm 1.8 \pm 2.2$ [66]	$29.1^{+5.0}_{-4.9} \pm 4.0$ [81]	$27.6^{+8.4}_{-7.4} \pm 4.2$ [94]	24.0 ± 2.5
$\bar{B}^0 \to \pi^0 \rho^0$	< 2.5 [64]	$6.0^{+2.9}_{-2.3} \pm 1.2$ [81]	< 5.5 [94]	< 2.5
$B^- \to \pi^- \omega$	$5.4 \pm 1.0 \pm 0.5$ [70]	$5.7^{+1.4}_{-1.3} \pm 0.6$ [80]	$11.3^{+3.3}_{-2.9} \pm 1.4$ [94]	5.9 ± 0.9 ($S = 1.4$)
$\bar{B}^0 \to \pi^0 \omega$	< 3 [78]	< 1.9 [80]	< 5.5 [94]	< 1.9
$B^- \to \eta \rho^-$	< 6.8 [83]	< 6.2 [83]	< 15 [96]	< 6.2
$\bar{B}^0 \to \eta \rho^0$	—	< 5.5 [83]	< 10 [96]	< 5.5
$B^- \to \eta' \rho^-$	—	—	< 33 [96]	< 33
$\bar{B}^0 \to \eta' \rho^0$	—	< 14 [83]	< 12 [96]	< 12
Penguin-dominated decays				
$B^- \to \pi^- \phi$	< 0.41 [72]	—	< 5 [97]	< 0.4
$\bar{B}^0 \to \pi^0 \phi$	—	—	< 5 [97]	< 5
$B^- \to K^- K^{*0}$	—	—	< 5.3 [94]	< 5.3

Mode	BaBar	Belle	CLEO	Average
Tree-dominated decays				
$B^- \to \pi^- \rho^0$	$23 \pm 16 \pm 6$ [64]	—	—	23 ± 17
$B^- \to \pi^0 \rho^-$	$-17 \pm 11 \pm 2$ [64]	—	—	-17 ± 11
$\bar{B}^0 \to \pi^+ \rho^-$	$-62^{+24}_{-28} \pm 6$ [68]	—	—	-62 ± 27
$\bar{B}^0 \to \pi^- \rho^+$	$-11^{+16}_{-17} \pm 4$ [68]	—	—	-11 ± 17
$\bar{B}^0 \to \pi^\pm \rho^\mp$:				
$A_{\rm CP}$	$-18 \pm 8 \pm 3$ [66]	$-38^{+19}_{-21}{}^{+4}_{-5}$ [81]	—	-21 ± 8
$C_{\pi^\pm \rho^\mp}$	$36 \pm 18 \pm 4$ [66]	—	—	36 ± 18
$S_{\pi^\pm \rho^\mp}$	$19 \pm 24 \pm 3$ [66]	—	—	19 ± 24
$\Delta C_{\pi^\pm \rho^\mp}$	$28^{+18}_{-19} \pm 4$ [66]	—	—	28 ± 19
$\Delta S_{\pi^\pm \rho^\mp}$	$15 \pm 25 \pm 3$ [66]	—	—	15 ± 25
$B^- \to \pi^- \omega$	$4 \pm 17 \pm 1$ [70]	$-48^{+20}_{-23} \pm 2$ [80]	$-34 \pm 25 \pm 2$ [95]	-20 ± 17 ($S = 2.0$)

References

[1] B. Aubert *et al.* [BaBar Collaboration], Nucl. Instrum. Meth. A **479** (2002) 1 [hep-ex/0105044].

[2] S. Mori *et al.* [Belle Collaboration], Nucl. Instrum. Meth. A **479** (2002) 117.

[3] M. Bauer, B. Stech and M. Wirbel, Z. Phys. C **34** (1987) 103.

[4] M. Neubert and B. Stech, Adv. Ser. Direct. High Energy Phys. **15** (1998) 294 [hep-ph/9705292].

[5] A. Ali and C. Greub, Phys. Rev. D **57** (1998) 2996 [hep-ph/9707251].

[6] A. Ali, G. Kramer and C. D. Lu, Phys. Rev. D **58** (1998) 094009 [hep-ph/9804363].

[7] Y. H. Chen, H. Y. Cheng, B. Tseng and K. C. Yang, Phys. Rev. D **60** (1999) 094014 [hep-ph/9903453].

[8] M. Beneke, G. Buchalla, M. Neubert and C. T. Sachrajda, Phys. Rev. Lett. **83** (1999) 1914 [hep-ph/9905312].

[9] M. Beneke, G. Buchalla, M. Neubert and C. T. Sachrajda, Nucl. Phys. B **591** (2000) 313 [hep-ph/0006124].

[10] M. Beneke, G. Buchalla, M. Neubert and C. T. Sachrajda, Nucl. Phys. B **606** (2001) 245 [hep-ph/0104110].

[11] T. Muta, A. Sugamoto, M. Z. Yang and Y. D. Yang, Phys. Rev. D **62** (2000) 094020 [hep-ph/0006022].

[12] D.-s. Du, D.-s. Yang and G.-h. Zhu, Phys. Lett. B **488** (2000) 46 [hep-ph/0005006].

[13] D.-s. Du, H.-u. Gong, J.-f. Sun, D.-s. Yang and G.-h. Zhu, Phys. Rev. D **65** (2002) 074001 [hep-ph/0108141].

[14] M. Z. Yang and Y. D. Yang, Phys. Rev. D **62** (2000) 114019 [hep-ph/0007038].

[15] H. Y. Cheng and K. C. Yang, Phys. Rev. D **64** (2001) 074004 [hep-ph/0012152].

[16] H. Y. Cheng and K. C. Yang, Phys. Lett. B **511** (2001) 40 [hep-ph/0104090].

[17] M. Diehl and G. Hiller, JHEP **0106** (2001) 067 [hep-ph/0105194].

[18] M. Beneke and M. Neubert, Nucl. Phys. B **651** (2003) 225 [hep-ph/0210085].

[19] D.-s. Du, H.-j. Gong, J.-f. Sun, D.-s. Yang and G.-h. Zhu, Phys. Rev. D **65** (2002) 094025 [Erratum: *ibid.* D **66** (2002) 079904] [hep-ph/0201253].

[20] D.-s. Du, J.-f. Sun, D.-s. Yang and G.-h. Zhu, Phys. Rev. D **67** (2003) 014023 [hep-ph/0209233].

[21] J.-f. Sun, G.-h. Zhu and D.-s. Du, preprint hep-ph/0211154.

[22] R. Aleksan, P. F. Giraud, V. Morenas, O. Pene and A. S. Safir, Phys. Rev. D **67** (2003) 094019 [hep-ph/0301165].

[23] N. de Groot, W. N. Cottingham and I. B. Whittingham, preprint hep-ph/0305263.

[24] C. H. Chen, Y. Y. Keum and H.-n. Li, Phys. Rev. D **64** (2001) 112002 [hep-ph/0107165].

[25] C. W. Bauer, D. Pirjol and I. W. Stewart, Phys. Rev. Lett. **87** (2001) 201806 [hep-ph/0107002].

[26] J. Chay and C. Kim, preprint hep-ph/0301262.

[27] A. Khodjamirian, Nucl. Phys. B **605** (2001) 558 [hep-ph/0012271].

[28] A. Khodjamirian, T. Mannel and B. Melic, preprint hep-ph/0304179.

[29] T. Feldmann, P. Kroll and B. Stech, Phys. Rev. D **58** (1998) 114006 [hep-ph/9802409].

[30] A. G. Grozin and M. Neubert, Phys. Rev. D **55** (1997) 272 [hep-ph/9607366].

[31] M. Beneke and T. Feldmann, Nucl. Phys. B **592** (2001) 3 [hep-ph/0008255].

[32] V. M. Braun and I. E. Filyanov, Z. Phys. C **48** (1990) 239 [Sov. J. Nucl. Phys. **52** (1990) 126].

[33] P. Ball, V. M. Braun, Y. Koike and K. Tanaka, Nucl. Phys. B **529** (1998) 323 [hep-ph/9802299].

[34] M. Beneke, Nucl. Phys. Proc. Suppl. **111** (2002) 62 [hep-ph/0202056].

[35] B. V. Geshkenbein and M. V. Terentev, Yad. Fiz. **40** (1984) 758 [Sov. J. Nucl. Phys. **40** (1984) 487].

[36] P. Kroll and K. Passek-Kumericki, Phys. Rev. D **67** (2003) 054017 [hep-ph/0210045].

[37] A. Khodjamirian, R. Rückl, S. Weinzierl and O. I. Yakovlev, Phys. Lett. B **410** (1997) 275 [hep-ph/9706303].

[38] P. Ball and V. M. Braun, Phys. Rev. D **58** (1998) 094016 [hep-ph/9805422].

[39] P. Ball, JHEP **9809** (1998) 005 [hep-ph/9802394].

[40] J. D. Bjorken, Nucl. Phys. Proc. Suppl. **11** (1989) 325.

[41] M. Neubert, Int. J. Mod. Phys. A **17** (2002) 2936 [hep-ph/0110301].

[42] S. B. Athar *et al.* [CLEO Collaboration], preprint hep-ex/0304019.

[43] Z.-m. Luo and J. L. Rosner, preprint hep-ph/0305262.

[44] T. Becher, M. Neubert and B. D. Pecjak, Nucl. Phys. B **619** (2001) 538 [hep-ph/0102219];
M. Neubert and B. D. Pecjak, JHEP **0202** (2002) 028 [hep-ph/0202128].

[45] A. S. Dighe, M. Gronau and J. L. Rosner, Phys. Rev. D **54** (1996) 3309 [hep-ph/9604233];
M. Gronau and J. L. Rosner, Phys. Rev. D **57** (1998) 6843 [hep-ph/9711246].

[46] R. Fleischer and T. Mannel, Phys. Rev. D **57** (1998) 2752 [hep-ph/9704423].

[47] M. Neubert and J. L. Rosner, Phys. Lett. B **441** (1998) 403 [hep-ph/9808493]; Phys. Rev. Lett. **81** (1998) 5076 [hep-ph/9809311].

[48] A. J. Buras and R. Fleischer, Eur. Phys. J. C **11** (1999) 93 [hep-ph/9810260].

[49] M. Neubert, JHEP **9902** (1999) 014 [hep-ph/9812396].

[50] M. Ciuchini, E. Franco, G. Martinelli and L. Silvestrini, Nucl. Phys. B **501** (1997) 271 [hep-ph/9703353].

[51] Y. Grossman and M. P. Worah, Phys. Lett. B **395** (1997) 241 [hep-ph/9612269];
Y. Grossman, G. Isidori and M. P. Worah, Phys. Rev. D **58** (1998) 057504 [hep-ph/9708305].

[52] Y. Grossman, Z. Ligeti, Y. Nir and H. Quinn, preprint hep-ph/0303171.

[53] T. Yoshikawa, preprint hep-ph/0306147.

[54] Y. Grossman, M. Neubert and A. L. Kagan, JHEP **9910** (1999) 029 [hep-ph/9909297].

[55] H. J. Lipkin, Phys. Lett. B **445** (1999) 403 [hep-ph/9810351].

[56] M. Gronau and J. L. Rosner, Phys. Rev. D **59** (1999) 113002 [hep-ph/9809384].

[57] M. Gronau and J. L. Rosner, preprint hep-ph/0307095.

[58] M. Ciuchini, E. Franco, A. Masiero and L. Silvestrini, Phys. Rev. D **67** (2003) 075016 [hep-ph/0212397].

[59] R. Aleksan, I. Dunietz, B. Kayser and F. Le Diberder, Nucl. Phys. B **361** (1991) 141.

[60] A. Khodjamirian and R. Rückl, Adv. Ser. Direct. High Energy Phys. **15** (1998) 345 [hep-ph/9801443].

[61] A. Höcker, M. Laget, S. Laplace and J. v. Wimmersperg-Toeller, *Using Flavor Symmetry to Constrain α from $B \to \rho\pi$*, LAL 03-17, BABAR Analysis Document #628, http://www.slac.stanford.edu/ laplace/doc/lal-03-17.ps.gz

[62] C. W. Chiang, M. Gronau and J. L. Rosner, preprint hep-ph/0306021.

[63] M. Beneke, in: *The CKM Matrix and the Unitarity Triangle* (edited by M. Battaglia *et al.*), preprint hep-ph/0304132, pp. 299.

[64] B. Aubert *et al.* [BaBar Collaboration], preprint hep-ex/0307087.

[65] M. Bona, talk at the Conference on Flavor Physics and CP Violation (FPCP 2003), Paris, France, June 3–6, 2003, to appear in the Proceedings.

[66] B. Aubert *et al.* [BaBar Collaboration], preprint hep-ex/0306030.

[67] G. Hamel De Monchenault [BaBar Collaboration], preprint hep-ex/0305055.

[68] G. Hamel de Monchenault, talk at the 38th Rencontres de Moriond: Electroweak Interactions and Unified Theories, Les Arcs, France, March 15–22, 2003, to appear in the Proceedings.

[69] B. Aubert *et al.* [BaBar Collaboration], preprint hep-ex/0303046.

[70] B. Aubert *et al.* [BaBar Collaboration], preprint hep-ex/0303040.

[71] B. Aubert *et al.* [BaBar Collaboration], preprint hep-ex/0303039.

[72] B. Aubert *et al.* [BaBar Collaboration], preprint hep-ex/0303029.

[73] B. Aubert *et al.* [BaBar Collaboration], preprint hep-ex/0303028.

[74] B. Aubert *et al.* [BaBar Collaboration], preprint hep-ex/0303022.

[75] B. Aubert *et al.* [BaBar Collaboration], preprint hep-ex/0207065.

[76] B. Aubert *et al.* [BaBar Collaboration], Phys. Rev. Lett. **89** (2002) 281802 [hep-ex/0207055].

[77] B. Aubert *et al.* [BaBar Collaboration], preprint hep-ex/0206053.

[78] B. Aubert *et al.* [BaBar Collaboration], Phys. Rev. Lett. **87** (2001) 221802 [hep-ex/0108017].

[79] K. Abe *et al.* [Belle Collaboration], conference paper BELLE-CONF-0317 (EPS-ID 535) submitted to the International Europhysics Conference on High Energy Physics, Aachen, Germany, July 17–23, 2003.

[80] K. Abe *et al.* [Belle Collaboration], conference paper BELLE-CONF-0312 (EPS-ID 527) submitted to the International Europhysics Conference on High Energy Physics, Aachen, Germany, July 17–23, 2003.

[81] K. Abe *et al.* [Belle Collaboration], preprint hep-ex/0307077.

[82] K. F. Chen *et al.* [Belle Collaboration], preprint hep-ex/0307014.

[83] H. Aihara, talk at the Conference on Flavor Physics and CP Violation (FPCP 2003), Paris, France, June 3–6, 2003, to appear in the Proceedings.

[84] T. Tomura, preprint hep-ex/0305036.

[85] K. Abe *et al.* [Belle Collaboration], preprint hep-ex/0301032.

[86] K. Abe *et al.* [Belle Collaboration], Phys. Rev. D **67** (2003) 031102 [hep-ex/0212062].

[87] A. Gordon *et al.* [Belle Collaboration], Phys. Lett. B **542** (2002) 183 [hep-ex/0207007].

[88] H. C. Huang [Belle Collaboration], preprint hep-ex/0205062.

[89] K. Abe *et al.* [Belle Collaboration], Phys. Rev. D **65** (2002) 092005 [hep-ex/0201007].

[90] B. I. Eisenstein [CLEO Collaboration], preprint hep-ex/0304036.

[91] A. Bornheim *et al.* [CLEO Collaboration], preprint hep-ex/0302026.

[92] E. Eckhart *et al.* [CLEO Collaboration], preprint hep-ex/0206024.

[93] R. A. Briere *et al.* [CLEO Collaboration], Phys. Rev. Lett. **86** (2001) 3718 [hep-ex/0101032].

[94] C. P. Jessop *et al.* [CLEO Collaboration], Phys. Rev. Lett. **85** (2000) 2881 [hep-ex/0006008].

[95] S. Chen *et al.* [CLEO Collaboration], Phys. Rev. Lett. **85** (2000) 525 [hep-ex/0001009].

[96] S. J. Richichi *et al.* [CLEO Collaboration], Phys. Rev. Lett. **85** (2000) 520 [hep-ex/9912059].

[97] T. Bergfeld *et al.* [CLEO Collaboration], Phys. Rev. Lett. **81** (1998) 272 [hep-ex/9803018].